ANL-6879
Physics
(TID-4500, 31st Ed.)
AEC Research and
Development Report

ARGONNE NATIONAL LABORATORY
9700 South Cass Avenue
Argonne, Illinois 60440

PHYSICS DIVISION SUMMARY REPORT

Annual Review

1 April 1963—31 March 1964

Lowell M. Bollinger, Division Director

Preceding Summary Reports:

ANL-6767, July-August 1963
ANL-6819, September-December 1963
ANL-6877, January-March 1964

Operated by The University of Chicago
under
Contract W-31-109-eng-38
with the
U. S. Atomic Energy Commission

DISCLAIMER

FOREWORD

This issue of the ANL Physics Division Summary Report presents a comprehensive picture of the work of the Division in the year ending in the spring of 1964. Instead of the usual small selection of relatively full accounts of individual researches reported at the random times at which they become available, this issue offers a complete and systematic overview of what is going on. Much of what is indicated briefly here has been described more fully in earlier issues of the Summary; most of the rest will appear in forthcoming issues.

In addition, the papers published in the 1-year period from 1 April 1963 through 31 March 1964 are listed immediately after the reports on the research. This list accounts for much the same effort but from a different point of view.

Still another picture of the relative emphases on the different programs of the Division is supplied by the roster of personnel, in which the staff members are grouped by program. (It must be understood, however, that staff members frequently do part of their work in another program.) This roster forms the last section of the report.

TABLE OF CONTENTS

I. EXPERIMENTAL NUCLEAR PHYSICS

INTRODUCTION

The over-all purpose of the program continues to be, as in the past, to obtain a much more complete understanding of the atomic nucleus. Consequently, most of the program consists of experimental and theoretical studies of the energies, quantum numbers, and lifetimes of nuclear energy levels and investigations of the mechanisms by which simple nuclear projectiles interact with nuclear targets. Experimenters and theorists work closely together so that new results in one area may suggest new approaches in another. An effort is made to stress work that can be done more advantageously at Argonne than elsewhere because of the special facilities available here. In view of the history and tradition of the Laboratory, it is natural that considerable emphasis is placed on studies of interactions between nuclei and neutrons; but this is balanced by a well diversified program of other nuclear investigations.

The experimental part of the program is most easily outlined by subdividing the work into various categories for which a major piece of equipment or an important experimental technique is the unifying factor. The categories formed in this way are the following:

(1) Studies of the neutron and of neutron-induced reactions at the reactor CP-5.

(2) Neutron and charged-particle-induced reactions at the 4.5-MeV Van de Graaff.

(3) Charged-particle reactions at the tandem Van de Graaff accelerator.

(4) Charged-particle reactions at the 60-in. cyclotron.

(5) Various experiments that use the Mössbauer effect.

(6) Atomic-beam studies.

(7) Studies of the decay of short-lived radionuclides.

Some physicists restrict their efforts to the use of a single machine or technique, whereas others investigate related problems with several systems of apparatus.

I - 1. RESEARCH AT THE REACTOR CP-5

The program of the Physics Division at the reactor CP-5 is devoted entirely to nuclear physics. The experiments fall into three broad categories—experiments on the fundamental properties of the neutron itself, studies of neutron cross sections, and a variety of experiments with neutron-capture gamma rays.

The first category includes an investigation of the neutron-electron interaction and studies of the decay of polarized neutrons.

Neutron cross sections are measured by the time-of-flight method with a fast chopper. During the past year, this system was used to measure total cross sections and especially to study the gamma-ray spectra that result from the capture of neutrons in resonances.

The largest area of investigation is concerned with the gamma rays from capture of thermal neutrons. A key instrument for these investigations is the 7.7-meter bent-crystal spectrometer, a precision instrument that is used for the range of energy up to about 2 MeV. A high resolution germanium diode system is currently being developed for the study of gamma rays of higher energy. In addition to the measurements made with these precision instruments, many useful studies are performed with NaI scintillation spectrometers of various kinds. These studies include measurements with an anticoincidence spectrometer to obtain the capture gamma-ray spectra for materials having exceptionally small neutron cross sections, delayed-coincidence measurements of the lifetimes of excited states formed by neutron capture, coincidence measurements to determine nuclear decay schemes, and angular-correlation measurements to determine spins and parities of excited states.

In addition to the above well-established experiments, during the past year a program of measurements on the resonant scattering of neutron-capture gammas was started.

I - 1.1. Instrumentation for Measurements of the Symmetry Properties of Neutron Decay (Project I-123)

M. T. Burgy and G. R. Ringo (and P. Doherty for the summer of 1963)

For the next phase of the experiment on the symmetry properties of neutron decay, it is necessary to know the polarization of the

neutrons with an accuracy of about ±2%. The work has progressed until it seems reasonably clear that this can be done, probably by use of double reflection in both polarizer and analyzer mirrors and certainly using elaborate compensating schemes to handle the small-angle scattering caused by the depolarizing steel foil in the measurement technique we have adopted. The technique is not sufficiently reliable yet, however, to permit describing the work as complete.

Some preliminary work has been done on a test for the uniformity of response of the proton detector, and the data-recording system is being improved. The next major step, however, will be to design and build a new polarizing mirror giving several times the intensity of the present one.

I - 1.2. Electron-Neutron Interaction (Project I-135)

V. Krohn and G. R. Ringo

The objective of this program is to achieve a precise measurement of the electron-neutron interaction by studying the fore-and-aft asymmetry in the scattering of thermal neutrons by noble gases.

The computer program for calculating the contribution of the motion of the center of mass of the scattering system to the observed asymmetry is now satisfactory. The neutron spectrum used in the asymmetry measurements and the scattering cross sections of the individual isotopes of the noble gases are needed as inputs for these calculations.

Plans to measure the scattering cross sections of the isotopes have suffered a serious setback. Isotopes of neon and argon are available but plans for a xenon separation by gaseous diffusion at Oak Ridge have been abandoned and krypton separation has been delayed. Also, it is not clear that this method of separation will be satisfactory for the intermediate-mass isotopes of xenon and krypton. This will be

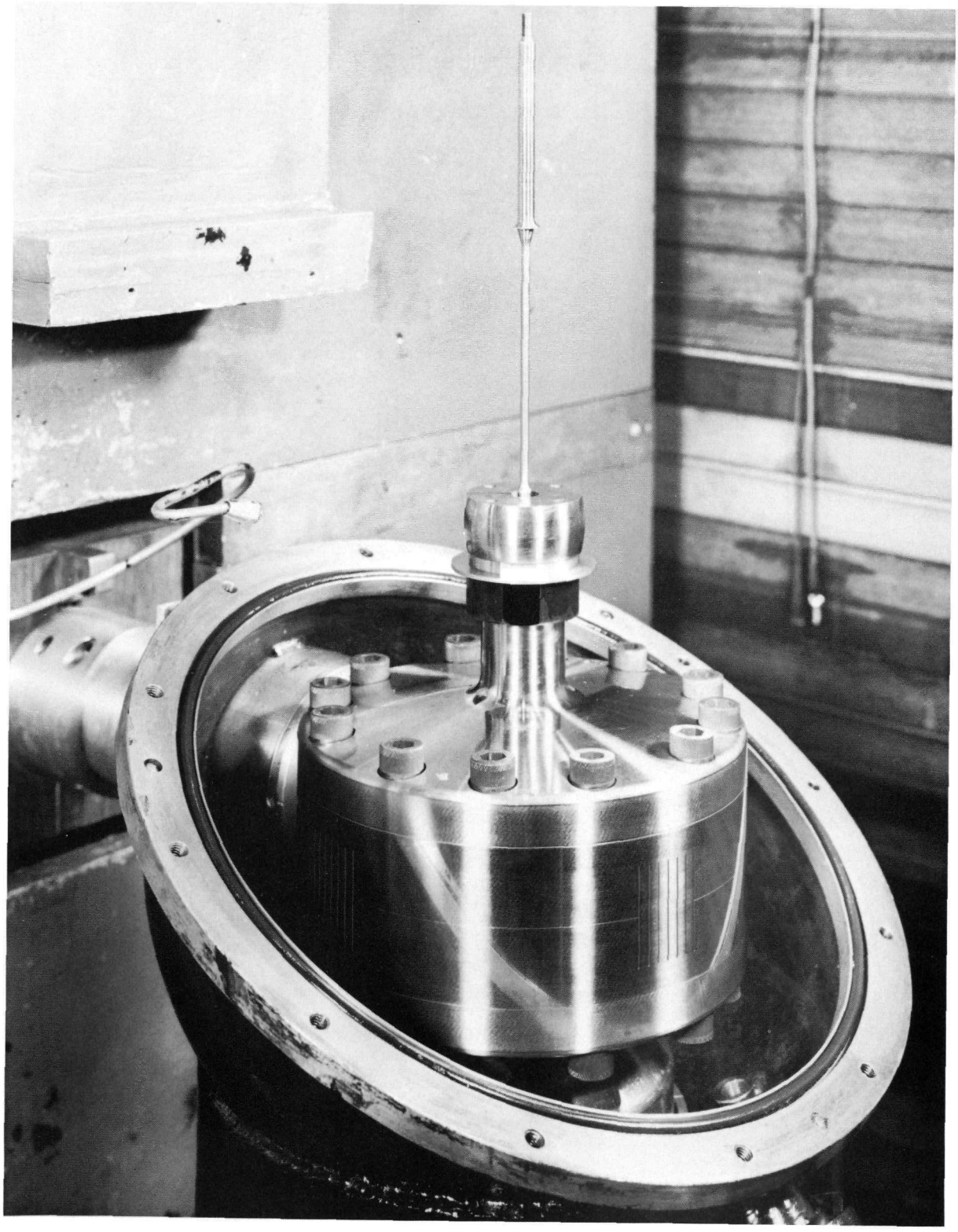

Fig. I-1-a. Rotor No. IV of the fast chopper. The rotor was built specifically for use in capture gamma-ray studies at neutron resonances. [See Sec. I-1.3(b).]

determined when the krypton is separated in the near future. If electromagnetic methods must be used for the desired separations, a satisfactory technique will have to be developed for the collecting of the separated isotopes.

The program to develop large-diameter ^{3}He proportional counters for the measurement of scattering asymmetries has been completed. Mixtures of ^{3}He, methane, and neon gave very satisfactory counter performance. These mixtures were then tested in smaller (0.936-in. i.d.) counters and shown to be superior to BF_3 for many routine applications involving thermal neutrons. The results obtained with these fillings have been submitted for publication.

Preparations for measurements of the scattering asymmetries are nearly complete; these measurements will be started in the near future at a CP-5 thermal column. A slow chopper will be used to determine the spectrum of the thermal neutrons used for these measurements.

I - 1.3. Neutron Resonances

L. M. Bollinger, R. E. Coté, H. E. Jackson, J. P. Marion and G. E. Thomas

During the past year the fast chopper time-of-flight neutron spectrometer has been used to study low-energy resonances in some 18 nuclides ranging from calcium to curium. The results of greatest physical interest are discussed below.

(1) p-Wave Resonances at Very Low Energy

A newly developed boron-loaded liquid scintillation neutron detector of large area has permitted us to obtain total-cross-section data of extremely good statistical accuracy. Such data for Th^{232} exhibit a structure of tiny resonances (Fig. I-1-b) which had previously been undetected.

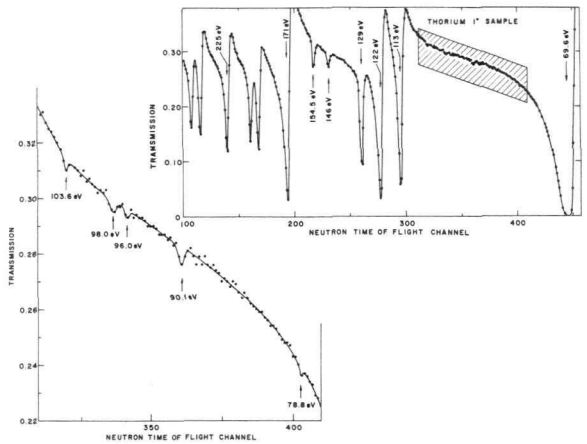

Fig. I-1-b. The transmission of a sample of thorium as a function of neutron time-of-flight. The enlarged area shows the very small size of the resonances that have been assigned as p-wave resonances.

The quantitative treatment[1] of the observed transmission dips indicates that they must be interpreted as resonances that are excited by p-wave neutrons. Thus the data permit, for the first time, a direct determination of the spacing and the strength function of p-wave resonances in a heavy target.

In earlier work at this Laboratory, the low-energy p-wave resonances in Nb^{93} was identified by studies of the capture γ-ray spectra.[2] Recently, total cross sections were measured precisely to determine the total radiation widths Γ_γ for these p-wave resonances.[3] The results (Table I-1-A) show that Γ_γ for p-wave capture is twice that for s-wave capture. No satisfactory explanation of this surprising difference has been advanced to date.

---

[1] L. M. Bollinger and G. E. Thomas, Phys. Letters 8, 45 (1964).

[2] H. E. Jackson, Phys. Rev. 131, 2153 (1963).

[3] H. E. Jackson, Phys. Rev. Letters 11, 378 (1963).

(2) Spin Assignments for Neutron Resonances

A method of spin assignment based on the intensity of two-step gamma-ray cascades is being systematically studied. The

TABLE I-1-A. Parameters for neutron resonances in niobium.

E_0 (eV)	Parity	Γ (10^{-3} eV)	$2g\Gamma_n$ (10^{-3} eV)	Γ_γ (10^{-3} eV)
35.9	-	215 ± 40	0.12 ± 0.01	215 ± 40
42.2	-	260 ± 20	0.09 ± 0.01	260 ± 20
94.3	-	215 ± 50	0.34 ± 0.03	215 ± 50
106	+	96 ± 50	0.05 ± 0.01	96 ± 50
119	+	113 ± 20	5.8 ± 0.6	107 ± 20
194	+	175 ± 25	41.7 ± 4	133 ± 30

method, which has been described previously,[1] depends on the fact that the intensity of two-step cascades to the ground state from the intial compound state formed by neutron capture depends on the density of states at the capturing level; the density, in turn, is proportional to (2J + 1), where J is the spin of the compound state. The spectra of the sums of coincident gamma rays in two large NaI scintillators is used to determine the intensity of the two-step cascades. Measurements on resonances of Se^{77}, Mo^{95}, Pd^{105}, Cd^{111}, Cd^{113}, Ba^{135}, W^{183}, Hf^{177}, Hf^{179}, and Hg^{199} show that the method is useful for almost all even-even compound nuclides (Table I-1-B). On the other hand, since the sum-coincidence spectra observed for silver and niobium resonances do not depend significantly on the spins of the resonances, the method does not appear to be useful for odd-odd compound nuclides.

---

[1] L. M. Bollinger and R. E. Coté in Argonne National Laboratory Report ANL-6146, p.1 (1960).

TABLE I-1-B. Summary of spin assignments made by observation of 2-step γ-ray cascades. Asterisks indicate cases in which results confirm previous assignments.

Isotope	Cd^{111}		Cd^{113}		Ba^{135}		Pd^{105}				Hf^{177}	
Spin & parity	0+	1+	0+	1+	1+	2+	2+		3+		3-	4-
Resonance energy (eV)		28	193	0.2*	24.5	82	13.2	161	11.8	127	1.1*	2.38*
		99		18		88	29.8	186	25.4	172	5.9	6.6
		138		64		106	45.5	208	37.6	231	11.0	8.8
		164*		108		223	78.7	264	55.7	260	14.1	13.7
				215		290	142.2	312	68.9	292		
						318	151	379	86.8	355		22.4
									104	389		

(3) Distribution of Partial Radiation Widths

The measurement of partial radiation widths of neutron resonances and the determination of the distribution that governs these widths has been the subject of a comprehensive study extending over the past several years. The greater part of this work has now been completed and reported.[1] The over-all result, based on the study of gamma-ray spectra from capture in resonances of Hg^{199}, Pt^{195}, W^{183}, and Se^{77}, is that the partial widths are consistent with the Porter-Thomas distribution (the chi-squared distribution with one degree of freedom), i.e., the widths are consistent with the predictions of the simple statistical model. The actual value of ν (the number of degrees of freedom) obtained from a statistical analysis of the data is $\nu = 1.34 \pm 0.33 \pm 0.21$. A similar treatment of previously reported partial radiation widths for resonances in Gd^{155}, Yb^{173}, Hf^{177}, and Hg^{201} leads to the value $\nu = 1.14 \pm 0.44 \pm 0.21$, a value that is also compatible with the expected value of unity.

---

[1] L. M. Bollinger, R. E. Coté, R. T. Carpenter, and J. P. Marion, Phys. Rev. 132, 1640 (1963).

At the time the above work was completed, only the experimental widths for U^{238} appeared to be inconsistent with the predictions of the simple statistical model; the widths for U^{238} had been reported to exhibit little variation from resonance to resonance. However, our recent measurements[2] show that the earlier experimental evidence was incorrect. These new data yield the value $\nu = 5.8 \pm 2.3$ for the distribution of the sum of widths for unresolved transitions at about 4.02 MeV. This value of ν is entirely consistent with the expected value 4.

---

[2] H. E. Jackson, Phys. Rev. (Summer 1964).

(4) s-Wave Neutron Strength Functions

Isotopes of selenium. Cross-section measurements on the isotopes of selenium yield a value of about 1.7×10^{-4} for the strength functions of both Se^{76} and Se^{77}. These relatively high values tend to confirm the previously reported structure in the dependence of the strength function on nuclear mass.

The transplutonic region. Theorists have shown that either a quadrupole or an octopole nuclear deformation could cause the neutron strength function to exhibit a peak near A = 240. The relatively high values of the strength functions for nuclides near uranium tend to support this possibility. However, any comprehensive experimental study in this mass region is severely restricted by the limited availability of samples, since the region is bounded on the low-energy side by very short-lived nuclides and on the high-energy side by the transuranic elements. Nevertheless, in a continuing program we have been studying the neutron cross sections of heavy elements as samples of sufficient size become available. Most recently, samples (prepared by H. Diamond and R. A. Barnes of the Argonne Chemistry Division) of Cm^{244} and Cm^{246} were

studied in transmission measurements.[1] An estimate of the strength function was obtained for each nuclide. These values, when combined with all other measured values of the strength function in this mass range, suggest rather strongly that there is, in fact, a peak in the strength function near A = 240. The data are shown in Fig. I-1-c.

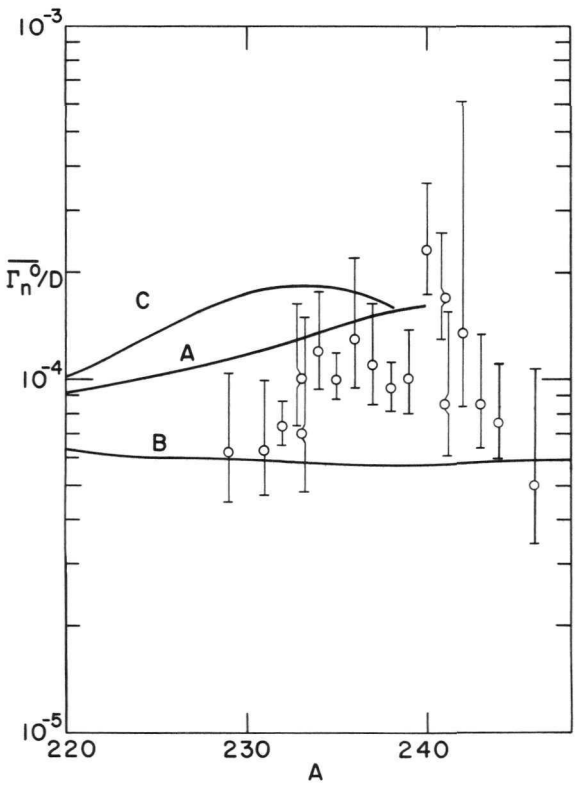

Fig. I-1-c. The strength function for the nuclides with nucleon numbers A between 220 and 246. The theoretical curves are all from Chase, Wilets, and Edmonds, Phys. Rev. 110, 1080 (1958). Curve A is based on a spheroidal potential that provides the best fit to the data near A = 160. Curve B is based on a spherical potential. Curve C corresponds to the same set of parameters as A except that the quadrupole deformation is 33% larger for C.

[1] R. E. Coté, R. A. Barnes, and H. Diamond, Phys. Rev. (Summer 1964).

(5) R-Matrix Fit of the Total Cross Section for Mn^{55}

The total neutron cross section of manganese has been measured from 0.01 eV to about 50 keV and a multilevel analysis of the data has been carried out from 0.01 eV to 15 keV.[1] An excellent fit

[1] R. E. Coté, L. M. Bollinger, and G. E. Thomas, Phys. Rev. (Summer 1964).

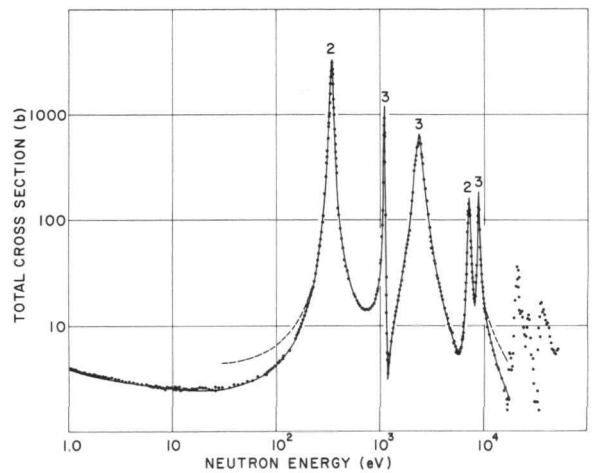

Fig. I-1-d. The observed total neutron cross section of manganese. The solid curve was computed with values of the nuclear radius that differ for each spin state and include the effects of bound levels. The dashed curve was computed with the same resonance parameters, but a constant nuclear radius (the same for both spins) was used and the effects of bound levels were ignored.

is obtained, as is shown in Fig. I-1-d. In addition to describing the total cross section accurately, the final parameters of the fit yield (a) a correct sign for the coherent scattering amplitude, (b) values of the thermal-capture cross section and coherent-scattering cross section that are in agreement with the measured values, (c) agreement with the results of measurements on the capture of polarized neutrons, and (d) agreement with measurements of the resonance-capture integral.

(6) Apparatus

A new rotor (Fig. I-1-a) for the fast chopper has been completed. It was designed to provide a relatively intense burst of neutrons at a high repretition rate without allowing neutrons from consecutive bursts to reach the sample simultaneously when the neutron flight path is 60 m. The rotor has been tested at speeds as high as 20 000 rpm, at which speed the neutron burst is about 1.5 μsec wide.

A 4096-channel time analyzer for transmission measurements is under construction in the Argonne Electronics Division. A novel feature of the analyzer is that the channel width can be selected independently for each block of 64 adjacent channels. The smallest channel width available is 0.125 μsec.

An effort is being made to develop a boron-loaded liquid scintillation neutron detector for which pulse-shape discrimination can be used to reject counts from various forms of background radiation.

I - 1.4. Neutron-Capture γ Rays and Lifetime Measurements of Excited States

H. H. Bolotin

A highly-collimated beam of thermal and subthermal neutrons, effectively free of fast neutrons and γ rays, is being used at the Juggernaut reactor to investigate the low-lying excited states of nuclei populated in the (n,γ) reaction. Gamma-gamma coincidence measurements between low-energy γ rays are providing new information concerning the levels and transitions between levels near the ground state. The levels in Sc^{46}, Ga^{72}, and Sb^{122} have been investigated by these methods. This is the first time some of these nuclides and information concerning these low-lying levels have been obtained by this technique. Plans for future investigations include lifetime measurements of excited states and angular-correlation measurements of cascade γ rays.

I - 1.5. Excited-State Spin Assignments Based on $(n,\gamma\gamma)$ Angular-Correlation Measurements on Medium-Weight Nuclei

R. E. Coté, H. E. Jackson, L. L. Lee, and J. P. Schiffer

A series of measurements of the angular correlations of two-step cascade gamma rays following neutron capture have been completed for Ca^{44}, Fe^{54}, Ni^{58}, Ni^{60}, and Ni^{62}. The results have been used to determine the spins of 9 levels in the compound nuclides formed by the capture of thermal neutrons in those targets. The results are shown in Table I-1-C. These results definitely show that the reported separation of levels associated with the $p_{3/2}$ and $p_{1/2}$ gross-structure groups is incomplete;

TABLE I-1-C. The measured angular correlations and the inferred spins. The quantities a_2 and a_0 are the coefficients of the Legendre polynomials that describe the angular dependence. The errors are standard statistical errors.

Nuclide	Spin	E (MeV)	$\frac{C(\theta=180^\circ)}{C(\theta=90^\circ)}$	a_2/a_0	
				Uncorrected	Corrected
Ca^{45}	$\frac{3}{2}^-$	2.24	1.39 ± 0.07	+ 0.22 ± 0.04	+ 0.26 ± 0.04
Fe^{55}	$\frac{1}{2}^-$	0.413	1.01 ± 0.01	+ 0.01 ± 0.007	+ 0.01 ± 0.007
Ni^{59}	$\frac{1}{2}^-$	0.470	1.01 ± 0.01	+ 0.01 ± 0.007	+ 0.01 ± 0.007
	$\frac{3}{2}^-$	0.870	0.74 ± 0.03	- 0.19 ± 0.025	- 0.21 ± 0.025
	$\frac{1}{2}^-$	1.310	0.92 ± 0.11	- 0.06 ± 0.08	- 0.06 ± 0.08
Ni^{61}	$\frac{1}{2}^-$	0.284	1.02 ± 0.015	+ 0.01 ± 0.01	- 0.02 ± 0.01
Ni^{63}	$\frac{3}{2}^-$	0.158	1.62 ± 0.10	+ 0.34 ± 0.04	+ 0.39 ± 0.05
	$\frac{3}{2}^-$	0.526	0.69 ± 0.06	- 0.23 ± 0.04	- 0.26 ± 0.05
	$\frac{1}{2}^-$	1.008	0.98 ± 0.05	- 0.02 ± 0.05	- 0.014 ± 0.035

$J=\frac{1}{2}$ levels exist within the $p_{3/2}$ group.[1] The results are of further interest in that they form the basis for the newly discovered method for determining spins in (d,p) experiments that is discussed in Sec. I-3.4(4).

---

[1] R. E. Coté, H. E. Jackson, L. L. Lee, Jr., and J. P. Schiffer, Phys. Rev. (Summer 1964).

I - 1.6. High-Resolution Studies of Thermal-Neutron-Capture Gamma-Ray Spectra (Project I-80)

R. K. Smither, A. P. Magruder, and A. I. Namenson

(1) Measurements with the Bent-Crystal Spectrometer

The 7.7-m bent-crystal spectrometer is used to investigate thermal-neutron-capture gamma-ray spectra between the energies of 20 keV and 2 MeV. The energy precision of the system is about one part in 15 000 when the spectrometer is operated in the normal automatic mode. The resolution width (FWHM) is 10 keV at 1 MeV and 100 eV at 100 keV. All data are automatically recorded on punched cards and processed in the IBM-704 computer. During the last 12 months, the bent-crystal spectrometer has been used to investigate the following reactions: $Te^{123}(n,\gamma)Te^{124}$, $U^{238}(n,\gamma)U^{239}$, $Hf^{179}(n,\gamma)Hf^{180}$, and $Sm^{152}(n,\gamma)Sm^{153}$. The last investigation is still in progress. All samples were highly enriched in the isotope under investigation. The observed gamma spectra were used to modify and extend the level schemes of Te^{124}, U^{239}, and Hf^{180}.

The investigation of Te^{124} is part of a series of experiments on spherical even-Z even-N nuclei in which a special effort is made to find missing 2-phonon states and evidence for 3-phonon states. Two possible candidates for the three levels of a 2-phonon triplet in Te^{124} were suggested by β-decay experiments. A third candidate for the triplet is suggested by the

present work. A considerable number of additional states are suggested at higher energies. Two of these higher states appear to be good candidates for members of a 3-phonon triplet, in that the cascade gammas to the 2-phonon states are much stronger than corresponding transitions to the 1-phonon first excited state.

The investigation of Hf^{180} is part of a series of experiments on even-Z even-N nuclei which are strongly deformed. The results are similar to those obtained in an earlier study of Hf^{178}. A group of strong lines are observed between 0.9 and 1.5 MeV. These can be interpreted as gamma transitions from excited-state rotational bands. Although the analysis is not complete, it appears possible to correlate some of the excited-state rotational bands observed in Hf^{180} with those observed in Hf^{178}. The strong enhancement of the low-energy (< 200 keV) gamma transitions between levels of the excited-state bands is also similar to the results found in Hf^{178}.

The experiment on $U^{238}(n,\gamma)U^{239}$ experienced trouble with warpage of the source and a consequent deterioration of the line shape of the gamma diffraction pattern. This experiment will be repeated.

The experiment on $Sm^{152}(n,\gamma)Sm^{153}$ is mainly a clean-up experiment designed to fix the identification of a number of weak gamma rays observed previously and assigned to the level scheme of either Sm^{152} or Sm^{153}. The identification of these gamma transitions is important because, when combined with the results of Coulomb-excitation measurements, the capture γ-ray data may enable one to obtain values of B(E2) for transitions between members of two rotational bands of excited states in Sm^{152}. In combination with the results of $Sm^{152}(d,p)Sm^{153}$ measurements being made with the magnetic spectrograph at the tandem Van de Graaff, the gamma-ray spectra associated with the level scheme of Sm^{153} will also be used to construct a level scheme for Sm^{153}. No information concerning

this level scheme is available at present.

(2) Angular-Correlation Measurements

To supplement the information obtained in precision measurements with the bent-crystal spectrometer, a series of experiments have been performed on the γ-γ angular correlation of the low-energy gamma rays (below 2 MeV) emitted following thermal-neutron capture. The reactions $Sm^{149}(n,\gamma)Sm^{150}$ and $Cd^{113}(n,\gamma)Cd^{114}$ were studied during the year. A relatively thin sample (40 mg/cm^2) of highly enriched material was used in both cases. The γ rays were detected with large NaI scintillators. The pulse-height data were stored and analyzed with the Argonne 3-parameter analyzer. An example of the results is given in Fig. I-1-e. Spin assignments obtained from the

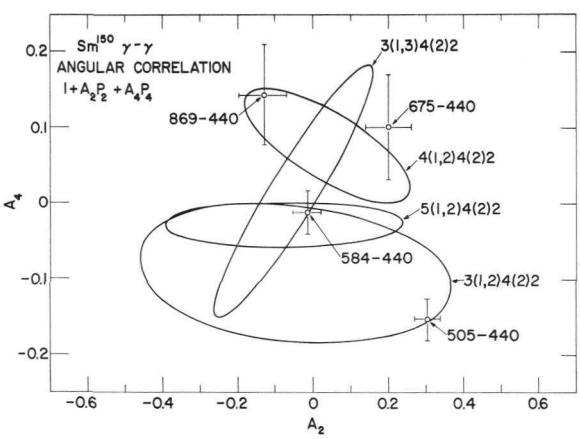

Fig. I-1-e. Angular correlation results for Sm^{150}. The ellipses give the possible theoretical values of the Legendre polynomial coefficients A_2 and A_4 when one transition has various admixtures of E1 and M2 or M1 and E2 radiation and the other gamma ray is a pure E2 transition from the first 4^+ state to the first 2^+ state (Fig. I-1-f). The experimental results are shown as crosses.

angular-correlation data were combined with the gamma-ray energies and intensities obtained with the bent-crystal spectrometer and with the internal-conversion coefficients measured in Germany and Russia to form a decay scheme for Sm^{150}. This decay scheme (Fig. I-1-f) is unusually complete.

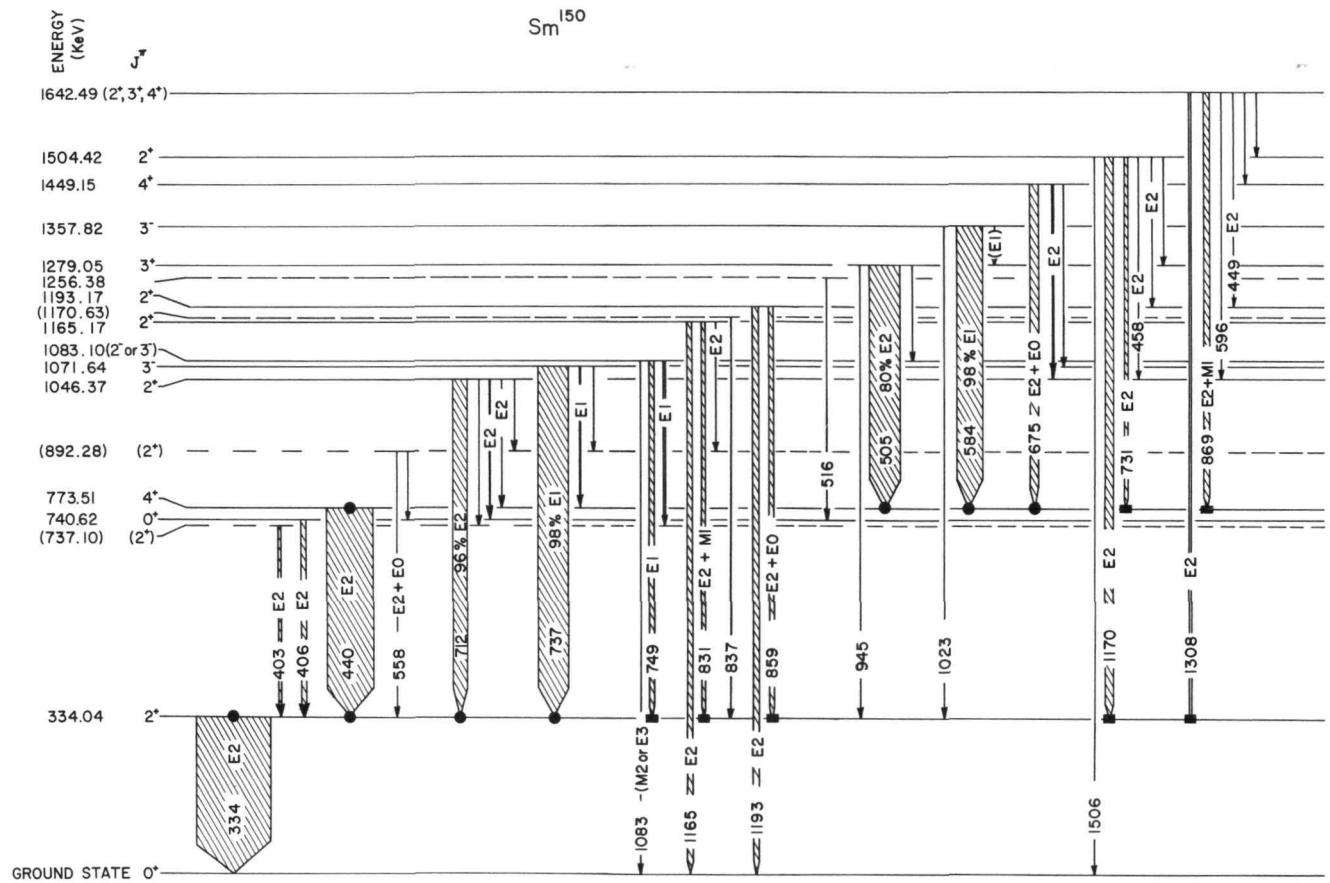

Fig. I-1-f. The level scheme of Sm^{150} as derived from thermal-neutron-capture gamma-ray studies. The excitation energies, which appear at the left in keV, are derived from the bent-crystal experiments. The intensities of the gamma transitions are represented by the widths of the lines. The gamma rays which were analyzed in the γ-γ angular correlation work to obtain spins and parities of the levels are indicated by the filled circles. The labels "80% E2, 98% E1, etc." on the gamma transitions refer to the multipole admixture of the gamma transition as derived from the γ-γ angular-correlation work and the conversion-electron work. The squares indicate γ-γ coincidence experiments.

(3) Modification of the Bent-Crystal Spectrometer

Major modifications now in progress are expected to improve the resolution, the counting rate, and the operational efficiency of the bent-crystal spectrometer. (1) A new quartz crystal 2 mm thick is being acquired. This is half the thickness of the present crystal. Measurements indicate that the change will reduce the line width to 60% of its present value with only a 30% loss in intensity. The thinner crystal is ideally suited for the low-energy part of the spectrum, where absorption in the quartz is appreciable. (2) An array of three Ge crystals is being acquired. The higher Z of Ge is expected to give a 10-fold increase in the counting rate at high energies (1 MeV—4 MeV). The Ge crystals will be used in second- and third-order diffraction to resolve gamma rays up to 6 MeV. (3) A new set of collimators is being built. The new design is expected to increase the counting rate at least 10-fold at low energies. (4) A new source-handling system is being built. It will allow samples to be changed during a 1-hr shutdown of the reactor, as compared with the several days that are now required. The greater convenience of the new system should make the spectrometer a much more effective research tool.

The combination of the thinner quartz cyrstal and the Ge crystal in the diffraction spectrometer and a Ge diode spectrometer (see below) will allow the whole capture gamma-ray spectrum to be examined with a resolution width of 0.2% (FWHM) or better.

(4) Ge Diode Gamma-Ray Spectrometer

An effort to use a lithium-drifted Ge diode detector to analyze neutron-capture gamma-ray spectra has been initiated in a new program. Many different kinds of experiments are planned.

The Ge diode for the detection system being assembled (all

components are on hand) was made by H. Mann of the Argonne Electronics Division. The Ge detector will be mounted within an annulus formed of four independent NaI scintillators. In this configuration the system can be used as a highly efficient annihilation pair spectrometer for the investigation of high-energy gamma rays (2 to 10 MeV) and also as a spectrometer with an anticoincidence ring (to reject scattered radiation) for the investigation of the low-energy portion of the spectrum. Since the resolution of the Ge diode detector is comparable to or better than any other instrument now used for the study of gamma rays with energies above 2 MeV and since its efficiency is much higher than that of other precision instruments, the new detector is expected to revolutionize many measurements on the neutron-capture gamma rays.

I - 1.7. Gamma Rays from Capture of Monoenergetic Neutrons (Project I-55)

S. Raboy and C. C. Trail

The gamma-ray spectra from capture of 0.01-eV neutrons by separated isotopes of Ca^{48}, Ca^{44}, and Ca^{42} have been observed with two anticoincidence NaI scintillation spectrometers.[1] Pulses from the spectrometers are fed into a 2D pulse-height analysis system which gives the coincidence spectra.[2]

In the case of capture by Ca^{48}, one sees the 5.1-MeV gamma rays corresponding to the full-energy jump to the ground state of Ca^{49} and two gamma rays corresponding to the cascade through the first excited state at 2 MeV. Other gamma-ray transitions are quite weak. These results are consistent with a shell-model interpretation of Ca^{49} as consisting of a Ca^{48}

---

[1] C. C. Trail and S. Raboy, Rev. Scti. Instr. 30, 425 (1959.

[2] M. G. Strauss, Rev. Sci. Instr. 34, 1248 (1963), and private communication.

core plus a nucleon in the $p_{3/2}$ shell for the ground state and $p_{1/2}$ shell for the first excited state.

The spectra obtained from capture by both Ca^{42} and Ca^{44} are much more complicated and cannot be interpreted as simply as that from Ca^{48}. One interesting result from the Ca^{42} data has been the indication that the previously reported capture cross section[3] for this isotope must be too large by at least a factor of 10. The earlier result could be explained by a Ca^{43} contaminant in the Ca^{42} sample if the Ca^{43} has a very large capture cross section. We have obtained a Ca^{43} sample for study.

---

[3] H. Pomerance, Phys. Rev. 88, 412 (1953).

I - 2. RESEARCH AT THE 4.5-MEV VAN DE GRAAFF ACCELERATOR

The experimental program with the 4.5-MeV Van de Graaff accelerator is continuing along much the same lines as in previous years. Experiments with fast neutrons are emphasized, especially measurements of the polarization of scattered neutrons. Other experiments include pulsed-beam measurements of the lifetimes of excited states, studies of Coulomb excitation by heavy ions, studies of nuclear reactions induced by charged particles, and measurements of total neutron cross sections. A continuing program is directed toward the improvement of the accelerator.

I - 2.1. Operation of the 4.5-MeV Van de Graaff Accelerator (Project I-11)

J. R. Wallace

The 4.5-MeV Van de Graaff accelerator has operated approximately 2500 hr from June 1963 to April 1964. It is currently operating on an 80-hr/week schedule.

Approximately 20 scientists have used this accelerator for research in the past year.

The long-range program[1] to increase the beam current of this accelerator and to improve the energy stability has continued. The machine has been moved and beam-steering equipment has been installed. The accelerator now has additional shielding, namely a roof above the machine and a shield wall between the output end of the tank and the beam-switching magnet.

It has been requested that a new chilled-water line and return lines should be brought to the accelerator area and that a complete water-cooling system for the accelerator and its accessories should be installed to replace the inadequate system that now exists.

---

[1] Physics Division Annual Review, ANL-6720 (June 1963).

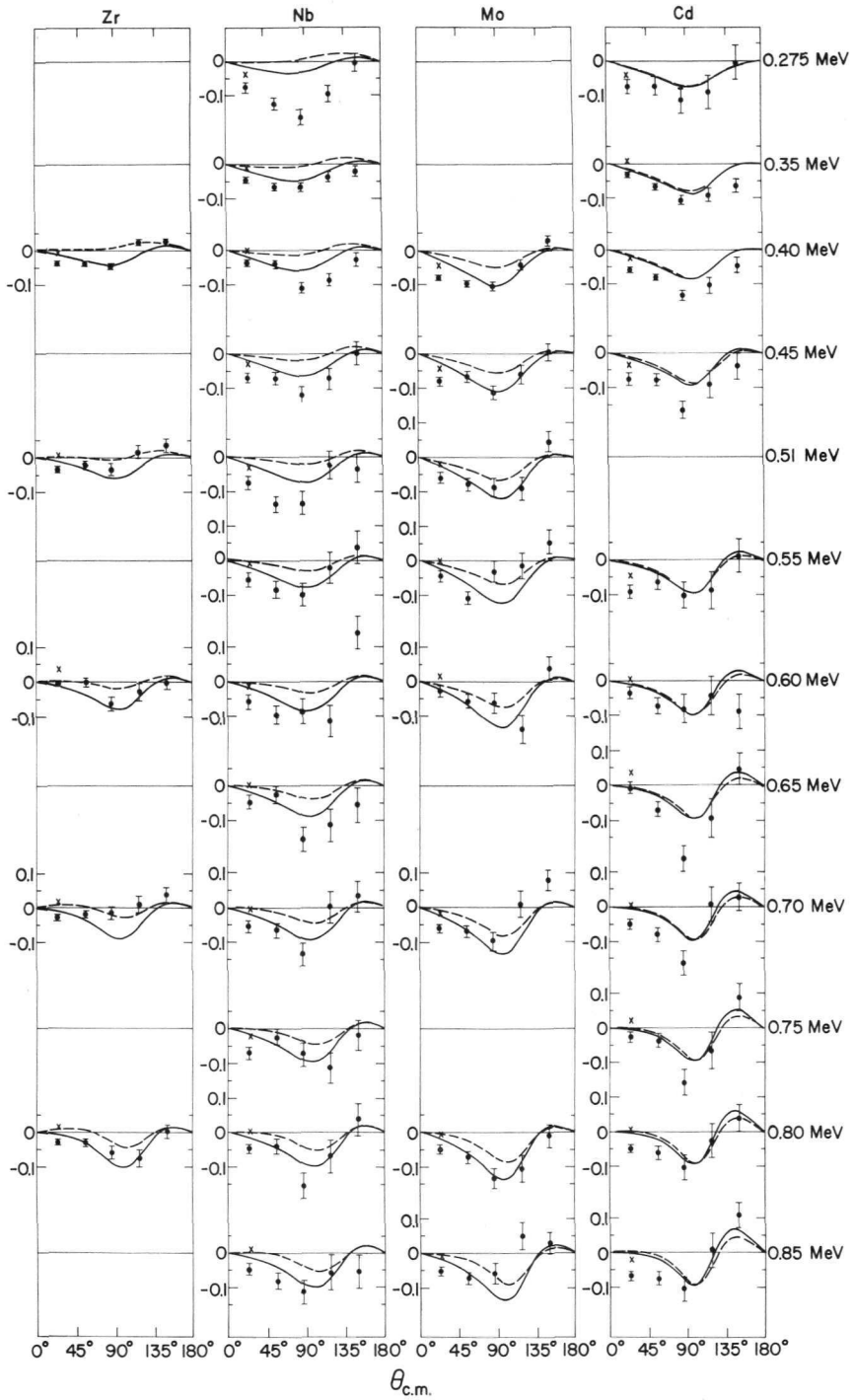

Fig. I-2-a. The angular dependence of the polarization $P_2(\theta)$ for each incident-neutron energy for Zr, Nb, Mo, and Cd. The solid curves are the predictions of the equivalent local optical model except that both a real and imaginary spin-orbit potential are employed with $V_S = 10$ MeV and $W_S = 4$ MeV. The dashed curve differs only in setting $W_S = 0$. The data points for Zr have been obtained by numerically averaging the actual data over a larger energy interval.

I - 2.2. Neutron Polarization and Differential Cross Section (Project I-18)

A. J. Elwyn, R. O. Lane, A. Langsdorf, Jr., and J. E. Monahan

We are continuing our studies of the polarization and differential cross sections for neutrons scattered from various nuclei. In these measurements, the polarized neutrons are produced in the $Li^7(p,n)Be^7$ reaction. Those selected for use are emitted at 51° to the beam direction. The neutron spins can be turned 180° by a beam-precessing electromagnet. After scattering, the neutrons are detected by banks of oil-moderated BF_3 counters enclosed in large shielding tanks. With this system we are able to measure both differential cross sections and polarization at five angles simultaneously.

(1) Optical-Model Studies of Neutron Scattering from Nuclei Near A = 100 at Energies Below 1 MeV[1]

A. J. Elwyn, J. E. Monahan, R. O. Lane, and A. Langsdorf, Jr.

The polarizations and differential cross sections for neutrons scattered from Zr, Nb, Mo, and Cd have been measured at five angles for incident neutron energies between 0.275 and 0.85 MeV. The experiment was carried out in the belief that a systematic investigation would lead to a more consistent interpretation of neutron-scattering data in terms of an optical model at energies below 1 MeV.

The results have been analyzed in terms of an optical model equivalent to the nonlocal model of Perey and Buck.[2] The analysis leads to the following conclusions: (a) While the measured differential cross sections can be fitted satisfactorily when a real spin-orbit potential $V_S = 10$ MeV is employed, consistency with both differential cross sections and polarization can be obtained within the framework of this particular optical model only by using a spin-orbit potential that includes both a

---

[1] A. J. Elwyn, R. O. Lane, A. Langsdorf, Jr., and J. E. Monahan, Phys. Rev. 133, B80 (1964).

[2] F. Perey and B. Buck, Nucl. Phys. 32, 353 (1962).

real term and a small imaginary term W_S of the Thomas type (Fig. I-2-a). (b) The magnitude and shape of the peak of the p-wave neutron strength function in the region near A = 100 are insensitive to the values chosen for the spin-orbit potential, at least for $7.2 \leq V_S \leq 20$ MeV and $0 \leq W_S \leq 7.2$ MeV. Therefore, for the model used, the reported splitting of the 3p strength-function peak cannot be interpreted in terms of a spin-orbit force alone.

(2) The Observation of Structure in the Neutron Scattering from Nuclei near A = 20[1]

A. J. Elwyn, J. E. Monahan, R. O. Lane, and A. Langsdorf, Jr.

The polarization and differential cross sections for neutrons scattered from F, Na, Mg, Al, and P were measured at five angles at energies between 0.2 and 2.2 MeV, with incident neutron energy spreads of 100—150 keV. Structure, characterized by peaks that are separated in most instances by energy intervals of 300—400 keV and that have widths from 100—200 keV, have been observed (Fig. I-2-b) in the total and differential cross sections and in the polarization for these nuclei.

Calculations based on a diffuse-surface optical model (with surface absorption) are in reasonable agreement with an energy average through the measured total and differential cross sections, but give poorer fits to an average through the measured polarizations. The observed fluctuations cannot be reproduced by any calculations based on an optical-model potential with fixed or slowly varying parameters. An effort is being made to interpret the observed fluctuations in terms of an intermediate structure similar to that proposed by Kerman et al.[2]

---

[1] A. J. Elwyn, J. E. Monahan, R. O. Lane, and A. Langsdorf, Jr., Nucl. Phys. (to be published).

[2] A. K. Kerman, L. S. Rodberg, and J. E. Young, Phys. Rev. Letters 11, 422 (1963).

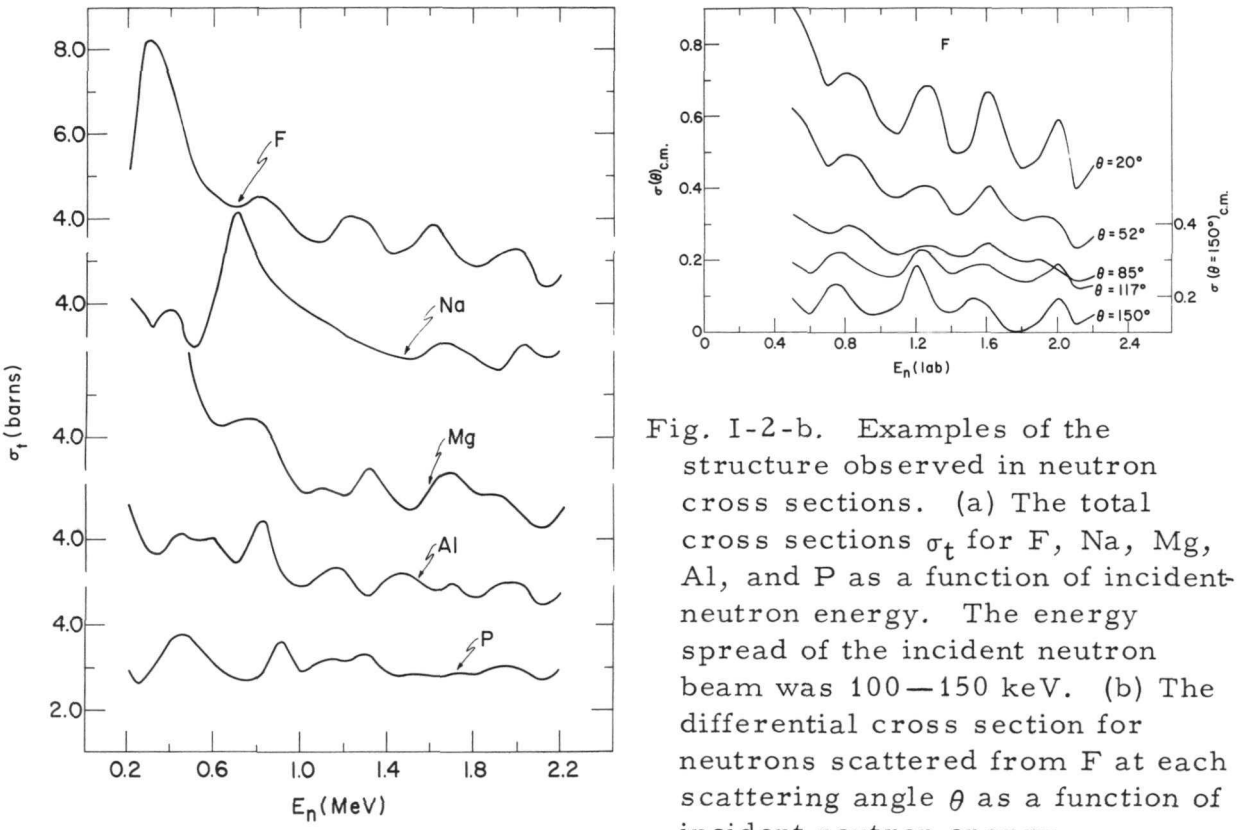

Fig. I-2-b. Examples of the structure observed in neutron cross sections. (a) The total cross sections σ_t for F, Na, Mg, Al, and P as a function of incident-neutron energy. The energy spread of the incident neutron beam was 100—150 keV. (b) The differential cross section for neutrons scattered from F at each scattering angle θ as a function of incident-neutron energy.

(3) The Inclusion of Mott-Schwinger Scattering in Optical-Model Calculations

J. E. Monahan and A. J. Elwyn

A large polarization in small-angle scattering of neutrons from heavy nuclei due to a spin-orbit force of electromagnetic rather than of nuclear origin was predicted by Schwinger. The same effect had been considered earlier by Mott for the scattering of electrons. The nature of this spin-orbit force is conveniently described in the rest system of the neutron. In this system a magnetic field is produced by the Coulomb field of the nucleus moving past the neutron. An interaction $\vec{\mu} \cdot \vec{B}$ arises between this field $\vec{B}$ and the magnetic moment $\vec{\mu}$ of the neutron. Since the direction of $\vec{B}$ is associated with the relative orbital angular momentum vector $\vec{\ell}$, and the magnetic moment $\vec{\mu}$ is associated with the neutron spin $\vec{s}$, the interaction is of the form $\vec{\ell} \cdot \vec{s}$.

Because of the long range of the Coulomb field, the largest effect of this interaction is at small scattering angles. However, the measurements of the polarization of neutrons scattered from Zr, Nb, Mo, and Cd, which are described above, indicated that this interaction may contribute significantly to the polarization at scattering angles as large as 20° to 30°. In order to investigate this possibility, it was necessary to include the $\vec{\mu} \cdot \vec{B}$ interaction in an optical-model potential that included a nuclear interaction of the form $\vec{\ell} \cdot \vec{s}$.

The method used to calculate the polarization in this case is described in Sec. II - 7. For Mott-Schwinger scattering of neutrons, the neglect of higher order terms in the perturbation expansion of the wave function in the intermediate region gives rise to a negligible error in the calculation of the polarization. The inclusion of the $\vec{\mu} \cdot \vec{B}$ potential in the optical-model calculations for neutrons scattered from Zr, Nb, Mo, and Cd indicates that this interaction contributes significantly to the polarization measured at 22°.

(4) Polarization and Differential Cross Section of Neutrons Scattered from Be^9: Parities of the 7.37- and 7.54-MeV States in Be^{10}

R. O. Lane, A. J. Elwyn, and A. Langsdorf, Jr.

Inherent ambiguities in the interpretation of data on differential scattering cross section alone have left the parities of the states in Be^{10} at 7.37 and 7.54 MeV excitation undetermined. To determine these parities, we measured the polarization of neutrons scattered near these resonances in Be^9 + n. This placed an added constraint on the theoretical assumptions. The new information enabled us to make the assignment $J^{\pi} = 3^-$, $\ell = 2$ for the state at 7.37 MeV and $J^{\pi} = 2^+$, $\ell = 1$ for the one at 7.54 MeV.[1]

---

[1] R. O. Lane, A. J. Elwyn, and A. Langsdorf, Jr., Phys. Rev. 133, B409 (1964).

(5) Polarization and Differential Cross Section for Neutrons Scattered from Li^6 and Li^7

R. O. Lane, A. J. Elwyn, and A. Langsdorf, Jr.

The understanding of the interaction of neutrons with Li^6 and Li^7 has been very limited in the past. In an effort to shed new light on these interactions, polarizations of the scattered neutrons were measured for neutron energies of 0.1 to 2.0 MeV. Surprisingly, at the higher energies (not measured previously) both nuclides exhibit sizable polarizations of the same form, $P(\theta) \approx -0.3 \sin 2\theta$. The interpretation of the data for Li^6 is complicated by the presence of a large (n, α) cross section. Extensive calculations were carried out on the CDC-3600 computer in an attempt to understand both the polarization and differential cross sections for Li in terms of states in Li^8 and alternatively in terms of phase shifts. The calculations show that the dominant features of the data can be represented by the known 3^+ ($\ell = 1$) resonance at $E_n = 0.25$ MeV, a broad hypothetical 2^- ($\ell = 0$) resonance at high energy, and a slowly varying phase shift of the character 3^- ($\ell = 2$). No known model at present predicts 2^- and 3^- states in this region. Preliminary calculations based on the optical model indicate that some of the main features of these data can also be reproduced for certain values of the parameters. Since the assumptions of the two models are fundamentally different, the calculations point up the degree of ambiguity still remaining in our understanding of the interaction.

(6) Triple-Interaction Experiment to Determine the Polarization of Neutrons

R. O. Lane, A. J. Elwyn, and A. Langsdorf, Jr.

In triple scattering the first interaction produces a polarized beam, the second acts on that polarization, and the third analyzes the effect of the second interaction. The polarization parameters that are necessary

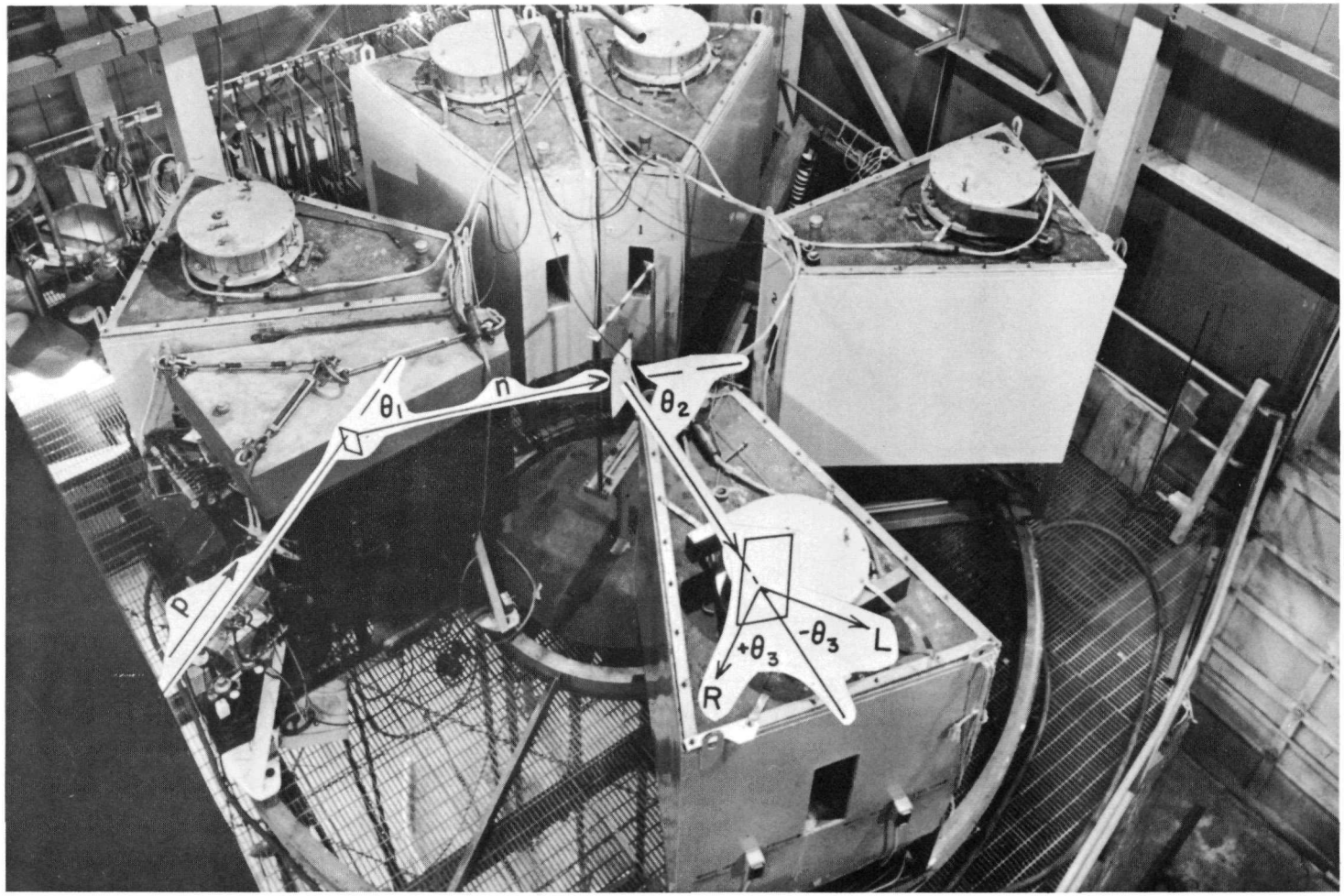

Fig. I-2-c. Triple-interaction experiment as adapted from the older double-interaction apparatus. Protons from the 4.5-MeV Van de Graaff accelerator produce a polarized neutron beam in the first interaction, a $Li^7(p,n)Be^7$ reaction. These neutrons scatter from targets of various materials (second interaction) into the collimators of the large trapezoidal tanks where they are again scattered (third interaction) from an analyzer. From the asymmetry in the intensities scattered to the right (R) and left (L), together with the polarization produced in each interaction, the Wolfenstein parameter D can be calculated for the nuclide in the second interaction.

to describe such triple scattering for neutrons determine all elements of the scattering matrix to within a phase factor. Thus triple-scattering measurements should remove the ambiguities inherent in the interpretation of differential-cross-section and polarization data described above. Exploratory measurements now underway utilize the existing 4.5-MeV Van de Graaff accelerator with polarized neutron beams being (a) produced in the $Li^7(p,n)Be^7$ reaction, (b) scattered from various nuclei, and (c) analyzed by scatterers of known polarizing power (Fig. I-2-c). These measurements, all done in the same plane, will measure the Wolfenstein "D parameter." This type of experiment has not yet been reported at these energies. The major problem is the low intensity implicit in the requirement of three successive interactions. We hope that the statistical accuracy attainable with our present apparatus will be sufficient for useful exploratory measurements. It is clear, however, that accurate results will require an accelerator capable of delivering a much larger beam than can be obtained from the present 4.5-MeV Van de Graaff.

I - 2.3. Ratio Method for the Measurement of Neutron Cross Sections (Project I-102)

A. Langsdorf, Jr.

An article prepared for publication describes high-resolution measurements of the total cross sections of Fe, Al, and F (as Teflon, CF_2) by a method not previously exploited for this purpose. The primary aim of the method is to minimize the statistical and systematic errors most likely to obscure true structure or to introduce spurious structure in the cross section measured as a function of neutron energy. The basic idea of the method is to use two neutron counters in a simultaneous measurement of the neutrons scattered by the sample and those transmitted through it. Another counter that monitors the flux enables the experimenter to

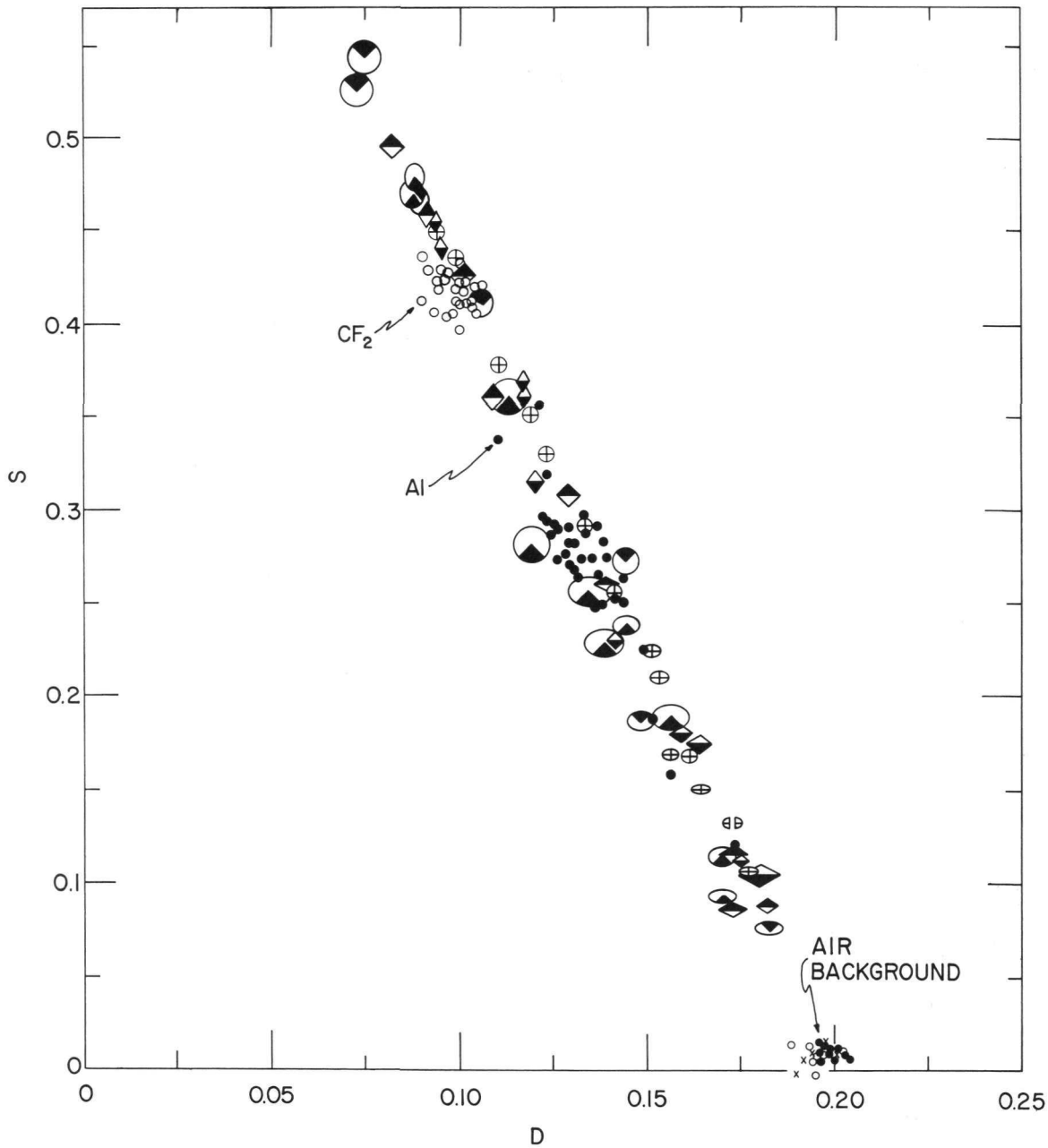

Fig. I-2-d. Plot illustrating the linear relation between S and D, the normalized net counts due respectively to scattered and transmitted neutrons. The neutrons were produced in a Li(p,n) reaction. Both the detector and the monitor used for normalization were set at 120° to the proton beam. Small open circles: teflon sample (CF_2). Small closed circles: aluminum sample (except cluster marked "air background," all taken with no sample). Other symbols: different runs on Fe; the dimensions measure the standard deviations due only to statistical errors of counting. The data were taken at various neutron energies from 130 to 160 keV and an energy spread of about 1.5 keV.

normalize to a fixed flux incident on the sample. In the absence of appreciable capture and after the data are normalized, the graph of scattered counts C_s against transmitted counts C_t is a straight line (Fig. I-2-d). When the background is negligible or corrected for, the neutron transmission T is given by the simple relation $1/T = 1 + r(C_s/C_t)$, where r is the slope of the plot of C_s vs C_t. Among the advantages of the method are that (1) T is determined by simultaneous instead of sequential measurements so drifts are less harmful, (2) it is more accurate than the conventional method when $C_s \approx C_t$, (3) for suitably chosen thin samples, the thickness does not have to be changed between resonance and off-resonance regions, (4) it can serve as a sensitive device to monitor the neutron energy or to reset on a given energy, and (5) it can be readily adapted to permit reliable self-indication studies.

I - 2.4. Unbound Nuclear Levels in the keV Region

Carl Hibdon

The study of unbound levels in light nuclei has been continued. The neutron total cross section of F^{19} was measured at neutron energies up to 300 keV and the results were published.[1] Some 56 peaks were observed; many of them are small so that their existence is difficult to establish. Most of the peaks appear to be due to neutron interactions with $\ell > 0$. However, no analysis of the peaks above about 120 keV is feasible because of the sizable amount of inelastic scattering which is known to be present. The amount of this scattering must be known for each peak if any analysis is to be meaningful. Considerable time was spent in checking the cluster of levels near 100 keV, which still persists as a cluster. Further checking in the region of 100—245 keV confirmed

[1] C. T. Hibdon, Phys. Rev. 133, B353 (1964).

the presence of the peaks observed previously.

A recheck of the clusters of levels in aluminum at neutron energies of 80—90 keV and 130—170 keV confirmed earlier results. Recent work in another laboratory shows similar patterns.

A study of the level structure of Li^6 and Li^7 in the keV region has been continued. Further work is planned on these nuclei.

I - 2.5. The Interaction of B^{11} with 0.5—4-MeV Protons

R. G. Allas, S. S. Hanna,* and R. E. Segel

The radiations from the various exit channels (namely elastically scattered protons, gamma rays following inelastic scattering, capture gamma rays, neutrons, and alpha particles) have been examined. Comparison of the neutron and alpha-particle yields reveals a fairly good separation of the two isotopic-spin states. The differential cross section for radiative capture indicates that the strength of the s-wave contribution to the giant-dipole resonance is carried mainly by two states which are at energies of 17.3 and 19.2 MeV. A threshold effect is seen in the alpha-particle angular distributions as the neutron channel opens.

---

*Now at Stanford University.

I - 2.6. Elastic Scattering of Protons by Mg^{26}

M. C. Mertz and J. P. Schiffer

During the past two years, differential cross sections for elastic scattering of 0.85—4.58-MeV protons by Mg^{26} have been measured, mostly at the 4.5-MeV Van de Graaff, and have been analyzed by use of dispersion theory. The ℓ values of 59 of the 73 levels seen up to 3.5 MeV

were assigned, and in some cases the values of J were determined as well. Negative-parity states are strongest, as would be expected from the shell model. One broad positive-parity state is seen. The report on this work is nearly complete.

I - 2.7. Studies of Corona Current

A. Langsdorf, Jr., and R. Wehrle

This study of the corona current i as a function of the voltage V was begun in the hope of raising the operating voltage of the Van de Graaff accelerator and improving its operation, but is of considerable fundamental interest in its own right. We have found that plots of $\sqrt{i}$ vs V have an ubiquitous tendency to be nearly linear over a considerable part of their length. A survey of an appreciable fraction of the approximately 1000 articles on this subject published in widely dispersed journals over a 70-year period uncovered a few curves previously plotted this way; and several theoretical studies suggest strong reasons for such behavior—but there seems to have been no general appreciation of this ubiquity of the linear relation nor of its usefulness.

We have performed a series of experiments and have systematically plotted the data as $\sqrt{i}$ vs V. Even the deviations from linearity help suggest explanations for the often very complex behavior of such systems. For example (Fig. I-2-e), when the wire is positive, moisture does not influence the position or slope of the straight portion of the curve for CO_2; but for a negative wire, there is no straight portion when the CO_2 is dry but one appears when moisture is added. Apparently the water vapor captures a substantial number of electrons and thereby leads to a slow-moving cloud of negative ions whose space charge limits the current. These results merely typify a large body of data obtained in this continuing experiment.

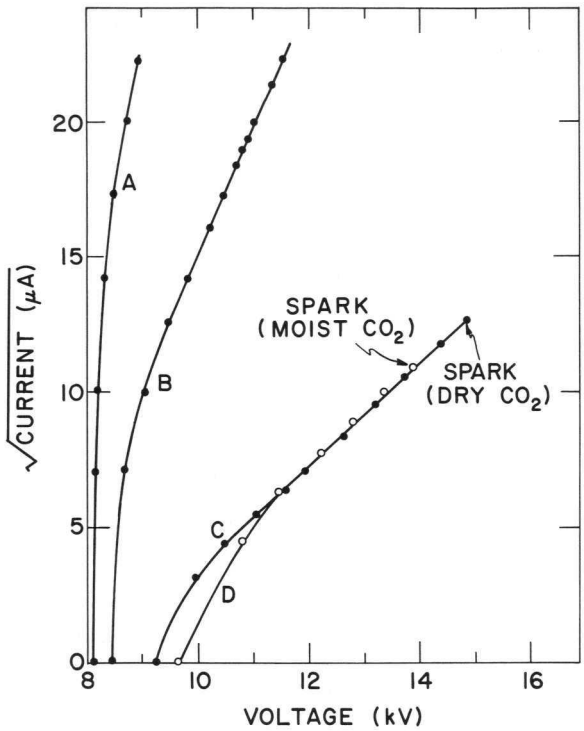

Fig. I-2-e. Corona current-voltage relation plotted as $\sqrt{i}$ vs V. The gas is CO_2 at a pressure of 1 atm. The corona is between a platinum wire of 0.016-in. diameter and a concentric cylinder 1 in. in diameter by 1.25 in. long, with a guard tube at each end. Curves A and B are for the wire negative, curves C and D for the wire positive. Curves A and C are for dry CO_2, curves B and D for CO_2 humidified by passage over water at 15°C.

I - 3. RESEARCH AT THE 12-MEV TANDEM VAN DE GRAAFF

The experimental research program on the tandem Van de Graaff has proceeded at a vigorous pace. Operation is now on a 152-hr/week schedule; continuous operation is planned in the near future. In addition to use by the Physics Division, the tandem facility is regularly used by members of the Chemistry Division and the Solid State Science Division. A program formally initiated in January 1964 makes the tandem available to qualified users from outside Argonne. Four groups from universities are now conducting experiments with this facility.

During the past year, all major pieces of apparatus planned for the initial phase at the tandem have come into operation. The broad-range magnetic spectrograph is now used for about 20% of the experimental program. The pulsed beam has been used for studies of (d,n) reactions and for the measurement of lifetimes of nuclear states. The scattering chambers and γ-ray angular-correlation apparatus are in routine operation. The ASI-2100 computer has been installed and is now in use for on-line operation with both the tandem and the 4.5-MeV Van de Graaff. This computer has a communication link with the CDC-3600 computer, whose capacity and speed can now be utilized for on-line experiments.

I - 3.1. Installation and Operation of the Tandem Van de Graaff Accelerator (Project I-10)

J. R. Wallace

The tandem has operated 4426 hours from June 1963 to April 1964. To date the tandem has 9413 hours of operation. At the present time the tandem is scheduled for 152 hours/week. There are plans to go to a full time operational schedule of 24 hr/day, 7 days/week. The main endeavor of the operational group has been to modify or improve the tandem and at the same time maintain a good operational schedule for the scientists doing research on the accelerator.

The major items of experimental equipment that have been completed and were in use during this past year at the tandem are: (1) an 18-in. scattering chamber, (2) angular-correlation equipment, (3) a beam

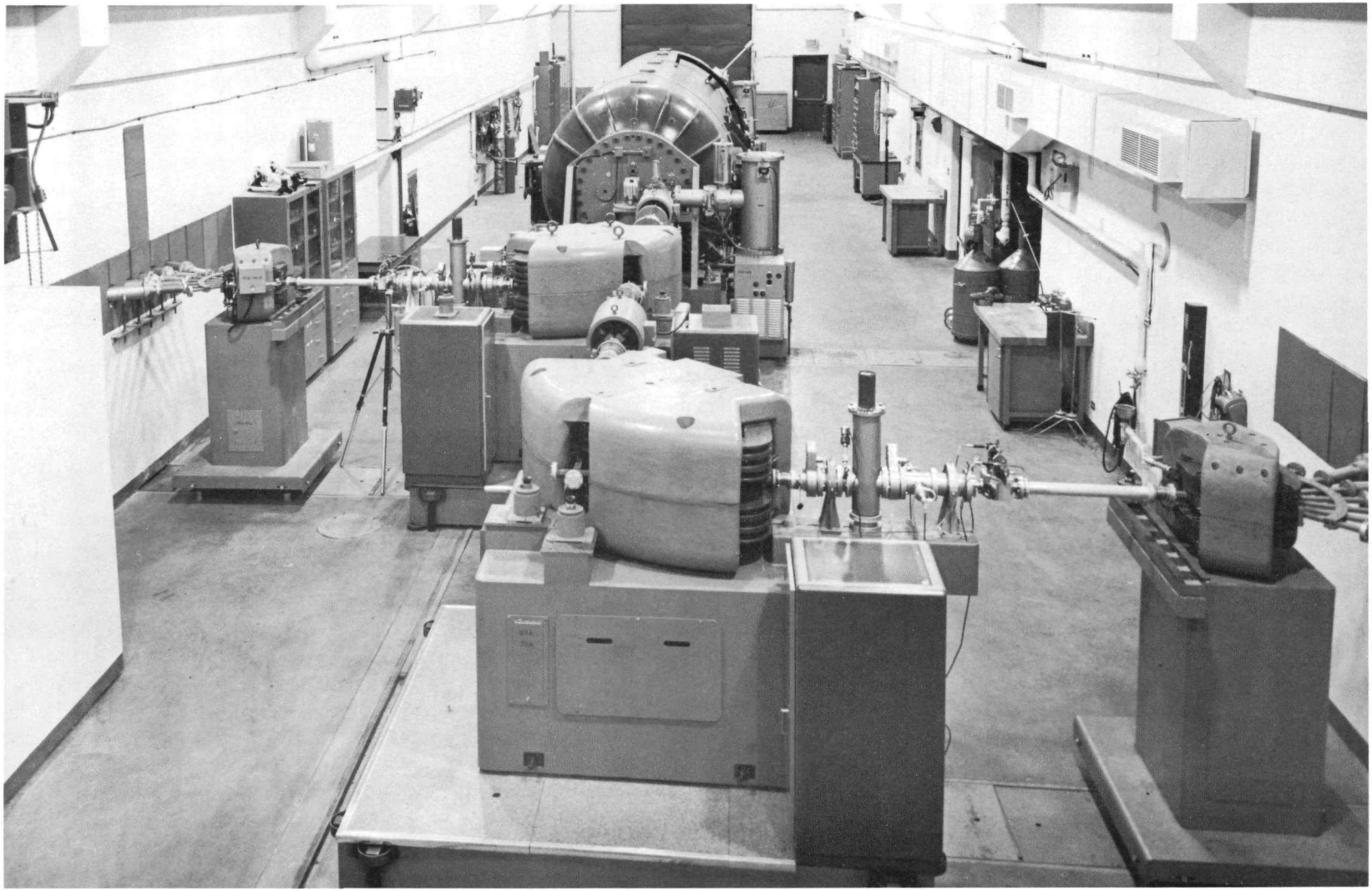

Fig. I-3-a. The Argonne 12-MeV tandem Van de Graaff accelerator. The negative ions of H, D, or O (or a focused neutral beam of He) is injected at the far end of the machine. After emerging from the accelerator tank, the high-energy beam is deflected to the west target room (left) or east (right) by the appropriate 90° analyzing magnet (center foreground) and is switched into the selected beam line by the switching magnet placed near the wall of the machine vault.

pulser and buncher, (4) a broad-range magnetic spectrograph, and (5) a 60-in. scattering chamber. A second 18-in. scattering chamber is under construction to serve the needs of the large number of experimenters now using the existing one.

An ASI-2100 computer has been installed. It will be used for multiparameter analysis and on-line data reduction and to feed partially-processed data directly to the CDC-3600 computer.

Plans for the coming year include: (1) further work on ion sources, (2) installation of inclined-field acceleration tubes, (3) installation of a high-transmission beam package from HVEC, (4) a heavy-ion program, and (5) work on a polarized ion source.

I - 3.2. The Physics Division On-Line Computing System

D. S. Gemmell

The PHYsics Division on-Line Information System (PHYLIS) was delivered in January 1964. Acceptance tests are scheduled for June 1964. The PHYLIS system is used for the on-line processing of data obtained in low-energy nuclear physics experiments at both the 4.5-MeV Van de Graaff and the 12-MeV tandem generator (Fig. I-3-b). The central processing unit is an ASI-2100 computer. This is a fast digital machine with a memory of 8192 words and a 21-bit word length. The memory cycle time is 2 μsec. The computer has two buffered input/output channels.

The hardware of the system is distributed into four distinct geographical locations. (1) Central station: central processer, digital plotter, typewriter, line printer, card reader/punch, and two magnetic tapes. (2) Tandem generator: ND-160 analyzer (2 parameters, 4096 channels) and three computer interrupts. (3) 4.5-MeV Van de Graaff: typewriter, card reader, card punch, line printer, and two computer interrupts. (4) CDC-3600: The ASI-2100 is satellited to the CDC-3600 in the Applied Mathematics Division by way of an 800-ft cable.

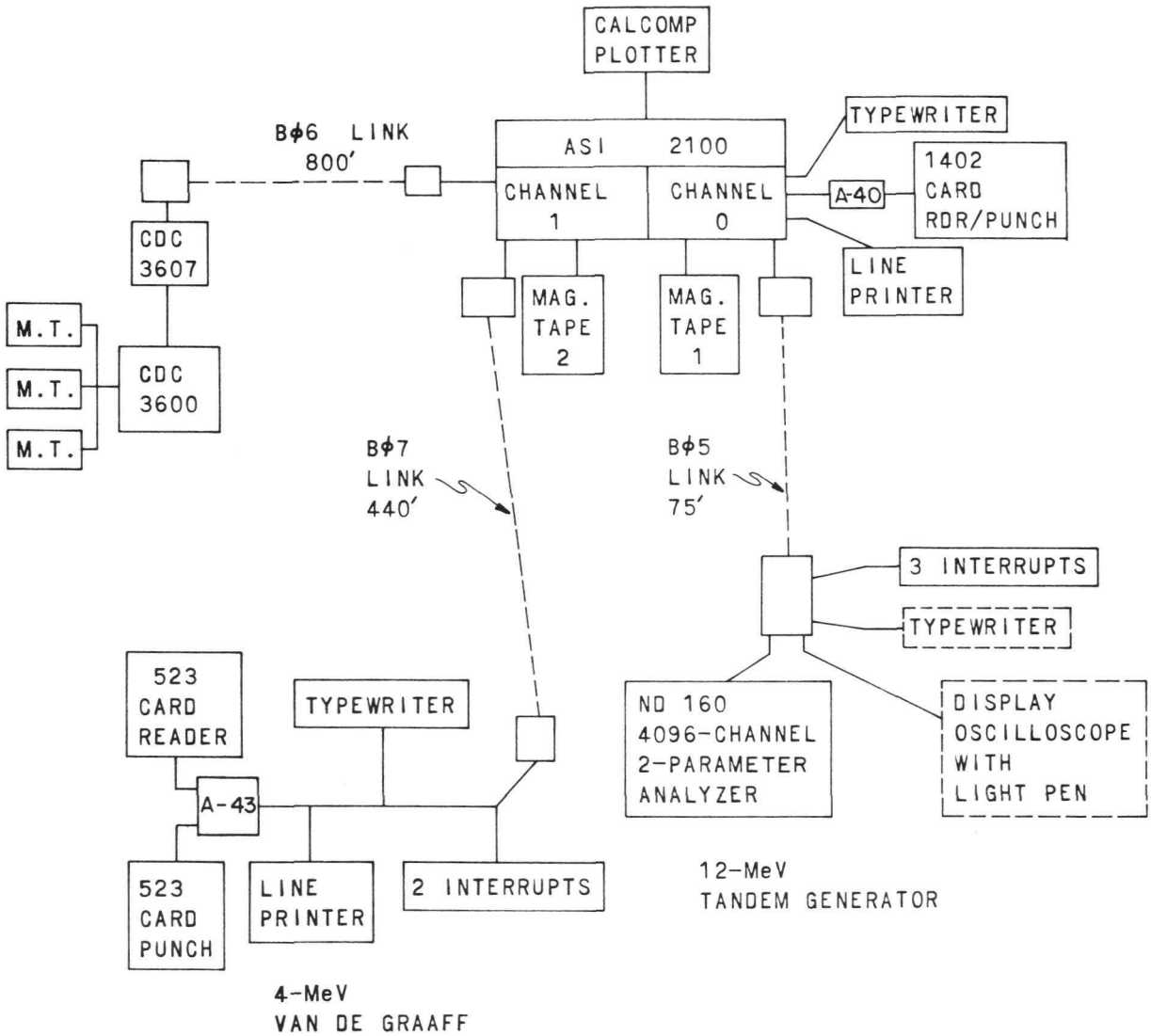

Fig. I-3-b. Block diagram showing how the individual devices making up the PHYLIS system are normally divided among the four experimental areas. (Devices shown as dashed blocks are proposed additions to the system.) Since the two In-Out channels of the ASI-2100 may be operated simultaneously, equipment at two different locations can operate simultaneously. Also, since the devices are connected to the channels in parallel, any equipment on a particular channel can be connected to any other equipment on it; e.g., the printer and 1402 card unit can be moved to the tandem and operated there. Each device depicted has a unique interrupt address which may be either "normal" or "priority." The four instruction addresses associated with the CDC-3600 link (Bϕ-6) are designated "priority" and as such may interrupt any "normal" interrupt routine.

An additional typewriter and an oscilloscope display unit with a light pen facility are scheduled for delivery in July 1964. This extra equipment will be located at the tandem generator.

The program interrupt features of the ASI-2100 and the CDC-3600 make the system very flexible. For example, an experimenter at the 4.5-MeV machine may interrupt the ASI-2100 which, in turn, can interrupt the CDC-3600. The CDC-3600 may then perform some calculation (such as the determination of polarization and cross sections as a function of angle from data taken in a neutron-scattering experiment). These results may then be used immediately to determine what further measurements are necessary.

Another common use of the system is in the recording of 2-parameter data at the tandem generator. Digitized pulses from the dual-ADC unit of the 4096-channel analyzer are transmitted to the ASI-2100 and stored on magnetic tape. When this process is finished the CDC-3600 is interrupted and the events on the tape are transmitted to it for pulse-height analysis into, say, a 256 × 256 array. This array is then transmitted back to the ASI-2100 and stored on the other magnetic-tape unit. In addition to this type of operation, it is also possible to read or write the 4096-channel analyzer memory from the ASI-2100.

There are many other ways in which the system can be used. When not in use on-line, the ASI-2100 is a very useful machine for performing off-line computations.

I - 3.3. Pulsed-Beam Experiments at the Tandem

(1) Pulsed-Beam Apparatus

F. J. Lynch

The beam-pulsing system consisting of a buncher and chopper has been used for neutron time-of-flight experiments [mainly

(d,n) reactions], charged-particle identification by time of flight, background reduction in (p,γ) experiments, and lifetime measurements of nuclear excited states. The system is convenient to use and stable in operation.

For measurements of lifetimes greater than 100 μsec, such as that of the first excited state in Sc^{43}, a slow pulsing system has been constructed. A RIDL multichannel pulse-height analyzer operated in the time mode advances its address at a rate determined by an external timing circuit so that the build-up and decay times are spread over the 400 channels of the analyzer. The voltage across the deflector plates of the beam chopper is reduced to zero for a specified time (corresponding to 2, 4, 8, 16, or 32 channels) during which the beam is allowed to strike the target; then a large voltage deflects the beam away. The analyzer records the induced gamma activity as a function of time. After the last channel is passed, the cycle restarts and a new beam pulse occurs.

A new time-to-pulse-height converter using an Esaki diode as a bistable element has been developed in the Electronics Division and is now in operation. The converter is stable and linear in response and is equally applicable to pulsed-beam and coincidence measurements. All electronic equipment in the energy and time channels now use solid-state elements exclusively.

(2) Pulsed-Beam Measurements of Lifetimes of Nuclear Excited States

R. E. Holland, F. J. Lynch, and K.-E. Nystén*

We have used the recently completed system for pulsing the beam from the tandem accelerator to extend our measurements of the

---

*Permanent address: University of Helsinki.

lifetimes of nuclear states. The higher particle energy available from the tandem allows us to excite states which we could not reach with the 4.0-MeV Van de Graaff.

We have used the pulsed beam to measure lifetimes of nuclear states in the mass region above Ca^{40}. The lifetimes of a number of levels have been measured in Ti^{45} and V^{48}, but the most interesting case involved the first excited states of Sc^{43} at 150 keV. This state was found to have a mean life of 628 ± 10 μsec, about 15 times the single-particle estimate for an M2 transition; such a retardation is to be expected for M2 transitions. The appearance of such a state in a nucleus so near Ca^{40} is surprising. It can be explained as arising from promoting a $d_{3/2}$ proton to the $f_{7/2}$ shell; such states are observed in (p,d) and (d,He^3) reactions. When this "hole" state is the first excited state, it should be metastable. Therefore one should observe other long-lived states. A search in scandium and titanium isotopes has not revealed other such isomers.

(3) Capture γ-Ray Measurements with the Pulsed Beam of the Tandem Generator

D. S. Gemmell and Z. Vager

If one can tolerate average beam currents as low as 50 to 100 mμA, then there are considerable advantages in using pulsed-beam techniques to study radiative-capture reactions. One can discriminate against neutrons from the target and against γ rays and neutrons from all locations other than the target (e.g., from the beam collimator, beam catcher, etc.). In addition, the effective cosmic-ray background is reduced by the duty cycle of the machine. We have developed a technique whereby we can obtain a timing resolution width as small as 2 nsec for 20-MeV γ rays when a 10 × 8-in. NaI(Tl) crystal is used. The technique uses the "cross-over" time for a delay-time clipped pulse. "Pile-up"

events are distinguished because they cause a delay in this cross-over time. We have tested the technique by means of the $B^{11}(p,\gamma)C^{12}$ reaction at E_p = 7 MeV where we observed a much cleaner spectrum than is normal with a dc beam. Initial attempts to observe the (d, γ) reaction with targets of B^{10} and C^{12} were unsuccessful.

(4) Particle Identification by Time-of-Flight Methods

D. S. Gemmell

A time-of-flight technique has been used to discriminate between different masses of particles emitted from nuclear reactions. The particles are detected with a silicon junction counter. A two-parameter pulse-height analyzer is used to record both the energy and the flight time of each particle detected. The Argonne tandem Van de Graaff provides a chopped and bunched incident beam. Pulses from the silicon detector are fed into both a fast (200-Mc/sec band width) amplifier and into a conventional charge-sensitive preamplifier with a slower response. The fast side of the circuit feeds into a time-to-pulse-height converter giving a pulse which is a measure of flight time. An energy pulse is provided by the slower circuitry. The experimental data show a time resolution width of 2 nsec and an energy resolution width of 50 keV for particles with energies between 400 keV and 10 MeV.

The technique has been tested with the reactions B^{10} + d, B^{11} + d, and C^{12} + d at energies up to 12 MeV. With flight paths of 40 cm, an excellent mass separation was achieved. The method should be very useful in the study of reactions with low Q values and of reactions involving the emission of complex nuclei. A systematic study of (d, Li^6) and (d, Li^7) reactions has been initiated.

I - 3.4. Charged-Particle Reactions at the Tandem

(1) Test of the DWBA in (d,p) Reactions

L. L. Lee, Jr., J. P. Schiffer, B. Zeidman, G. R. Satchler,* R. H. Bassel,* and R. M. Drisko*

The measurements of elastic deuteron scattering from Ca and the reaction $Ca^{40}(d,p)Ca^{41}$ are being used as a test of the Distorted-Wave Born-Approximation (DWBA) analysis of (d,p) reactions. Extensive analysis of the elastic scattering indicates that many discrete sets of optical potentials fit the measured differential cross sections (Fig. I-3-c).

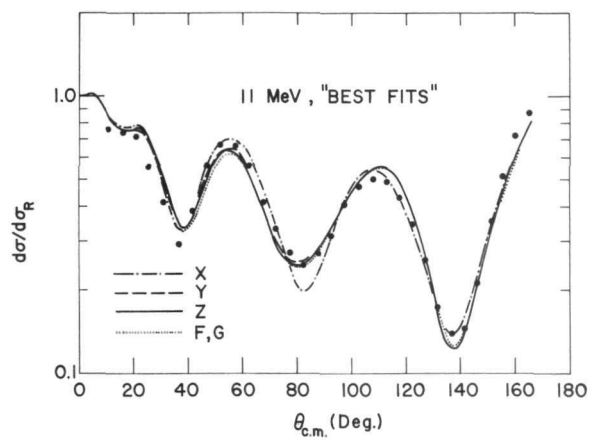

Fig. I-3-c. Comparison of the measured 11-MeV deuteron scattering from Ca with five "best fit" surface-absorption potentials. Parameters for the potentials are listed in Table I-3-A.

In all cases the potential is of the Saxon form with surface derivative absorption. The parameters of the potentials used in the figure are listed in Table I-3-A. The measured (d,p) differential cross sections can be fitted with all of the potentials if a radial cutoff is used in the calculations. However, only the deeper potentials ($V > 100$ MeV) give satisfactory fits without cutoff. Since Ca^{40} is a doubly magic nucleus, the Ca^{41} states observed strongly in the (d,p) reaction should be good single-neutron states for which the spectroscopic factor in the (d,p) reaction is unity.

*Oak Ridge National Laboratory.

TABLE I-3-A. Parameters of the optical-model potential

$$U(r) = -V(e^{x}+1)^{-1} - i\left(W - 4W_D \frac{d}{dx'}\right)(e^{x'}+1)^{-1}$$

used to obtain the theoretical curves plotted in Fig. I-3-c. In this expression, $x = (r - r_0 A^{1/3})/a$ and $x' = (r - r_0' A^{1/3})/a'$.

Potential	V (MeV)	r_0 (F)	a (F)	W (MeV)	W_D (MeV)	r_0' (F)	a' (F)
X	32.5	0.943	0.905	0	5.6	1.703	0.691
Y	72.4	0.936	0.945	0	11.8	1.511	0.542
Z	120.7	0.966	0.846	0	16.4	1.479	0.492
G	176.9	1.002	0.769	0	21.0	1.466	0.453
F	240.0	1.040	0.707	0	26.4	1.462	0.415

While this is not strictly the case, the $Ca^{40}(d,p)Ca^{41}$ reaction can be used to test the ability of the DWBA analysis to extract meaningful spectroscopic factors from the experimental data. The present results indicate that one can obtain spectroscopic factors by DWBA analysis with an accuracy of about 30%.

Measurements of elastic deuteron scattering from Fe^{54} and the reaction $Fe^{54}(d,p)Fe^{55}$ have been made at deuteron energies of 8.0, 10.0, and 12.0 MeV. Analysis of the elastic scattering yields sets of potentials similar to those obtained from the Ca data. Spectroscopic factors extracted from DWBA analysis agree with those obtained elsewhere with 15-MeV deuterons.

(2) Elastic Scattering of Protons and Deuterons from Isotopes of Ca

L. L. Lee, Jr., A. Marinov, and J. P. Schiffer

The scattering of intermediate-energy protons and deuterons from nuclei is usually interpreted in terms of an optical model in which the nucleus is represented by an average potential. It is of considerable interest to determine whether a dependence on the neutron excess of the target should be included in the potential. We have previously reported[1] an investigation of the nickel isotopes in which the need for such a term was demonstrated. To further investigate the importance of a neutron-excess term in the optical potential, we have studied the elastic scattering of 9- and 12-MeV protons and deuterons by Ca^{42}, Ca^{44}, and Ca^{48}. Deuteron scattering from Ca^{40} had already been studied and the excitation function for proton scattering from Ca^{40} showed so much fluctuation with proton energy that analysis in terms of an optical potential does not seem reasonable in this energy range. Analysis of the scattering from Ca^{42}, Ca^{44}, and Ca^{48} is now in progress. Preliminary results indicate the need for a neutron-excess term in the potential, but the evidence is not as striking as it was for the nickel isotopes.

[1] L. L. Lee, Jr., and J. P. Schiffer, Phys. Rev. (25 May 1964).

(3) The $F^{19}(He^3,d)Ne^{20}$ Reaction

L. L. Lee, Jr., and R. H. Siemssen

Angular distributions of deuteron groups from the reaction $F^{19}(He^3,d)Ne^{20}$ leading to the ground state and the six lowest excited states of Ne^{20} have been measured at a bombarding energy of 10 MeV. The transitions to the 5.63-and 5.80-MeV levels have been only partly resolved. Particles were identified with the aid of a solid-state dE/dx counter and a pulse multiplier based on the method of Stokes.[1]

[1] R. H. Stokes, Rev. Sci. Instr. 31, 768 (1960).

The angular distributions of the transitions to the ground state and the levels at 1.63, 5.80, and 6.72 MeV in Ne^{20} show clear stripping patterns. The values of ℓ for proton capture into these states are ℓ = 0, 2, 1, and 0, respectively. The angular distributions of the transitions to the levels at 4.25 and 4.97 MeV are nearly symmetric about 90°. Similarly the transition to the 5.63-MeV level very probably does not show stripping. These results are in agreement with the predictions by Elliot[2] from calculations based on the SU_3 classification scheme. Reduced widths have been extracted with the help of distorted-wave Born-approximation calculations.[3] Agreement between the measured and the calculated angular distributions, however, has not been too good so far. We intend to supplement our results with a measurement of the elastic scattering of He^3 on F^{19} at 10 MeV to obtain the distorting potential of the entrance channel for the DWBA calculation directly from experiment.

---

[2] J. P. Elliot, in Proceedings of the Rutherford Jubilee Conference, edited by J. B. Birks (Heywood and Co., London, 1961), p. 248.

[3] The calculations employed the code TSALLY developed by R. H. Bassel, R. M. Drisko, and G. R. Satchler, Oak Ridge National Laboratory Report ORNL-3240.

(4) Evidence for J Dependence of the Angular Distribution from (d,p) Reactions (Project I-27)

L. L. Lee, Jr., and J. P. Schiffer

A number of recent measurements in this laboratory have been directed toward determinations of the spins of low-lying states formed by ℓ_n = 1 neutron transfer in (d,p) reactions on medium-weight nuclei. Another line of investigation has been the careful study of (d,p) angular distributions on these nuclei. The results of these studies have now led to the discovery of a systematic difference between the ℓ_n = 1 angular

distributions to $J = \frac{3}{2}^-$ and $J = \frac{1}{2}^-$ final states.[1] Heretofore, measurements of (d,p) angular distributions have yielded only the orbital angular momentum transfer ℓ_n but no definite assignment of the total angular momentum J of the final state. Observation of this new effect makes it possible in many cases to assign J directly from the (d,p) angular distribution rather than from the much more difficult and lengthy angular correlation or polarization measurements necessary previously.

The effect observed is illustrated in the (d,p) angular distributions (Fig. I-3-d) from the reaction $Fe^{54}(d,p)Fe^{55}$ to two states in

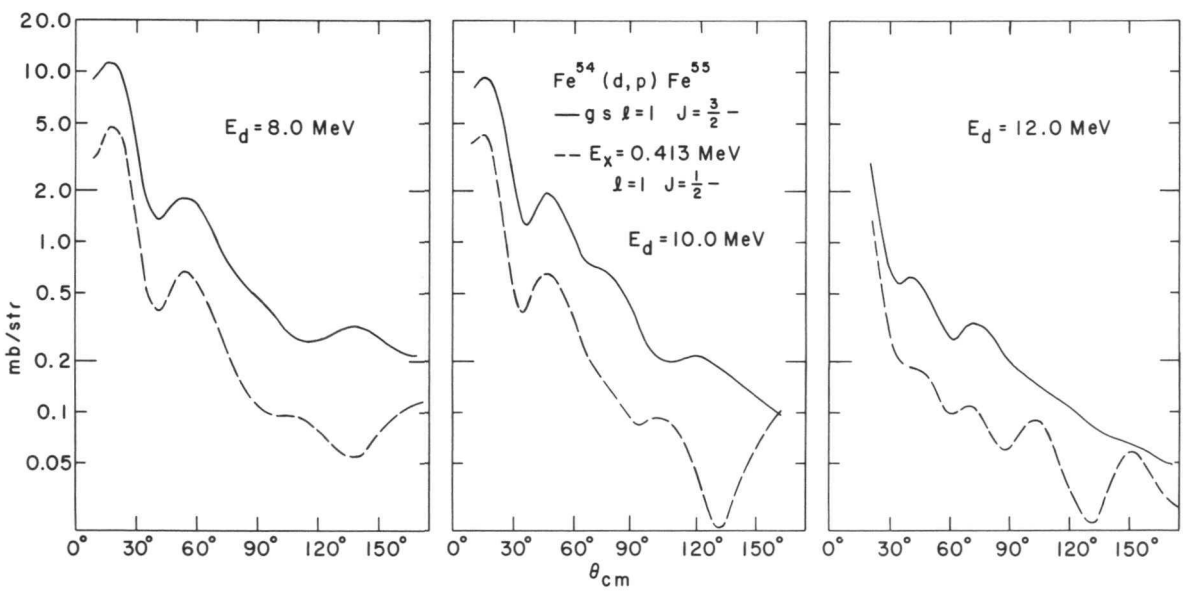

Fig. I-3-d. Measured angular distributions at 8, 10, and 12 MeV for the reaction $Fe^{54}(d,p)Fe^{55}$ leading to the $J = \frac{3}{2}$ ground state and the $J = \frac{1}{2}$ first excited state.

Fe^{55} for deuteron energies of 8.0, 10.0, and 12.0 MeV. The angular distribution for the $\frac{1}{2}^-$ final state shows a sharp dip at about 135° at all of the energies used while the $\frac{3}{2}^-$ group shows no such effect. This effect has been investigated for twenty transitions in targets for which $40 \leq A \leq 62$ and in which the J of the final state has been determined in angular-correlation experiments. In all of these cases the $J = \frac{1}{2}^-$ states have

[1] L. L. Lee, Jr., and J. P. Schiffer, Phys. Rev. Letters 12, 108 (1964).

TABLE I-3-B. Spin assignments based on $\ell_n = 1$ (d,p) angular distributions.

Nuclide	Excitation energy (MeV)	Spin J
Ca^{41}	1.95	3/2 [a]
	2.47	3/2 [a]
	3.95	1/2 [a]
Ca^{43}	2.03	3/2
Ca^{45}	1.43	1/2
	1.90	3/2
	2.25	3/2 [a]
	2.34	3/2
Ca^{49}	0	3/2
	2.03	1/2
Ti^{47}	1.56	3/2
	1.80	1/2
	2.58	1/2
	3.31	3/2
	3.95	3/2
Ti^{49}	1.38	3/2 [a]
	1.72	1/2 [a]
	3.17	1/2
	3.26	3/2
Ti^{51}	0	3/2
	1.16	1/2
	2.13	3/2
Cr^{51}	0.77	3/2 [a]
	1.92	(3/2) [a]
Fe^{55}	0	3/2
	0.41	1/2 [a]
	2.49	3/2 [a]
	3.56	3/2 [a]
	3.80	(3/2)
Fe^{59}	0	3/2
	0.73	3/2
	1.21	1/2
	1.92	(3/2)
Ni^{59}	0	3/2
	0.47	1/2 [a]
	0.89	3/2 [a]
	1.32	1/2 [a]
Ni^{61}	0	3/2
	0.29	1/2 [a]
Ni^{63}	0	1/2
	0.16	3/2 [a]
	0.53	3/2 [a]
	1.01	1/2 [a]
Ni^{65}	0.063	1/2
	0.325	3/2
	0.703	3/2
	1.42	(1/2)

[a] Confirms assignment based on earlier angular-correlation measurements.

shown the sharp dip in the backward direction and the $J = \frac{3}{2}^-$ states have not. This effect can then be used with some confidence as a spectroscopic tool to measure the J values of states formed in $\ell_n = 1$ transitions in (d,p) reactions (Table I-3-B). Considerable work is now being done, both at Argonne and elsewhere, to determine the extent of the J dependence in angular distributions, to understand the effect, and to use it as a spectroscopic tool.

(5) Isobaric Analogue States in Cu^{65}

L. L. Lee, Jr., A. Marinov, and J. P. Schiffer

In recent experiments on the elastic proton scattering from heavy nuclei,[1] sharp resonances in the excitation function of the compound nucleus (the target nucleus T plus a proton) have been interpreted as compound states which are isobaric analogues of the low-lying states in the nucleus T+ neutron. We have observed the excitation of such isobaric analogue states in Cu^{65} formed in elastic proton scattering from Ni^{64}. The excitation functions (Fig. I-3-e) agree with the expected analogue states calculated for a Coulomb-energy difference of 9.246 MeV; all of the expected strong states are observed. Angular momenta and widths calculated from the shapes of the observed resonances also agree very well with predictions. It is evident from the results (Table I-3-C) that the isobaric analogue states retain the energy separation and widths of the low-lying states to a greater degree than previously expected in medium-weight nuclei.[2]

---

[1] J. D. Fox, C. F. Moore, and D. Robson, Phys. Rev. Letters 12, 198 (1964).

[2] L. L. Lee, Jr., A. Marinov, and J. P. Schiffer, Phys. Letters 8, 352 (1964).

TABLE I-3-C. Summary of data on widths and energies.

Excitation[a] energy in Ni^{65} (MeV)	Calculated c.m. proton energy in Cu^{65} (MeV)	Observed c.m. proton in Cu^{65} (MeV)	ℓ[a]	$(2J+1)S$[a]	J[b]	S	Γ_p Calc.[c] (keV)	Γ_p Obs.[d] (keV)
0	3.123		3	1.49	5/2	0.25	0.06	
0.065	3.178	3.185	1	1.23	1/2	0.62	4	5
0.315	3.428	3.471	1	0.17	1/2	0.08	1	1
0.699	3.812	3.841	1	0.62	1/2	0.31	6	(17)
					3/2	0.16	3	5[e]
1.021	4.138		4	8.3	9/2	0.83	0.2	
1.33	4.44		1	0.02	1/2	0.017	0.3	
1.417	4.530	4.463	1	0.14	1/2	0.07	3	
					3/2	0.035	1.4	3[e]
1.603	4.716		2	0.09	5/2	0.015	0.3	
1.779	4.892		1	0.015	1/2	0.008	0.3	
1.919	5.032	5.02	(2)	1.3	5/2	0.22	5	9
2.153	5.266	(~5.3)	(1)	0.1	1/2	0.05	3	
⋮								
2.794	5.907	(~5.9)	2	0.74	5/2	0.15	2	
⋮								
3.401	6.514		0	0.27	1/2	0.13	10	

[a] Excitation energy, orbital angular momentum ℓ, and reduced width $(2J+1)S$, as measured by R. H. Fulmer and A. L. McCarthy, Phys. Rev. 131, 2133 (1963).

[b] J is the assumed total spin.

[c] Calculated from S.

[d] Obtained from the data.

[e] The shape of this resonance suggests a $\frac{3}{2}^-$ rather than $\frac{1}{2}^-$ assignment.

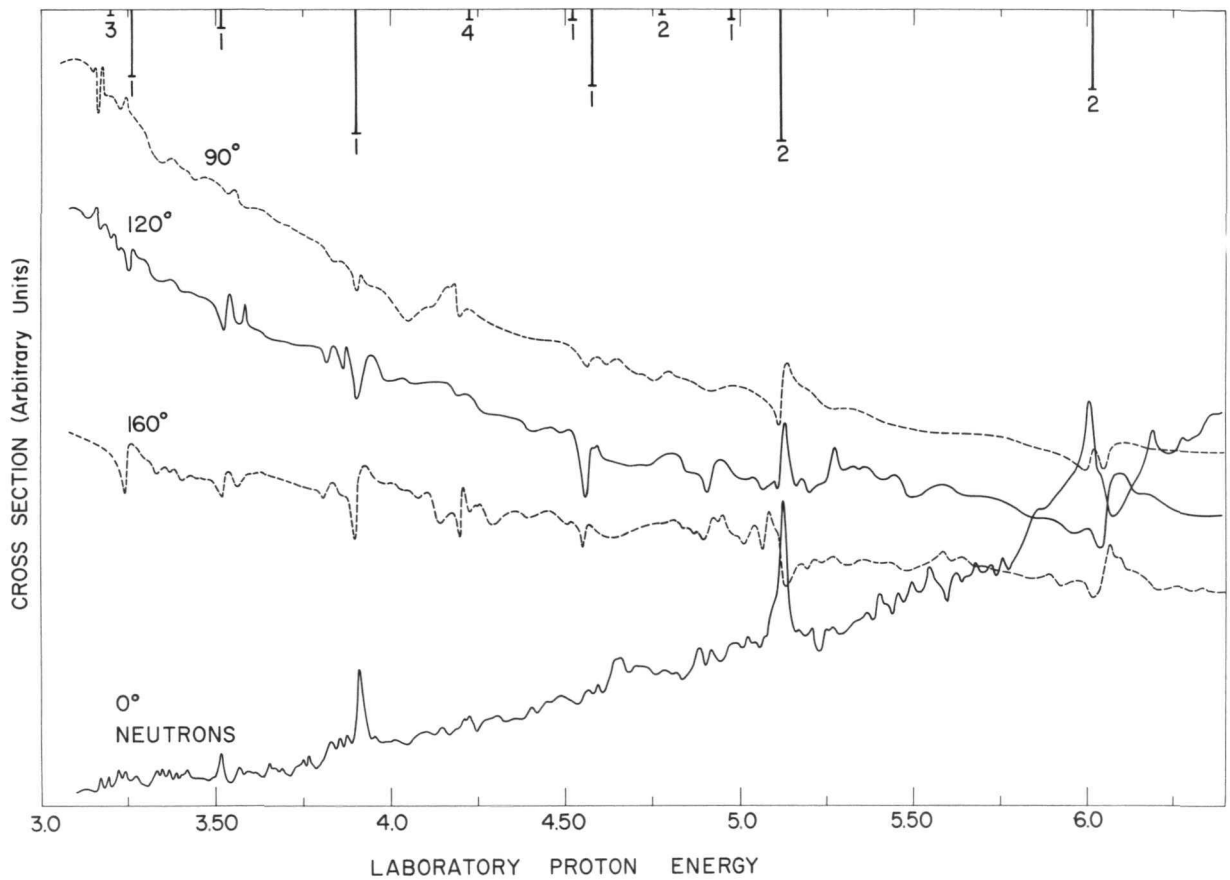

Fig. I-3-e. Measured excitation functions for elastic proton scattering from Ni^{64} and for the $Ni^{64}(p,n)Cu^{64}$ reaction. The vertical lines at the top of the figure indicate the predicted locations of the analogue states.

(6) (He^3, α) Reactions

L. Meyer-Schützmeister and T. H. Braid

In these reactions, studied in the 18-in. scattering chamber at the tandem, a proton is picked up from the target nucleus. They are thus related to the (d, T) reactions performed at the cyclotron. We have started to measure angular distributions and spectroscopic factors in nuclei whose 1f and 2p shells are being filled. First results in Fe^{54} indicate that states are excited with relative intensities quite different from those in (d, T) reactions.

In addition, the reaction (He^3, $\alpha\gamma$) performed on target nuclei with spin zero should offer a nice tool for determining spins in the final nucleus, by measuring the α-γ correlation with the α-particle detector kept fixed at either 0° or 180° to the incoming He^3 beam. Such targets as C^{12}, Mg^{24}, Si^{28}, and Ca^{40} seem to be promising for this reaction.

(7) Isotopic-Spin Selection Rule in the $C^{12}(d, \alpha)B^{10}$ Reaction

R. G. Allas, J. R. Erskine, L. Meyer-Schützmeister, and D. von Ehrenstein

With the ANL tandem, the 18-in. scattering chamber, and the broad-range magnetic spectrograph, we have measured the α-particle group in the $C^{12}(d, \alpha)B^{10}$ reaction which leads to the first T=1 state in B^{10}. No such group should exist if the isotopic-spin selection rule holds. The fact that the cross section $\sigma(T=1)$ of this particular α group is small, only about a hundredth of those leading to the T=0 states in B^{10}, indicates that the isotopic-spin selection rule holds at least partially. Our study showed that $\sigma(T=1)$ decreases by about a factor of 7 as the deuteron energy increases from 8 to 12 MeV. This suggests that possibly the high-energy region, in which the isotopic-spin selection rule is supposed to be valid, begins in this energy range. In the energy region studied, the angular distribution of the T=1 α-particle group changes very little although the cross section varies appreciably.

(8) The Elastic Scattering of 12.0-MeV He^3 by Nuclei

R. H. Bassel (ORNL), J. L. Yntema, and B. Zeidman

The angular distributions of the elastic scattering of 12.0-MeV He^3 particles by Mg^{24}, Ca^{40}, Sc^{45}, Ti^{46}, Ti^{48}, Ti^{50}, V, Fe^{54}, Ni^{58}, Zn^{64}, and Zr^{90} have been measured on the Tandem. This experiment was also used as a test of the operation of the 60-in. scattering chamber. The

experiment used a preliminary setup of the chamber. When completed, the chamber will accommodate four detectors with remote control of the distance to the center of scattering and eight targets with remote control of the angle between target and beam direction. Provisions have been made to accommodate a detector that could be moved throughout the top hemisphere. The results, which are necessary for the interpretation of (d,He^3) reactions on various nuclei studied at the 60-in. cyclotron, have given the parameters for the optical-model potential to be used in the distorted-wave theory. A single set of parameters, with the appropriate dependence on A and Z, fits all of the angular distributions except the ones for Mg^{24}. A paper is being prepared for Physics Letters.

I - 3.5. Research with the Magnetic Spectrograph

Since September 1963, when the magnetic spectrograph became ready for general use at the tandem, various experimental groups have used it to make a large number of measurements. The most complete studies are reported below. A number of other reactions are also being studied, but not enough progress has been made to warrant detailed discussion. Several groups outside the Physics Division have also been using the instrument. In their work targets of N^{14}, Ne^{20}, Mn^{55}, Fe^{56}, Co^{59}, and Pt^{192} have been bombarded.

The Argonne magnetic spectrograph is a general-purpose device for the study of charged-particle reactions. Protons with energies of 45 MeV or other charged particles of equivalent magnetic rigidity can be studied. Protons, deuterons, tritons, He^3 ions, alpha particles, and O^{16} ions have been analyzed to date. The particles recorded at one time have energies varying over a range of 2.4 to 1. The energy resolution width and the uncertainty in the energy calibration are both less than 0.1%. The usual method of detection is with photographic emulsions, a strip of nuclear emulsion 1 cm by 125 cm being exposed at one time. This is equivalent to an electronic pulse-height analyzer which has about 2500 channels. Most of the emulsions are scanned by an outside contractor. This arrangement has been quite successful. A program to develop an automatic plate-reading machine has been started.

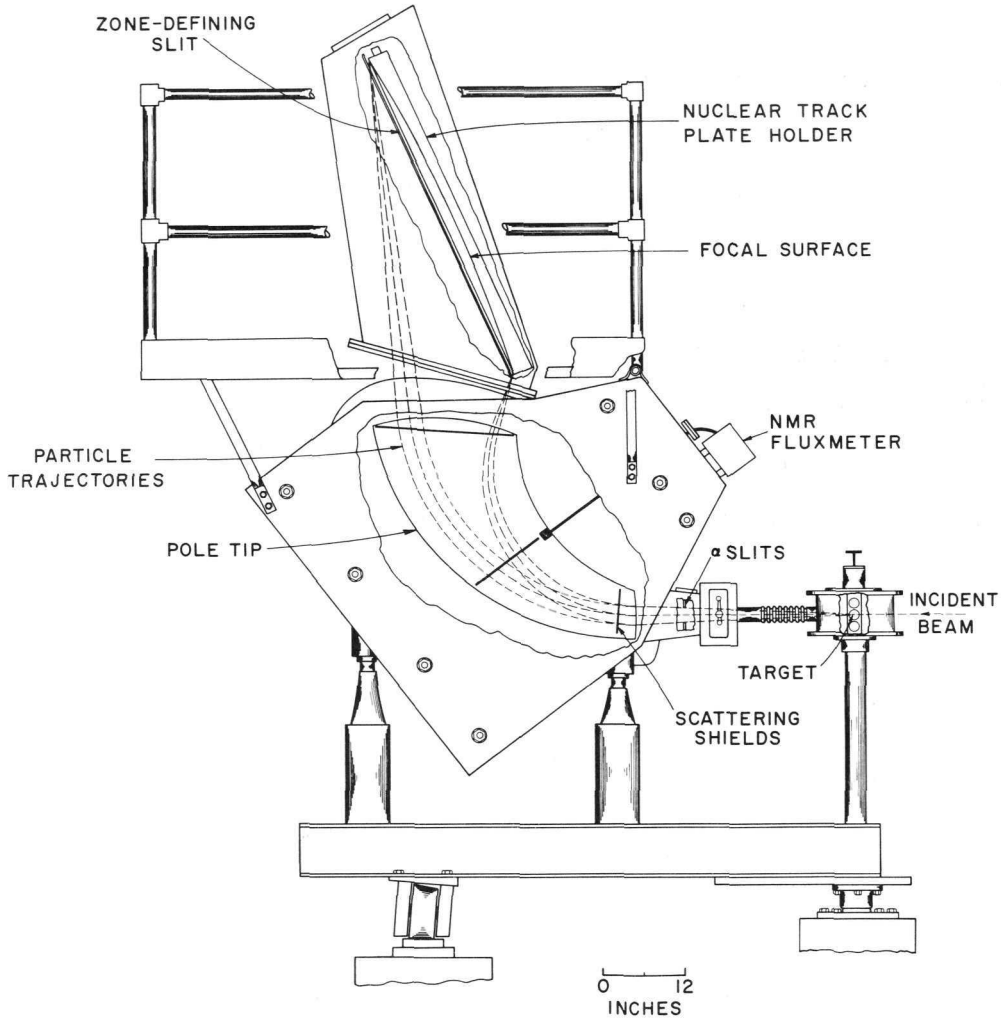

Fig. I-3-f. The Argonne broad-range magnetic spectrograph. This is a general-purpose instrument for the study of charged-particle reactions in which high resolution and/or accurate energy measurements are essential. It can be used to study protons with energies up to 45 MeV, or other particles with equivalent magnetic rigidity. The ion trajectories have a radius of curvature of 30 in. in a magnetic field of 11 kG. The ion optics are such that the ratio of maximum to minimum particle energies in a single exposure is 2.4: 1. Nuclear track plates are used to register the analyzed particles; low-sensitivity emulsions or absorbing foils enable the experimenter to study protons or alpha particles separately without competition from other particles. Seven separate exposures can be taken on one plate. The spectrograph moves on a semicircular track to cover the range of scattering angles from $0—150^{\circ}$. The solid angle of the instrument is about 3×10^{-4} sr. The resolution width is less than 0.1% in energy. The energy, calibrated with reference to a standard Po^{210} source, is reproducible to better than 0.1%.

(1) Reactions on Heavy Elements

J. R. Erskine

The energy-level structure of nuclei near the doubly-magic nucleus Pb^{208} should be relatively easy to interpret because of the presence of an inert core. A number of reactions leading to nuclei near Pb^{208} have been studied for the first time with enough resolution to observe the individual energy levels. The levels in Bi^{208} have been studied with the $Bi^{209}(d,t)Bi^{208}$ reaction. In the nuclear shell model, Bi^{208} is described as a Pb^{208} core plus a proton and a neutron hole. The observed levels agree well with the shell-model calculations of Kim and Rasmussen. Tl^{206} (described as Pb^{208} plus a proton hole and a neutron hole) is being investigated with the $Tl^{205}(d,p)Tl^{206}$ reaction. Early results indicate that the agreement with theory is not as good as for Bi^{208}. A study of the $Pb^{206}(d,p)Pb^{207}$ reaction to identify the single-particle states at high excitations in Pb^{207} is also starting.

The low-lying levels of highly deformed odd-A nuclei should be well described by the simple model of a rotating core plus an odd nucleon. The odd-A tungsten isotopes have been explored with (d,p) reactions in an effort to test this model. For the first time, the energy levels of W^{187} have been observed. Many new levels in W^{185} and W^{183} have also been found. The model consisting of a rotator plus an odd nucleon was found to give a simple interpretation of the observed energy levels within 500 keV of the ground state for W^{183}, W^{185}, and W^{187}.

(2) A Study of the Mechanism of (d,p) Reactions on Tungsten

R. H. Siemssen and J. R. Erskine

Angular distributions of the reaction $W^{182}(d,p)W^{183}$ have been measured with the magnetic spectrograph at a bombarding energy of 12 MeV to study the mechanism of a stripping process on a strongly

deformed nucleus. In addition to a modification of the optical-model potentials as a consequence of the deformation, it might be necessary to take account of two-step processes if the initial or final state is excited by inelastic scattering before or after the stripping process. A measurement of the intensity of the transition from the ground state to the first excited state of W^{183}, which is very small for normal stripping, gives an upper limit for the importance of such two-step processes. In addition, elastic scattering of deuterons on the isotopes W^{182}, W^{183}, and W^{186} has been measured. The deformation is known to change in this mass region. It was therefore hoped that the differences in the deformation might show up in the optical potentials. The bombarding energy of 12 MeV, however, appeared too low to bring out these differences significantly since the elastic scattering at this energy is still dominated by Rutherford scattering.

(3) Reactions on Ca^{48}

J. P. Schiffer, A. Marinov, and J. R. Erskine

The nuclei next to the doubly magic nucleus Ca^{48} are being studied by use of the (He^3, d), (He^3, α), (He^3, p), (d, p), and (d, α) reactions. Most of these reactions on Ca^{48} produce nuclear energy levels which have never before been observed. The (d, α) reaction leads to K^{46}, a nucleus which in itself has not been observed before. The study of the $Ca^{48}(He^3, d)Sc^{49}$ reaction is nearly complete; about 2 dozen energy levels are observed. These states are the single-particle proton states and are theoretically quite interesting. Energy levels in Sc^{50}, Ca^{47}, and Ca^{49} have also been observed and the data are being analyzed.

(4) The $Cd^{113}(d,p)Cd^{114}$ Reaction

R. K. Smither and J. R. Erskine

Some nuclei which have been studied with the bent-crystal spectrometer at the Argonne CP-5 reactor are also being examined with (d,p) reactions with the spectrograph. The excitation energies measured by the spectrograph are valuable clues in identifying the gamma-ray transitions which have been measured with very high precision by the bent-crystal spectrometer. Data have been taken on the $Cd^{113}(d,p)Cd^{114}$ reaction and plans are being made to study the $Hf^{177}(d,p)Hf^{178}$ reaction.

(5) Level Structure of Ar^{38} Below 6.3 MeV

R. G. Allas, L. Meyer-Schützmeister, and D. von Ehrenstein

The level structure of Ar^{38} was investigated with the $K^{41}(p,\alpha)Ar^{38}$ reaction at the Argonne tandem accelerator by means of a broad-range magnetic spectrograph. This structure was compared with that of Ar^{36}, whose level structure was earlier shown to be quite complicated, with several closely spaced multiplets. Although Ar^{38} (having only two $d_{3/2}$ proton holes) has a simpler make-up than Ar^{36} (with two additional neutron holes), its level structure is equally complicated. In particular, a rather low-lying single level at 3.381 MeV has been seen for the first time. Such low-lying levels are of special interest for nuclear shell-model calculations.

(6) Automatic Plate-Reading Machine

R. Vonderohe* and J. Erskine

An automatic plate-reading machine for scanning the nuclear track plates from the magnetic spectrograph is being developed. It is hoped

*Applied Mathematics Division.

that this new machine can be similar to the CHLOE film-scanning machine now in operation at Argonne and can use many components already designed. The CHLOE scanner was designed to automatically scan spark-chamber photographs. A nuclear-track-plate scanner requires higher resolution and a more complicated lighting system. However, the problem of pattern recognition is simpler. Initial estimates indicate that such a machine should be able to scan plates two orders of magnitude faster than a human scanner.

I - 3.6. Fluctuations of the Cross Section for the $K^{39}(p,\alpha)Ar^{36}$ Reaction

R. G. Allas, L. Meyer-Schützmeister, and D. von Ehrenstein

Eleven different final-state groups from the reaction $K^{39}(p,\alpha)Ar^{36}$ have been investigated at the Argonne tandem between

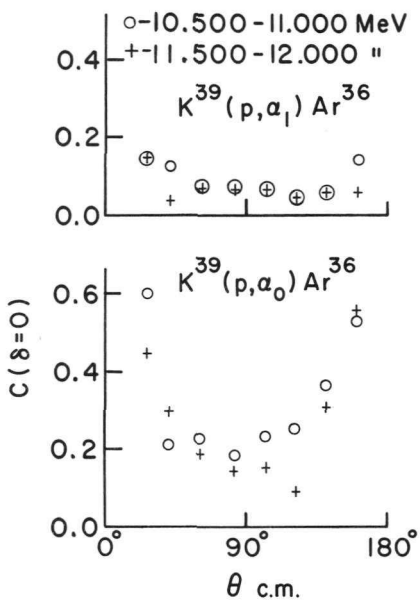

Fig. I-3-g. Auto-correlation coefficient $C = \langle\sigma^2\rangle/\langle\sigma\rangle^2 - 1$ as a function of angle. The fact that the ground-state transition peaks strongly at small and large angles shows the decrease in the number N of degrees of freedom by which the reaction can go. This effect is much stronger for the transition to the ground state (spin 0) where N is already small than for that to the first excited state (spin 2) which has a larger N.

10.000 and 13.000 MeV at 8 angles. We found strong fluctuations in the cross sections. Interpretation in terms of the statistical nuclear model[1] seems to be justified; in particular, we computed angular cross-correlations and probability distributions of the cross section as a function of the

[1] T. Ericson, Ann. Phys. (N.Y.) 23, 390 (1963).

angle (Fig. I-3-g). Such an analysis has not been published heretofore for a complete angular distribution. As a by-product of this investigation, a more complete and accurate level scheme of Ar^{36} up to 7 MeV has been established.

I - 3.7. Radiative-Capture Studies of the Giant-Dipole Resonance

R. G. Allas, S. S. Hanna, L. Meyer-Schützmeister, P. P. Singh, and R. E. Segel

We have completed a study of the giant-dipole resonances as seen through radiative capture in C^{12} and Si^{28}. In both cases, the photonuclear giant resonance as well as a giant resonance built upon the first excited state is clearly discerned. The fine structure varies considerably from case to case: for the ground-state gamma ray from B^{11} + p, the structure is very mild and the yield is usually monotonic over ranges of several MeV. For $B^{11}(p,\gamma_1)$ the peaks are about 1 MeV apart, while for the giant resonances from Al^{27} + p there is a great deal of structure with peaks about every 100 keV and fluctuations of up to about 2:1 in the cross section. The structure is uncorrelated between the two capture gamma rays in Si^{28}. For all four gamma rays studied, the angular distributions vary only slightly with energy. Both $B^{11}(p,\gamma_0)$ and $Al^{27}(p,\gamma_1)$ are peaked near 90°, while $B^{11}(p,\gamma_1)$ and $Al^{27}(p,\gamma_0)$ are almost isotropic. Some forward throw is seen in all four reactions: for B^{11} + p this forward peaking increases with increasing energy, while for Al^{27} + p no energy trend is discernible.

Some preliminary data on the capture gamma rays from F^{19} + p indicate that the angular distributions are again constant. In this case, γ_0 is apparently peaked at 90° and γ_1 more nearly isotropic.

A statistical analysis of the $Al^{27}(p,\gamma)$ reaction treats the variations in cross section as Ericson fluctuations. With this study, it

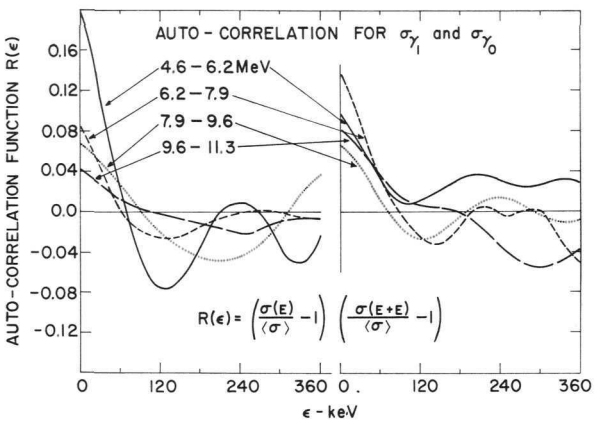

Fig. I-3-h. Auto-correlations of the 90° yield from the $Al^{27}(p,\gamma)Si^{28}$ reaction. Left: γ_1 to the first excited state in Si^{28}. Right: γ_0 to the ground state. The width of the auto-correlation curves is roughly independent of the averaging interval. Thus consistent values of the widths of the strongly overlapping states composing the giant resonance can be extracted.

has been possible to extract reasonable and consistent values for the widths of the strongly overlapping states which comprise the giant resonance (Fig. I-3-h). On the other hand, it has not been possible to extract mean values for the other physical parameters that are used to calculate Ericson fluctuations. Thus, the present theory of fluctuations is of use in this case but also has important limitations.

I - 3.8. Spins of Excited Nuclear States by p-γ Angular Correlations

D. S. Gemmell, L. L. Lee, Jr., A. Marinov, and J. P. Schiffer

In an effort to determine the fragmentation of the $\ell_n = 1$ single-particle neutron states in Fe^{55}, we have measured p-γ angular correlations for the prominent $\ell_n = 1$ states in the reaction $Fe^{54}(d,p\gamma)Fe^{55}$. Our measurements yield spin assignments as follows: $E_x = 0.41$ MeV, $\frac{1}{2}^-$; 2.49 MeV, $\frac{3}{2}^-$; 3.56 MeV, $\frac{3}{2}^-$; 3.80 MeV, $\left(\frac{3}{2}^-\right)$. These results indicate a much larger mixing and spread of the $2p_{1/2}$ and $2p_{3/2}$ strengths than expected from simple shell-model considerations.

I - 3.9. Study of (d,n) Reactions on Medium-Weight Nuclei

D. S. Gemmell, L. L. Lee, Jr., J. P. Schiffer, P. P. Singh, and A. B. Smith*

A program has been started to study (d,n) reactions on target nuclei with $40 \leq A \leq 64$. Studies of these reactions can in principle yield the same wealth of information for odd-proton nuclei as studies of (d,p) reactions have given for odd-neutron nuclei. In addition, one may hope to observe effects of isobaric-spin splitting in the states of the final nucleus. The pulsed beam from the tandem has been used in conjunction with a 10-m flight path and large liquid scintillation detectors. The over-all resolution width of the system is 0.2 nsec/m. This corresponds to a resolution width of 180 keV for 10-MeV neutrons and is good enough to resolve the low-lying states of many medium-weight nuclei. With the 10-m flight path, measurements can be made over an angular range from 5° to about 150°.

The first reaction chosen for study is $Fe^{54}(d,n)Co^{55}$. In preliminary measurements over an angular range from 0° to 60° at a deuteron energy of 7.0 MeV, we have observed neutron groups for which we have assigned the following excitation energies and orbital angular momentum transfers: g.s., $\ell_p = 3$; $E_x = 2.15$ MeV, $\ell_p = 1$; 2.55 MeV, $\ell_p = 1$; 2.92 MeV, $\ell_p = (1)$; 3.55 MeV, $\ell_p = (3)$, 4.15 MeV, $\ell_p = (1)$.

*Reactor Physics Division.

I - 3.10. Proposal for Construction of a Source for the Production of Polarized Ions

D. von Ehrenstein and D. C. Hess

A considerable effort is being made to develop a source of negative ions of known polarization, for use with the tandem Van de Graaff.

These ions will be produced by separating the different spin states of a beam of atoms in a magnetic lens. The degree of polarization can be increased by an rf transition. Since an rf transition is used, the subsequent ionization by electron bombardment can take place in a strong magnetic field without destroying the polarization—in fact, a strong field is needed to maintain it. The higher current densities attainable in a strong magnetic field should, in turn, lead to a high ionization efficiency. After ionization, the ions are accelerated, passed through a mass analyzer to eliminate those which might contribute undesired background, and then made negative by passage through an adding channel. The requirement of mass analysis introduces the possibility of general control of the final state of polarization. The mass analyzer will consist of a Wien filter. Thus, the angle through which the direction of polarization is precessed can be changed by changing the magnetic field while the deflection caused by the magnetic field is canceled by a suitable choice of electric field. This general control assumes that it is possible to pass ions with any direction of polarization through the charge-exchange channels. If this is not possible, special additional deflection magnets will be required at the output of the Tandem.

At present the effect of charge exchange on polarization is not known and no polarized ion source for use with a tandem Van de Graaff has been completed.

I - 3.11. University Use of the Argonne Tandem

In a new program of cooperation with Midwestern Universities, qualified physicists from the universities have been invited to make use of the Tandem Van de Graaff accelerator for about 32 hr of running time weekly. This program started informally with several individual requests for running time. Two requests of this kind were granted in 1963. A more

formal program, in which the availability of the Tandem was widely announced, was initiated on January 1, 1964. In this formal program, a committee consisting of three university representatives and two from Argonne allocate time to university users.

The experiments that have been proposed and accepted to date are listed below. The first two experiments have been in progress for some months and the other two will soon begin.

1. Multiple Coulomb Excitation and the Reorientation Effect

   R. P. Scharenberg (Case Institute of Technology)

2. Studies of Energy Levels in Light Nuclei with the Magnetic Spectrograph

   C. P. Browne (Notre Dame University)

3. Alpha-Gamma Correlation Studies of the Reaction $C^{12}(O^{16}, \alpha)Mg^{24*}_{1.37}$

   W. W. Eidson, J. G. Cramer, Jr., and R. D. Bent (Indiana University)

4. Magnetic Spectrograph Studies of the Reactions (He^3, α) and (He^3, d)

   W. P. Alford, L. M. Blau, D. Cline, and J. J. Schwartz (University of Rochester)

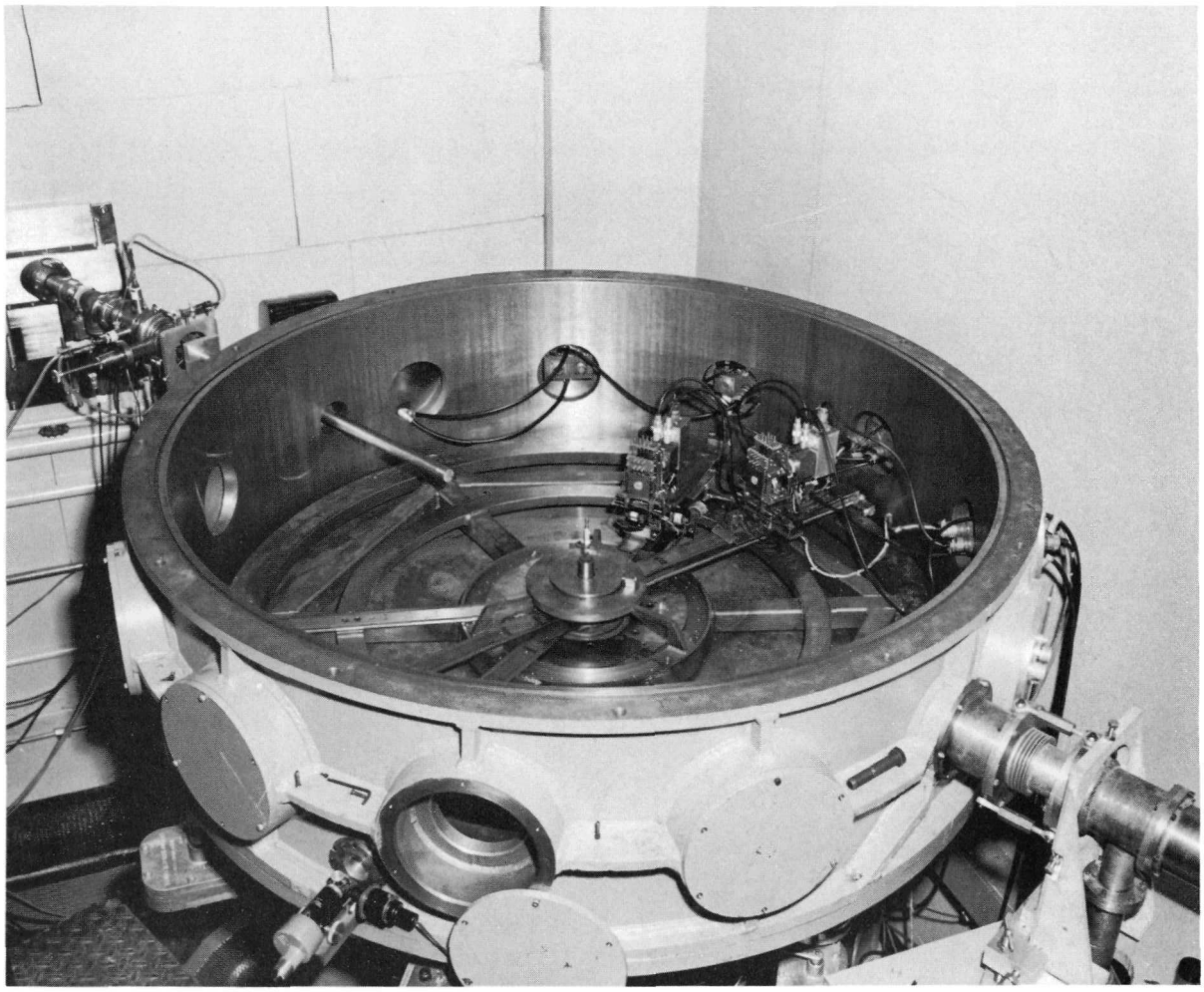

Fig. I-4-a. The 60-in. scattering chamber at the cyclotron, shown with the lid of the vacuum box removed. The beam collimator (upper left) has two circular apertures 3 mm in diameter and 1 m apart. The target is mounted accurately on the axis of rotation of the table. Each of the five detector units (two shown in the figure) includes an assembly by which aluminum absorber disks with a total thickness up to 700 mg/cm^2 can be inserted in front of the detectors in 7-mg/cm^2 steps. The arms carrying the detectors are provided with scales so that the distance from the defining aperture to the center of scattering can be read directly within about 0.25 mm. The position of the table is read through a microscope by means of a closed-circuit television system. The angle of scattering can be read to ±2 min of arc. All components of the scattering chamber are remotely controlled.

I - 4. RESEARCH AT THE 60-IN. CYCLOTRON

The 60-in. cyclotron is one of the low-energy accelerators operated by the Chemistry Division. It accelerates α particles to 43.2 MeV, deuterons to 21.6 MeV, and protons to 10.8 MeV. For all three of these projectiles, it can produce external beams at the shutter in excess of 0.1 ma. In addition, it accelerates Li^6 to an energy of 66 MeV with usable external beams of the order of 0.01 μa. Modifications which are now being made will enable the machine to accelerate He^3 to 28 MeV and (probably) Li^7 —in addition to the nuclei now accelerated.

The beam-handling equipment currently consists of a beam squeezer, three sets of quadrupole lenses, and two sets of left-right and up-down deflection magnets. A switching magnet permits the use of five different experimental stations. The energy of the incident particles can be lowered by use of a remotely controlled foil changer at the focal point of the first set of quadrupole lenses.

Now that a second experimental area has been built, it has become feasible to install a beam-analyzing magnet system. It is anticipated that this system will be ready near the end of 1964 and will provide a resolution width of 0.1% or less. The cyclotron is in operation approximately 80 hr/week. On the average, the Physics Division uses 25-30% of the operation time of the machine.

I - 4.1. The 60-In. Scattering Chamber at the Cyclotron (Project I-22)

Elastic scattering of deuterons by He^4 at 21.0 MeV (H. W. Broek and J. L. Yntema). The elastic scattering of deuterons by He^4 has been measured at 21.0 MeV. The results differ from those obtained at 19.0, 20.2, and 24.85 MeV elsewhere. A few points of the $He^4(d,p)He^5$ reaction to the ground state were also measured.

(d,He^3) and (d,t) reactions (J. L. Yntema). The (d,He^3) reaction on Ca^{40}, Ca^{42}, Ca^{43}, Ca^{44}, Ca^{46}, Ti^{46} (Fig. I-4-b), Ti^{47}, Ti^{48}, Ti^{49}, Ti^{50}, Y^{89}, and Zr^{90} and the (d,t) reaction on Ca^{42}, Ca^{43}, Ca^{44}, Ca^{46}, and Ca^{48} have been measured. The results obtained for the titanium

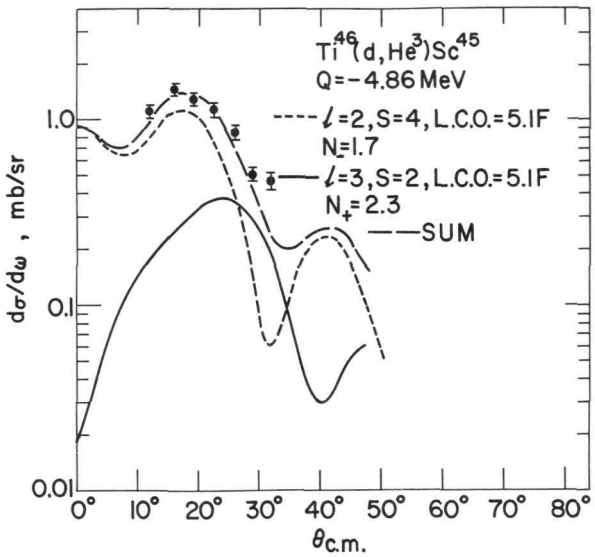

Fig. I-4-b. Angular distribution for the $Ti^{46}(d,He^3)Sc^{45}$ reaction to the region near the ground state. The solid line represents the prediction from distorted-wave calculations for the capture of $f_{7/2}$ protons with a strength of two. The calculations were normalized by means of the ground-state transition of $Ti^{48}(d,He^3)Sc^{47}$. The experimental points are clearly not in agreement with the prediction. The $Ti^{46}(d,He^3)Sc^{45}$ ground-state transition proceeds between two states of known spin and parity and is not forbidden. The experimental points are in good agreement with distorted-wave calculations when the group near the ground state of Sc^{45} is assumed to contain the transition to the $\frac{7}{2}^-$ ground state of Sc^{45} and the $\frac{3}{2}^+$ excited state of Sc^{45} from the $(d_{3/2})^3(f_{7/2})^2$ configuration. Therefore, the existence of an isomeric state in Sc^{45} at an excitation energy of less than 100 keV is predicted.

isotopes have been compared with distorted-wave calculations made by G. R. Satchler (ORNL). These experiments provide information on the ground-state wave functions of the target nuclei as well as on the nucleon-nucleon interaction in the nucleus.

Elastic and inelastic scattering of alphas (H. W. Broek and J. L. Yntema). A paper describing the scattering of 43-MeV alphas by Zr^{90}, Zr^{91}, Zr^{92}, and Zr^{94} and another for the five isotopes of titanium are in preparation. A letter on the elastic scattering and the excitation of the 2, 4, and 3^- states of Ni^{58} from 15^o to 165^o, together with the distorted-wave analysis of these data, is being prepared in collaboration with G. R. Satchler (ORNL).

I - 4.2. Studies of Pickup Reactions

T. H. Braid and B. Zeidman

The 21.5-MeV deuteron beam of the 60-in. cyclotron is used in a continuing study of the pickup of neutrons and protons by means of (d,t) and (d,He^3) reactions. The reactions are observed in an 18-in. scattering chamber with solid-state counters to detect the reaction products.

The measurements of (d,t) reactions on nuclei in the f-p-shell region have been improved and extended to nuclides not previously covered in this survey. These measurements identify the states which are formed by pickup of f and p neutrons. Discrepancies in the total strength of the $f_{7/2}$ states formed from targets with 28 neutrons indicate that distorted-wave calculations are needed for proper interpretation of the data.

The (d,He^3) reaction on $f_{7/2}$ nuclei (Sc^{45} through Fe^{54}) shows the positions and strengths of states due to pick up of $1f_{7/2}$ protons primarily, but also of 2s and 1d protons. The intensities observed are in general agreement with predictions made by Lawson on the basis of wave functions with mixed seniority. With a Ca^{40} target, weak groups near 5.8 MeV excitation are observed; they are identified as pickup of $d_{5/2}$ protons.

I - 4.3. Short-Lived Fission Activities

T. H. Braid, P. R. Fields,* and A. M. Friedman*

We have observed a spontaneous fission activity decaying rapidly after bombardment of Pu^{239} by deuterons from the 60-in. cyclotron. The target is oscillated rapidly to-and-fro between one position where it is exposed to the cyclotron beam and another where it is placed in front of a solid-state detector. Counts are recorded only when the

*Chemistry Division.

source is in the latter position. A pulse-height discrimination selects only fission fragments. The fissioning state (or states) shows a complex lifetime with at least two components, one of 6—8 msec half-life and the other about 70 msec. The yield has been observed to rise by a factor of ten as the energy of the incident deuterons is raised from 15 to 21 MeV. We have not yet identified the nuclide or the nature of the state which is responsible. Flerov has reported similar activities from the bombardment of Pu isotopes by α particles and deuterons. It seems possible that a number of such cases exist in this region of the periodic table.

I - 4.4. Delayed Proton Emission

T. H. Braid, R. Fink,* and A. Friedman*

This experiment is a search for delayed proton emission following the positron decay of Ne^{17}, which is a proton-rich nucleus. This is analogous to delayed neutron emission following the β decay of N^{17}. The protons are expected from excited states of F^{17} which are populated by the positron decay. The end product is O^{16}. A target of N^{14} is bombarded by a beam of Li^{6} ions accelerated to 66 MeV in the cyclotron. After being irradiated for a brief time in the beam, the sample is moved rapidly in front of a solid-state counter to observe the proton spectrum. Because of a weak Li beam and background of positrons from the β-active parent and neutrons from the cyclotron beam, our observations on the proton spectrum are not yet conclusive. The experiment is being continued. It has been predicted that a large number of cases of delayed proton emission should exist (several have been seen at another laboratory). Since the emitted particle is charged, this effect should be much easier to study than delayed neutron emission and should provide information about certain levels of nuclei on the proton-rich side of the line of nuclear stability.

*Chemistry Division.

I - 5. OTHER NUCLEAR EXPERIMENTS

Several experimental nuclear investigations in the Physics Division are not closely associated with any of the major sources of neutrons or charged particles. These independent studies are collected for convenience in this section.

I - 5.1. Atomic-Beam Research

W. J. Childs, L. S. Goodman, and J. Dalman

Since the last annual report, a large quantity of data has been obtained with the Mark II atomic-beam magnetic-resonance apparatus. A full report[1] on the hyperfine structure (hfs) of Cr^{53} has drawn interest from solid-state physicists. A paper on the electronic g factors of three metastable states of Sn I and Ge I has been accepted for publication,[2] and a paper on the hfs of three odd-Z isotopes of Sn in two different metastable states has been submitted for publication. The ability of the machine's universal detector to do useful work on metastable states of the 0.35% abundant isotope Sn^{115} establishes its unequalled sensitivity. These studies have revealed interesting details of admixtures between the atomic states. The theory is, at present, unable to account for the observed results, although the discrepancies are thought to be due to complexities of the calculations rather than to fundamental flaws in the theory.

More data have been obtained on the hfs of Fe^{57}, whose atomic ground-state multiplet is $^5D_{4,3,2,1,0}$. The magnetic field at the iron nucleus has been measured in both the $^5D_4$ and $^5D_3$ states. The

---

[1] W. J. Childs, L. S. Goodman, and D. von Ehrenstein, Phys. Rev. 132, 2128 (1963).

[2] W. J. Childs and L. S. Goodman, Phys. Rev. 134, A66 (1964).

contributions to this magnetic field are from the usual combination of electron orbit and electron spin (H_{LS}), and to the effect of polarization of the electron core (H_{CP}). These two contributions depend differently on the total electronic angular-momentum quantum number J; the measurement of the hfs of two different J states, therefore, allows one to determine H_{LS} and H_{CP} as independent quantities. H_{CP} is of opposite sign and almost twice the magnitude of H_{LS} in the $^5D_4$ states. This large contribution of H_{CP} is close to 5 times as large as the value from recent unrestricted Hartree-Fock calculations.

A considerable amount of data on the hfs of Ge^{73} in two metastable states has been obtained. The work is continuing. A value for the nuclear electric quadrupole moment will be obtained. The hfs of Au^{197} in its $^2D_{5/2}$ metastable state at 9161 cm^{-1} is being examined. This work should lead to an evaluation of the nuclear electric quadrupole moment of Au^{197}.

During the past year, an auxilliary potassium atomic-beam source and detector have been installed for use in precision calibration of the homogeneous magnetic field. Other parts of the apparatus have also been improved, particularly the electron-multiplier detector and the oven-loading system. Further improvements are in progress.

The most important improvement planned is the change from the present single-channel system of detection to a multichannel mode. This new counting system should lead to better averaging-out of nonrandom fluctuations and to increased sensitivity for detection.

The high-precision atomic-beam apparatus planned for the future is under preliminary investigation. It is expected that design can be begun this year.

I - 5.2. Determination of the Properties of Low-Lying Nuclear States Through the Investigation of Radioactive Decay Schemes

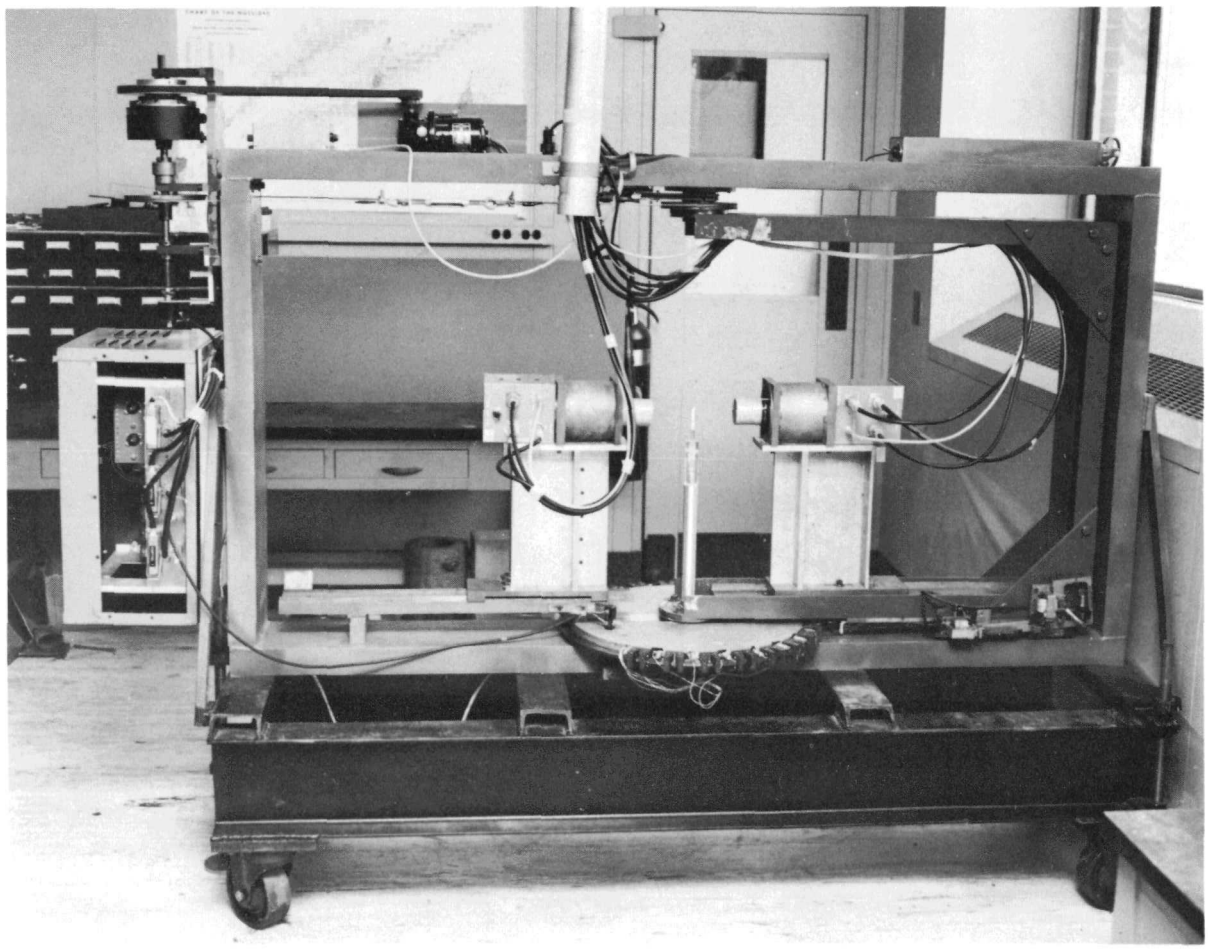

Fig. I-5-a. Fully automated suspension for the two scintillation detectors of the angular-correlation apparatus. The yoke supporting the movable detector pivots about a vertical axis. It is driven by a reversible motor and gear train and is precisely indexed at pre-set positions by means of a tapered pin and set of V-blocks clamped to the protractor plate. The complete sequence of operations needed to locate the yoke at any prescribed position is initiated by a single pulse on any one of the 21 address lines. Such an address pulse can be provided either from a symbol on the punched tape in the programming unit or from one of a set of buttons on the control console of the system.

(1) Directional-Correlation Apparatus

S. B. Burson, E. B. Shera, and T. Gedayloo

One of the most definitive experiments to determine a nuclear spin is the measurement of the directional correlation between two cascaded gamma rays. The automated directional-correlation apparatus (Fig. I-5-a) has been significantly improved by the addition of a 4096-channel two-parameter analyzer. This facility accumulates correlation data over large regions of the gamma-ray spectrum simultaneously so that a number of correlations can be measured at the same time. The apparatus exhibits the same advantages when used in conjunction with standard gamma-gamma and beta-gamma coincidence experiments. A number of new computer programs have been written to cope with the large amounts of numerical data accumulated and to perform the more complex analyses made feasible by the more comprehensive measurements.

(2) The Decay of Cs^{129} and the Levels of Xe^{129}

S. B. Burson and E. B. Shera

Among other recent theoretical developments leading toward an improved understanding of spherical nuclei, it has become possible to calculate the properties of nuclei consisting of several particles outside closed shells. The energies, spins, and parities of the levels of Xe^{129} have been investigated by means of the techniques of scintillation spectroscopy. These measurements have been discussed in the light of the recent pairing-model calculations of Kisslinger and Sorensen.

(3) Properties of the Odd-Odd Nucleus $_{75}Re^{188}_{113}$

S. B. Burson, E. B. Shera, T. Gedayloo, and R. G. Helmer*

*Phillips Petroleum Co., Idaho Falls, Idaho.

There are few signposts leading to the interpretation of the observable properties of odd-odd nuclei. Except for some treatments of the ground states, there is no comprehensive review of the available data and no general agreement regarding the adequacy of possible nuclear models.

The energies, spins, and parities of the ground state and five excited states of $_{75}Re^{188}$ have been determined through experimental studies of the radioactive species $_{74}W^{188}$ (69.4 hr), $_{75}Re^{188}$ (18 hr), and $_{75}Re^{188m}$ (18.5 min). Beta-ray and gamma-ray spectroscopy, coincidence methods, and directional-correlation techniques were employed in these investigations.

The level scheme was interpreted in terms of the spin-spin-coupling model for odd-odd nuclei presented by Gallagher and Moszkowski. All of the observed levels can be explained by various couplings of a proton in the $\frac{5^+}{2}$ [402] Nilsson level to a neutron in one of three different available neutron levels.

I - 5.3. Levels Populated by Beta Decay

H. H. Bolotin

(1) Sn^{166} Levels Populated by the Decay of 1-hr Sb^{116}

The use of the pairing-correlation assumption in short-range residual-force calculations has generated interest in singly-closed-shell nuclei in general and in the Sn isotopes (Z = 50) in particular. Since Sn^{116} may well provide the most comprehensive test of the theory for the even-A Sn isotopes, the Sn^{116} levels populated by the decay of Sb^{116} were studied in detail. A versatile counting system having an 800-channel pulse-height analyzer as the key element was used for gamma-gamma coincidence studies,

gamma-gamma angular-correlation measurements, and internal-conversion measurements. A complete set of spin, parity, and multipolarity assignments was obtained (Fig. I-5-b). The lifetime of the third excited

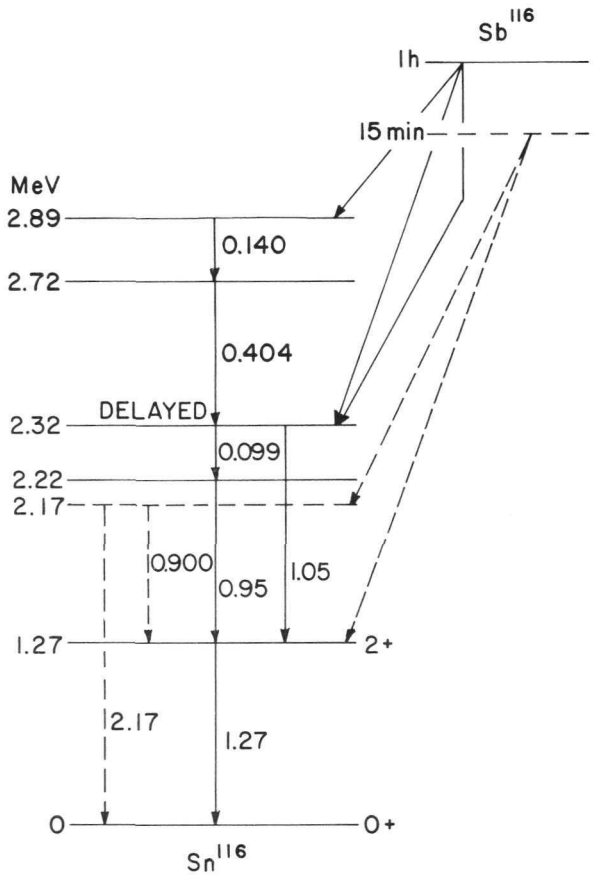

Fig. I-5-b. Proposed decay scheme for 1-hr Sb^{116}.

state (previously unreported) was determined from delayed-coincidence measurements to be $t_{1/2} = 2.4 \times 10^{-7}$ sec. In addition, triple-coincidence measurements involving annihilation radiation disclosed the existence of an important cross-over transition and resulted in a determination of the positron decay energy from measurements of the ratio of positron emission to electron capture.

(2) Sn^{116} Levels Populated by the Decay of the 54-min In^{116} Isomer

For many of the same reasons that motivated the Sb^{116} study, the Sn^{116} levels populated by the β^- decay of the 54-min In^{116}

isomer were investigated. Spins, parities, and multipolarities of the most prominent levels and transitions were assigned by use of techniques similar to those employed in the Sb^{116} investigation. With the exception of the first excited state, the levels populated are different from those populated in the decay of Sb^{116}. This is primarily due to the large spin and parity differences of the parent levels and, to some extent, to the detailed makeup of the Sn^{116} levels.

Gamma-gamma coincidence measurements disclose the presence of a level at 1.72 MeV, previously seen only in the decay of the 13-sec In^{116} ground state and tentatively assigned a spin and parity of 0^+. Preliminary results on internal-conversion electrons, measured by means of a solid-state detector, suggest that the transition from the 1.72-MeV level to the 0^+ ground state proceeds solely by internal conversion. This E0 character of the transition corroborates the 0^+ assignment of the level at 1.72 MeV. (The investigation of the E0 transition is being carried out with E. B. Shera.)

A comparison of the results from the decay of In^{116} with those from the decay of Sb^{116} and with the results of other workers on the decay of neighboring even-A In isotopes provides a broad experimental base for a comparison with theory.

(3) Ga^{66} Levels Populated by the Decay of 2.4-hr Ge^{66}

By means of time-to-pulse-height conversion techniques, the lifetime of the first excited state in Ge^{66} was measured to be $p_{1/2} = 21 \pm 2$ nsec. This is an ℓ-forbidden M1 transition, a type that is of current interest. Internal-conversion measurements have been made and gamma-gamma angular-correlation studies are in progress. These measurements should allow a determination of various spins, parities, and multipolarities. The results obtained to date have shown that for certain important features of the decay the proposals by previous workers are in error.

I - 5.4. Fission of Cf^{252}

T. H. Braid and H. Diamond

In coincidence studies with a Cf^{252} source, we have observed triple coincidences in which the total energy of the three particles appears to exceed the total energy from binary fission. We believe that these are due to fission of the nucleus into three fragments of comparable size. We are continuing this measurement and preparing a similar measurement on other spontaneous-fission sources and on the thermal fission of U^{234}.

I - 5.5. Study of Mesic X Rays

J. A. Bjorkland,* S. Raboy, C. C. Trail, R. Powers,† and R. Ehrlich†

A second series of measurements of muonic x rays was made at the FM cyclotron of the University of Chicago. As in the previous experiment,[1] extreme care was exercised to keep the counting rate in the photomultiplier of the detection system the same for calibration as for measurement. In addition, partly to take advantage of the high intensity of muons in the μ channel, the electronics and the detection system (NaI crystal with anticoincidence annulus) were improved. The improved experimental setup removed troublesome drifts and enabled us to measure the K x rays of the intermediate region (Al, Mg, V, Fe, Zn, and Ni) to a precision that will reduce the error in the nuclear radii to not more than half that in the electron-scattering experiments at Stanford University.

---

*Electronics Division.

†University of Chicago.

[1] H. L. Anderson, C. S. Johnson, E. P. Hincks, S. Raboy, and C. C. Trail, Phys. Letters 6, 261 (1963).

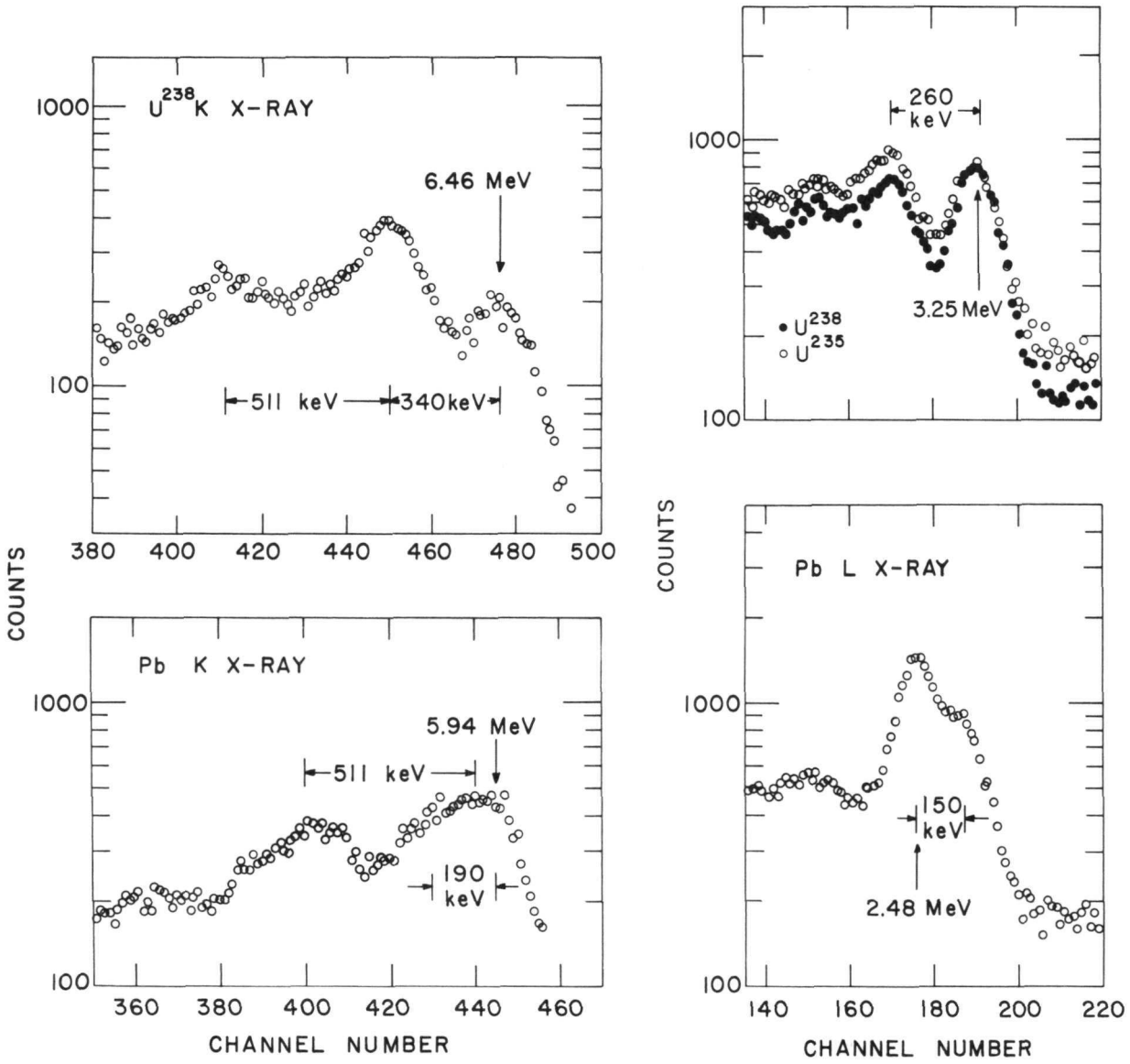

Fig. I-5-c. Mesic x-ray spectra for U and Pb. Left: K x rays. Right: L x rays. The qualitative difference between the spectra is expected from the facts that the rotational model holds somewhat for U^{238} and that Pb has no low-lying nuclear levels.

The L x rays of V, Fe, Zn, Cu, and Ni were measured with similar precision to replace our previous erroneous measurements. The slight differences between the L x rays and the point-charge calculation is a measure of the vacuum polarization.

The isotope shift between Ca^{44} and Ca^{40} was remeasured under these superior conditions. The final result was $K_\alpha(Ca^{40}) - K_\alpha(Ca^{44}) = 0.8 \pm 0.3$ keV.

We have initiated a series of measurements of μ-mesic x rays from highly deformed nuclei to which the rotational model applies. These nuclei have large intrinsic quadrupole moments and their low-lying levels have been identified as rotational states. The first targets selected were U^{235}, U^{238}, Pu^{239}, and natural Th. The K and L x rays show a complex spectrum which is attributed to the quadrupole interaction between the muon and the nucleus. We hope that the sign of the intrinsic quadrupole moment of the nucleus can be determined from these experiments. The qualitative difference between the spectra of Pb and U^{238} (Fig. I-5-c) is expected from the absence of low-lying nuclear levels in Pb and the large deformation of U^{238}.

Similar measurements on Bi, Ta, and Au suggest some quadrupole splitting in the mesic x rays. This would be expected if the excitation energies of the low-lying levels are comparable to the splitting due to the quadrupole interaction.

I - 5.6. Mössbauer Measurements (Project I-19)

In the last few years the Mössbauer effect has become a powerful tool for the study of many phenomena in solid-state, chemical, and low-energy nuclear physics. The experiments are aimed in two directions: (a) to yield accurate measurements of previously unobtainable nuclear properties (e.g., the deviation from roundness of a nucleus whose lifetime is only a few billionths of a second), and (b) to make accurate determinations of the environment in which a nucleus is immersed (e.g., to determine how the electron "borrowed" from the potassium atom in the compound KI is spatially distributed around the iodine nucleus or how the different atoms are distributed around an iron atom in a solid solution of vanadium and iron). Recent Argonne experiments have included such diverse nuclear and chemical species as Fe^{57}, Sn^{119}, Xe^{129}, and I^{129}, and more will be added.

(1) Mössbauer Effect in an External Magnetic Field

In Mössbauer experiments it is often desirable to apply strong magnetic fields to the nuclei under study. The advent of high-field superconductors has made possible the construction of suitable magnets. Two useful superconducting magnets[1] have been built and applied to experimental investigations (Fig. I-5-d).

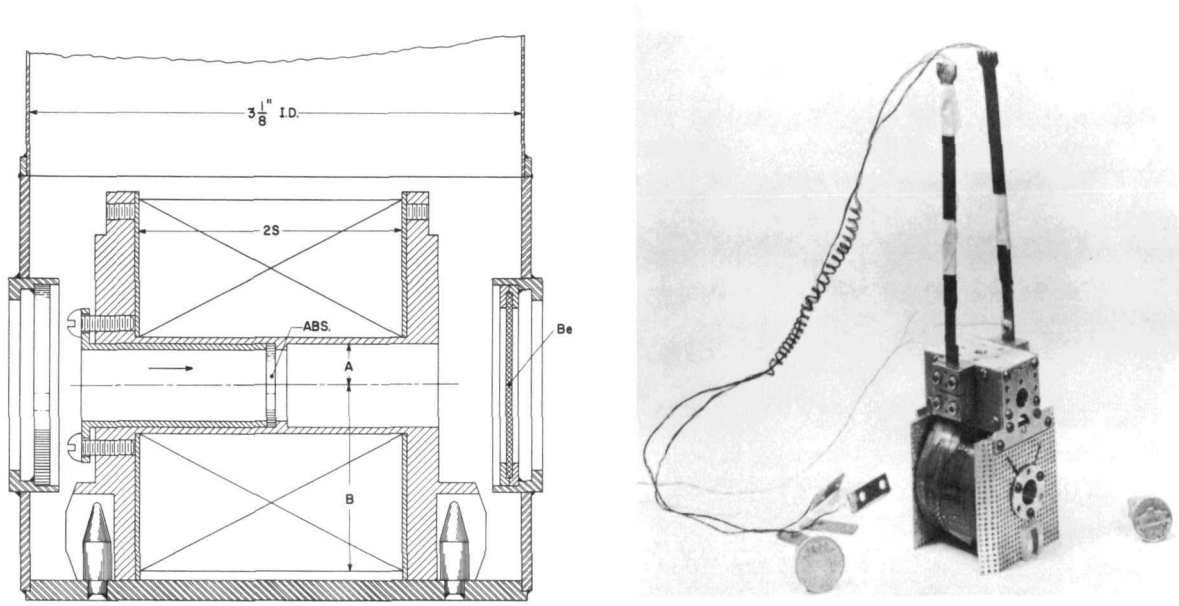

Fig. I-5-d. Superconducting magnet M8 which produces 50.7 kG at a current of 22.0 A: (a) cross-sectional diagram; (b) photograph.

Sn^{119} and Fe^{57} Metals[2] (J. Heberle, M. Schulhof, and S. S. Hanna). There had been some indications from other laboratories that an externally applied magnetic field produces an isomer shift. In order to explore this question, the nuclides Sn^{119} and Fe^{57} were investigated. In a field of 48 kG (applied along the direction of the gamma rays),

---

[1] J. Heberle, Rev. Mod. Phys. 36, 408 (1964).

[2] J. Heberle, M. Schulhof, and S. S. Hanna, Rev. Mod. Phys. 36, 407 (1964).

a foil of white tin (nonferromagnetic) produced a 4-line absorption spectrum, as expected. In the case of iron (ferromagnetic), the two inner lines were measured in fields of 11 and 48 kG. In neither case was any significant change in the isomer shift detected upon application of the magnetic field.

Manganese-Tin Alloys[3] (S. S. Hanna, J. Heberle, J. Diaz, and R. W. Reno). Other investigations have shown that the internal magnetic field at the Sn^{119} nucleus is 40 kOe in Mn_3Sn and 200 kOe in Mn_2Sn. We have attempted to determine the sign of these internal fields by applying a strong external field. In the case of Mn_3Sn, the lines broaden—for reasons that are not understood. The hyperfine spectrum of Mn_2Sn contracts upon application of an external field of 46 kOe. This behaviour indicates that the internal field in Mn_2Sn is negative, i.e., its direction is opposed to that of the bulk magnetization. This result is interesting because, with the exception of Sn^{119} in nickel, the internal fields in all other known cases are also negative. The sign of these internal fields is not yet fully understood theoretically.

Gadolinium[4] (L. Meyer-Schützmeister, S. S. Hanna, J. Heberle, J. Diaz, and R. W. Reno). The second excited state in Gd^{155} decays to the ground state by the emission of 87-keV gamma rays. The Mössbauer effect of this radiation has been observed previously; it has now been studied in $GdAl_2$, an intermetallic compound with a cubic Laves structure. A source of $Eu^{155}Al_2$ was prepared by irradiating unenriched $SmAl_2$ in the Argonne research reactor. The resonant absorption of the 87-keV radiation in an annealed sample of $GdAl_2$ produced a single line 2.2 mm/sec wide. From the measured half-life, a natural width of 0.63 ± 0.03 mm/sec

---

[3] S. S. Hanna, J. Heberle, J. Diaz, and R. W. Reno, Rev. Mod. Phys. 36, 407 (1964).

[4] L. Meyer-Schützmeister, S. S. Hanna, J. Heberle, J. Diaz, and R. W. Reno, Rev. Mod. Phys. 36, 329 (1964).

is predicted. If all the line broadening is attributed to an unresolved magnetic splitting, the observed width places an upper limit of 640 kOe on the internal field at the Gd nucleus. Measurements with the absorber in a field of 46 kG yield the same width as before.

Niobium Stannide (J. Heberle). The intermetallic compound Nb_3Sn is well known for its remarkable superconductive properties. Its critical field H_{c2} is so high that it has not yet been determined by experiment. An earlier investigation[5] of the Meissner effect in Nb_3Sn yielded the result that at most 25% of the sample was completely shielded from an externally applied field of 20 kG. Our superconducting magnet was used to apply a longitudinal field of 48 kG to an absorber of Nb_3Sn enriched to 50% in Sn^{119}. The splitting in the observed 4-line Mössbauer spectrum corresponded to the nuclear Zeeman effect of Sn^{119}

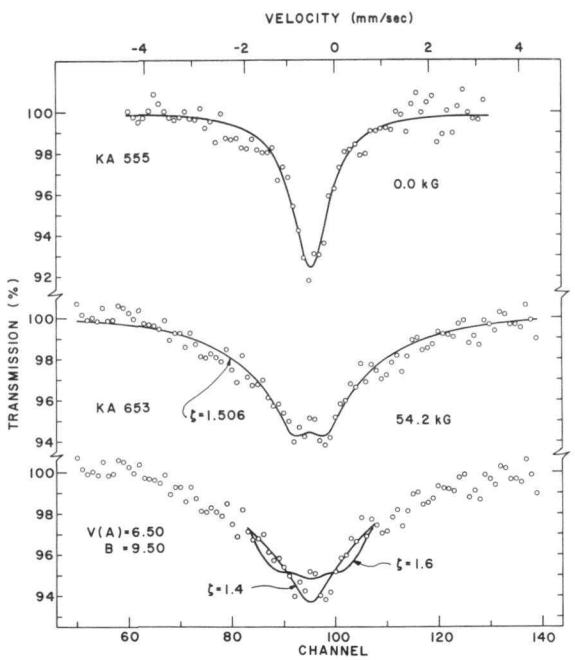

Fig. I-5-e. Experimental Zeeman spectrum of KI^{129}. The parameter ζ is the ratio of the Zeeman splitting of the 26.8-keV level to that of the ground state. In the center curve, a best fit is obtained for $\zeta = 1.506$. In the bottom curve, the same data are fitted with $\zeta = 1.4$ and 1.6.

[5] V. Vali, T. W. Nybakken, and J. G. Dash, Rev. Mod. Phys. 36, 359 (1964).

in a field of 48 kG. The absence of an unsplit line at the center of the spectrum places an upper limit of 5% on the fraction of sample from which the applied magnetic field is excluded. This result is in harmony with current theoretical ideas about high-field superconductivity.

Magnetic Moment of the 26.8-keV state in Iodine-129

(J. Heberle and H. de Waard). The magnetic moment of the $\frac{5^+}{2}$ state at 26.8-keV has been measured by observing the Mössbauer spectrum of a KI^{129} absorber in fields of 48 and 54 kG (Fig. I-5-e). The spectrum consists of 12 overlapping Zeeman components whose relative intensities are known. Of the many parameters required to specify the spectrum, only two (the Zeeman splitting of the excited state and the absolute intensity) are unknown. Therefore it is possible to determine these by the technique of curve fitting. A preliminary analysis yields $\mu_{exc} = +2.80 \pm 0.18$ nm.

Knowledge of this moment will be useful in analyzing the rather complicated Mössbauer spectra obtained with ferromagnetic compounds of tellurium. (Te^{129} is the parent nucleus of I^{129}.) This is the first instance in which an exclusively external magnetic field was used to determine a nuclear magnetic moment by means of the Mössbauer effect. It is also the first time that a superconducting magnet has been used to measure a nuclear magnetic moment.

(2) Short-Range Ordering in V-Fe Alloys

R. S. Preston, C. W. Kimball,* D. J. Lamm,** M. V. Nevitt,** and D. O. Van Ostenburg**

---

*Solid State Science Division.

**Metallurgy Division.

The Mössbauer absorption by Fe^{57} in V-Fe alloys has been measured to determine the isomer shift as a function of iron concentration.[1] Each sample was quenched from about 1000°C so that a disordered (random) arrangement of V and Fe atoms would be frozen into a regular body-centered cubic lattice. In each case, x-ray diffraction measurements confirmed the existence of bcc structure with no long-range ordering of the vanadium and iron within the structure. Magnetization measurements showed no magnetic ordering at room temperature below about 34% Fe. Above 34%, the magnetizations were mixtures of small ferromagnetic parts with large paramagnetic parts.

The Mössbauer patterns were all symmetric structureless single lines. The widths and the isomer shifts relative to Fe in iron are shown in Fig. I-5-f. Contrary to expectations of minimum inhomogeneous quadrupole broadening at 2% Fe and a monotonic rise to maximum broadening at 50% Fe, there is a broad maximum at 25% followed by a slight dip and a sharp rise. Also, contrary to expectations of considerable variations in isomer shift with concentration, the isomer shift remains nearly constant.

We attribute this behaviour to the existence of a peculiar type of short-range order which is illustrated in Fig. I-5-g. The figure shows a bcc lattice as two interlocking simple cubic sublattices. One of the sublattices (e.g., that of the black dots) is entirely vanadium for any concentration of iron less than 50%; the other sublattice (white dots) is a random mixture of vanadium and iron. Thus every Fe atom has only V atoms as nearest neighbors, independent of concentration, and the isomer shift is therefore very nearly constant. Also, the ordered vanadium sublattice has cubic symmetry about every iron atom, and therefore contributes

---

[1] R. S. Preston, C. W. Kimball, D. J. Lam, and D. O. Van Ostenburg, Bull. Am. Phys. Soc. 9, 112 (1964).

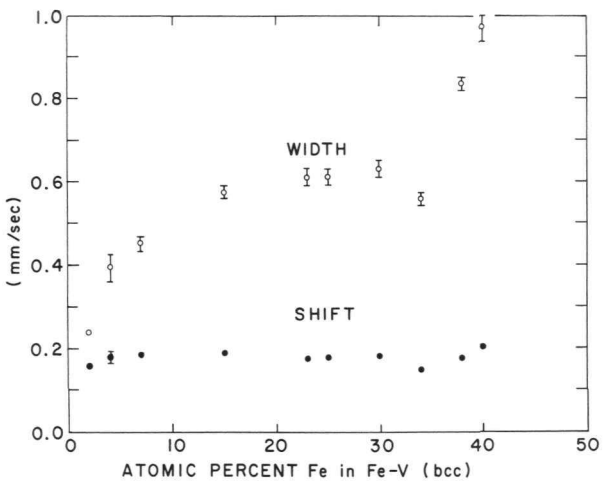

Fig. I-5-f. Mössbauer line widths and isomer shifts as functions of the iron concentration. The isomer shifts shown are relative to Fe^{57} in iron.

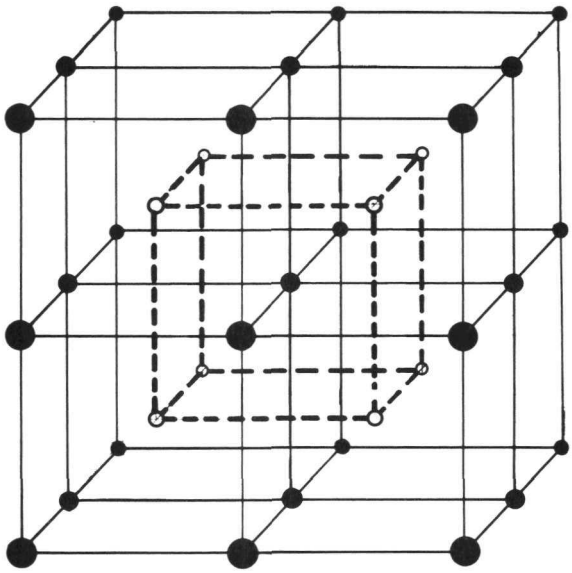

Fig. I-5-g. Part of a body-centered cubic lattice, shown as two interlocking simple cubic lattices.

nothing to the quadrupole field at any iron site. Thus the disordered sublattice is responsible for all the inhomogeneous quadrupole broadening, which is therefore maximum when the sublattice is 50% iron. This accounts for the local maximum in line width at 25% total concentration of iron.

The existence of this mixture of disorder and short-range order has been confirmed by additional experimental evidence. (1) At 50% Fe, the short-range ordering should be of the CsCl type—one sublattice being entirely vanadium, the other entirely iron. Ordered 50% V-Fe does have the CsCl structure. (2) The line width should fall off again above 25% iron to a minimum at 50%. A disordered 50% sample was ferromagnetic with a wide Mössbauer pattern. However, a measurement at 350°C gave a vastly reduced line width—about the same as for a 10% Fe sample. Likewise, after a 38% sample has been annealed for about $\frac{1}{2}$ hr at 600°C, the ferromagnetic component of its susceptibility

was greatly diminished and the Mössbauer line width was down to 0.5 mm/sec (less than at 34% Fe) but x-ray diffraction showed that it was still disordered.

(3) Mössbauer Effect in Xenon Compounds

G. J. Perlow and M. R. Perlow

Nuclear Quadrupole Moments. With XeF_4 as absorber and single-line (periodate) sources, the Mössbauer effect has been employed to study the transition from the first excited state to the ground state in Xe^{129} and in Xe^{131}. The parameters of the states involved are interchanged by the change of 2 in the neutron number. It had been expected that the quadrupole moments of the $\frac{3^+}{2}$ states would be nearly the same in the two isotopes; as a result of our having made this assumption earlier, a puzzle had arisen in interpreting the electronic structure of the xenon fluorides. The measurements now show that the moment of the first excited state in Xe^{129} is 3.45 ± 0.09 times that of the ground state in Xe^{131}. The chemical puzzle is removed by this value of the ratio, which is believed to signal the onset of a region of permanent deformation predicted earlier by others.

Xenon Compounds Formed by Beta Decay in Iodine Compounds. This experiment showed that a xenon compound is often formed by beta decay in an iodine compound. The evidence thus far is that the xenon takes on the complete set of iodine ligands. The formation of a compound of xenon is indicated by a large increase in the recoilless fraction (relative to the value for an unattached atom) and, in appropriate cases, by a quadrupole splitting. The occurrence of this process has been clearly demonstrated by comparing the splitting observed with an $I^{129}O_3^-$ source and a single-line abosrber (a clathrate compound, in which the xenon is trapped in a molecular "cage") with that seen with a single-line source

(IO_4^-) and XeO_3 absorber. The identical splitting shows that the decay is, at least for the most part, characterized by $IO_3^- \rightarrow XeO_3$. By starting with compounds of I^{129}, one may now make previously unknown chemical compounds of xenon. In the present investigation, $XeCl_4$ was made in this way from $KI^{129}Cl_4 \cdot H_2O$. The quadrupole splitting enables one to compare its structure with that of XeF_4 and (by virtue of the measured ratio of quadrupole moments reported in the first paragraph) with ICl_4^-.

Sign of the Quadrupole Moment of Xe^{129*}. With oriented crystals of $KICl_4 \cdot H_2O$ as source and a xenon clathrate absorber, the sign of the quadrupole coupling in $XeCl_4$ was measured. Let the four-fold molecular symmetry axis be called the z axis. The coupling is positive; and with only very weak assumptions about the bonding in $XeCl_4$, the quadrupole moment of the first excited state in Xe^{129} is negative. This is in agreement with expectations. The intensity ratio of the absorption dips gives evidence that $XeCl_4$ is indeed the compound being formed and that its orientation is not shifted appreciably from that of the ICl_4^- molecular ion.

I - 5.7. Pattern Recognition for Nuclear Events

D. H. Jacobsohn (AMD) and G. R. Ringo

The mechanization of the procedure for identifying interesting events is a problem of increasing importance in nuclear and particle physics. It is particularly critical in the case of emulsions in which it is desirable to scan large volumes of material with microscopes showing volumes of 10^{-8} cc or less in a view. A general-purpose computer has been programmed to simulate a four-layer random-connection network similar in its general character to the Perceptron of F. Rosenblatt. This program is designed to separate patterns presented in the form of 80-bit words into wanted and unwanted classes after a learning phase using 100 cases of each. The approach differs from that of the original Perceptron in which the random

connections were reinforced or weakened on the basis of the learning performance. In the version here, many completely different sets of connections are tried and the most useful (in the learning phase) kept.

Preliminary results show significant but not yet useful discrimination in a realistic but difficult case approximately equivalent to distinguishing X's from Y's of random size, orientation, and opening angle.

A tally counter, which will permit 100 times the previous speed of testing, is now being built. With this counter an 8 × 10 pattern can be tested in about 0.01 sec. A test of this general strategy on a large enough scale to settle the question of its usefulness should be under way by the fall of 1964.

I - 5.8. Microscopic Location of O^{17}, O^{18}, and N^{15}

G. R. Ringo and J. P. Schiffer

Some important problems in biological research call for development of a technique for finding the location of O^{17}, O^{18}, and N^{15} (used as tracers) with a resolution of 1 μm or better. It is proposed to do this by sweeping a proton beam of about 1 μm diameter over a thin specimen of interest and using a semiconductor counter to detect the α from the (p,α) reaction on the three isotopes mentioned. The output of the counter would be fed to a pulse-height analyzer (to select alphas from a particular isotope) and thence to a TV display synchronized with the proton-beam sweep. It appears that low-energy protons incident on the typical elements in biological materials would produce no other nuclear reactions that would yield confusing particles. A magnetic quadrupole lens to produce an appropriate proton beam is now being constructed.

II. THEORETICAL PHYSICS

The theoretical group consists of permanent staff and long- and short-term visitors. The principal subject of investigation is nuclear structure, but the theoretical effort includes research in diverse areas of theoretical physics. In particular, there are vigorous programs in high-energy theoretical physics and in the mathematics of quantum theory.

Activities of the group include several regular seminars. The general theoretical physics seminar draws in theorists from other divisions at Argonne and from nearby universities. A nuclear physics seminar is shared with experimental physicists at Argonne, and at Northwestern University and the University of Chicago. These formal programs are supplemented by a variety of informal contacts with the above-mentioned groups, with many research collaborations. Members of the Argonne theoretical group also offer occasional courses at Northwestern University. The theoretical group continues to attract large numbers of well-qualified applicants for temporary positions. Only a small number of these can be accepted for year-long visits. An active summer program makes it possible to accommodate many more visitors on a short-term basis. These are supported by Argonne National Laboratory, by Associated Midwest Universities, and by various outside agencies.

The largest single theoretical research project is the automated shell-model program, using the CDC-3600 computer. This project is now producing many valuable results, some of which are reported below. The project has also made valuable fundamental contributions in the area of automated computation.

II - 1. Theoretical Nuclear Spectroscopy

S. Cohen, D. Kurath, R. D. Lawson, M. H. Macfarlane, and M. Soga

The nuclear shell model provides the link between theoretical descriptions of nuclear matter and the excitation energies and transition rates measured in experimental laboratories. We report here on a program of calculations whose over-all purpose is the study of shell theory and its connection with the observed nucleon-nucleon scattering. This

connection will be made when theories of nuclear matter provide the self-consistent single-particle wave functions and residual two-body interaction for shell-model calculations.

Our program of shell-model studies therefore has three principal facets: (a) To study the techniques and approximations involved in very large shell-model calculations. Such work is basic to future progress. If an extreme degree of truncation of the basis is an essential part of any accurate shell-model calculation, it will be impossible to obtain a meaningful test of the basic parameters predicted by theories of nuclear matter. (b) To determine the best phenomenological effective interaction directly from experimental data in as many situations as possible. (c) To carry out detailed shell-model calculations of nuclear level structure and transition rates.

A basic set of interlinked FORTRAN programs for carrying out such calculations is now operational on the CDC-3600 computer. The system is constantly being augmented and improved. What is in fact emerging is a large collection of subroutines, each of which performs one of the mathematical operations which arise in computing the properties of a system of interacting fermions in a single-particle basis. Since the number of such distinct mathematical operations which can arise is limited and since each has been programmed in a fashion which makes no reference to the context in which it appears, it is clear that the programming of new calculations involves less and less effort as the system evolves. In this sense the system is more valuable than any of its particular applications.

The following is a brief list of the calculations that have already been carried out and an even briefer sketch of our plans for the immediate future.

(1) The effective interaction in the oxygen isotopes: $(1d_{5/2}, 2s_{1/2})^n$, identical nucleons.[1] Neutrons outside the O^{16} core

[1] S. Cohen, R. D. Lawson, M. H. Macfarlane, and M. Soga, Phys. Letters 9, 180 (1 April 1964).

populate the $1d_{5/2}$ and $2s_{1/2}$ single-particle orbits. The eight possible T = 1 two-body matrix elements are treated as independent parameters and determined by a least-squares fit to observed energy levels of O^{18}, O^{19}, and O^{20}. The best-fit theoretical spectra are compared with experiment in Table II-1-A.

(2) Isotopes of oxygen, fluorine, and neon: $(1d_{5/2}, 2s_{1/2})^n$. The isotopes of O, F, and Ne are treated in the fashion described in the preceding paragraph. Since both neutrons and protons are involved, we now have 16 independent two-body energies, eight for T = 0 and eight for T = 1. These are again determined by a least-squares fit to observed excitation energies. The fit is less impressive than for the O isotopes alone, and furthermore the F and Ne data force considerable changes in the T=1 matrix elements. Clearly the effects of configurations (such as $1p_{3/2}^{-m}, 1d_{3/2}^{n}$) excluded from our model are least critical in systems of identical nucleons.

(3) Isotopes of Y, Zr, Mo, Nb, and Tc: $(1g_{9/2}, 2p_{1/2})^n$, identical nucleons. A study of exactly the sort described above for the O isotopes has been carried out for the nuclei $_{39}Y^{89}$, $_{40}Zr^{90}$, $_{41}Nb^{91}$, $_{42}Mo^{92}$, and $_{43}Tc^{93}$ in which protons populate the $2p_{1/2}$ and $1g_{9/2}$ levels. An extremely interesting physical result emerges—seniority is a very good quantum number for the $g_{9/2}^n$ neutron configuration.

(4) The nuclear 1p shell. Work on the effective interaction in the 1p shell is in progress. In particular, the wealth of transition-rate data available here should give some insight into the relative degree of sensitivity with which the interaction parameters depend on transition rates and excitation energies.

(5) The isotopes of Ni: $(1f_{5/2}, 2p_{3/2}, 2p_{1/2})^n$, identical nucleons. In the Ni isotopes we consider neutrons in the $1f_{5/2}$, $2p_{3/2}$, and $2p_{1/2}$ orbits and assume a 4-parameter potential form for the effective interaction (central triplet and singlet, two-body spin-orbit,

TABLE II-1-A. Spins and excitation energies of states in the oxygen isotopes. All the states of the $1d_{5/2}$, $2s_{1/2}$ configuration are given in O^{18}. In O^{19} and O^{20} we have arbitrarily cut off our theoretical spectrum at 4.5 MeV and 5 MeV, respectively.

Nucleus	Experimental data		Theoretical spins and excitation energies (MeV)			
	Spin	Excitation energy (MeV)	Spin	Our results	Pandya	Talmi and Unna
O^{18}	2^+	1.98	2^+	1.93	1.99	1.87
	4^+	3.55	4^+	3.60	3.83	3.52
	0^+	3.63	0^+	3.52	3.63	3.42
	2^+	3.92	2^+	3.87	3.70	3.45
			3^+	5.46	6.20	5.77
O^{19}	$\frac{3}{2}$	0.096	$\frac{3}{2}$	0.04	0.04	0.18
	$\frac{1}{2}$	1.469	$\frac{1}{2}$	1.51	1.79	1.47
			$\frac{9}{2}$	2.66	2.76	2.66
			$\frac{3}{2}$	3.07	3.03	2.44
			$\frac{5}{2}$	3.24	2.81	4.07
			$\frac{7}{2}$	3.30	1.97	3.79
O^{20}	2	1.672	2	1.82	1.92	1.87
	4	3.568	4	3.53	3.54	3.52
	2	4.065	2	4.02	3.47	4.36
	0	4.446	0	4.46	4.33	4.60
			1	4.78	4.32	4.69

and tensor). Serious difficulties are encountered here, most of them stemming from the well-known tendency of potential interactions with harmonic-oscillator wave functions to produce very low 0^+ excited states.

(6) Effective interaction potential. It is of interest to determine to what extent the shell-model effective interaction can be parameterized in terms of a simple local potential, with central, two-body spin-orbit, and tensor components. There are two possible procedures here. (a) A least-squares fit to observed energy spectra and transition rates can be carried out with the potential parameters as independent variables. This has been done for various 1p-shell nuclei, for the isotopes of O and F within the configurations $(1d_{5/2}, 2s_{1/2}, 1d_{3/2})^n$, and, as described above, for the isotopes of Ni. (b) Alternatively, the two-body energies can be determined from the data and a potential can then be obtained by fitting these two-body energies.

This series of studies is as yet incomplete. It is, however, quite clear that to assume a local potential interaction with harmonic-oscillator radial wave functions imposes an unduly severe restriction on the two-body matrix elements. How much of the difficulty here stems from the assumption of a local potential and how much from the inappropriateness of harmonic-oscillator wave functions remains to be seen.

(7) BCS approximations. It has been stressed that approximate ways of handling shell-model calculations are of great importance. One such class of approximations which has been widely applied in the literature is based on the Bardeen-Cooper-Schrieffer (BCS) theory of superconductivity. The physical basis for this type of approximation is the goodness of the seniority quantum number for identical nucleons. We have analyzed a special model, involving neutrons in $1d_{5/2}$, $1d_{3/2}$, and $2s_{1/2}$ orbits with various interaction potentials and have compared the exact and approximate excitation energies and transition

rates. Preliminary results have been published[2] and a fuller account is in preparation.

(8) Projection of number eigenstates from BCS wave functions. BCS wave functions for nuclear ground states and excited states are superpositions of states corresponding to different eigenvalues of the particle number operator N. Simple explicit expressions have been obtained for the true-N components of BCS wave functions for the ground state and excited states, and also for the energy matrix elements between those states. These expressions are being used, first in analyzing the simple model outlined in (7) above, and then in studying isotopes of Sn and Pb.

Further developments in the immediate future will go in two directions: the first is to add new types of programs to the system, the second concerns the nature of the system itself. The approximate methods based on the BCS theory of superconductivity have one important limitation—they are strictly applicable only to systems of identical nucleons. We plan to study approximation methods which are free of this limitation. One such method involves treating neutrons and protons as separate entities; the T=1 part of the interaction is diagonalized first and the separate neutron and proton systems are coupled by the np interaction. The approximation involved is that of separately truncating the complete manifolds of neutron and proton states, the main question being how seriously this separate truncation violates isobaric-spin conservation. Another promising approximation method is that of projecting angular-momentum eigenstates from determinants of deformed-oscillator eigenfunctions. Both methods should be suitable for discussion of Ne^{20}

---

[2] S. Cohen, R. D. Lawson, M. H. Macfarlane, and M. Soga, Phys. Letters 9, 180 (1 April 1964).

within $(1d_{5/2}, 2s_{1/2}, 1d_{3/2})^n$. Since this problem can also be handled exactly, our first step will be to study the proposed approximation methods in detail for this special case. Finally, the system of programs is continually being improved as a research tool. Ideally such a system should perform all the drudgery involved in a given set of calculations while offering immediate access to any numerical information which we desire to examine. Considerable effort is being invested in studying how on-line display of data on an oscilloscope (Fig. II-1-a) can be used to further these aims.

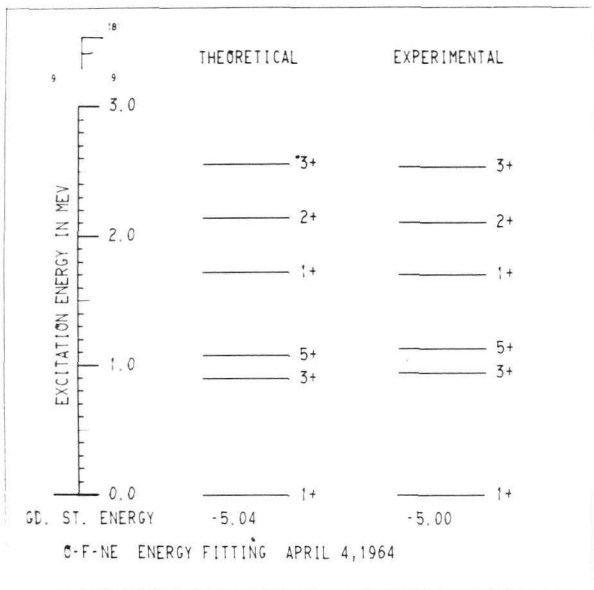

Fig. II-1-a. Typical oscilloscope display used to monitor the calculation in progress on the computer. This particular display occurred during the process of obtaining a best fit to the energy spectra of the isotopes of oxygen, fluorine, and neon.

II - 2. Interpretation of Inelastic Electron Scattering

Dieter Kurath

Nuclear excitation by inelastic scattering of electrons provides a rich source of information about nuclear structure. In addition to measuring excitation probabilities for various transitions, one can study the dependence of transition probability on momentum transfer. Such form-factor measurements provide information about the radial

distribution of nucleons in the nucleus. In particular, magnetic-dipole transitions reflect this radial dependence for the nucleons in the outer shells with larger orbital angular momentum. An interpretation of experiments on Li^6 and C^{12} is contained in an article, submitted to the Physical Review, entitled "Form Factors for Magnetic-Dipole Electron Scattering."

Such studies will be continued for more complicated nuclei, with the aid of the shell-model programs developed for the CDC-3600 computer.

II - 3. Effective Interactions and Nuclear Coupling Schemes in the 1s 0d Shell

S. P. Pandya

The nature of the effective nuclear interaction and its relationship to coupling schemes in nuclei has been investigated, particular attention being paid to the region of the 1s 0d shell in view of the occurrence of a distinctive rotational type of spectra early in the shell. A rather simple model for the effective interaction has been considered; it assumes the nuclear forces to operate only in $\ell=0$ states of relative orbital angular momentum of the two nucleons. It has been shown that the SU_3 coupling scheme and a coupling scheme having the major features of the pairing forces[1] emerge as special extreme cases of this s-state interaction model. It is further shown that the repulsive core in the interaction plays the important role of enhancing the component of the interaction which leads to the SU_3 coupling scheme, and is thus related to the appearance of nuclear deformations and rotational spectra. Detailed calculations in the framework of this simple model gave level schemes of O^{18}, F^{18}, O^{20}, and Ne^{20} that were in fairly good agreement with the observed level

---

[1] S. P. Pandya, Phys. Letters 7, 342 (1963).

schemes if the parameters of the interaction were suitably chosen. These values of the parameters agree well with the values one would expect from the realistic interaction which explains well the results of the nucleon-nucleon scattering experiments (such as Gammel-Thaler or Hamada-Johnston potentials).

Most of this work is carried out in collaboration with I. M. Green of the University of California at Los Angeles.

II - 4. On the Theory of Stripping Reactions

David R. Inglis

Stripping reactions, such as (d,p) reactions, have been extensively used since 1950 to identify the particle angular momenta involved in nuclear states, and the techniques of interpretation in terms of the distorted-wave Born approximation have been highly developed and extensively applied. However, the fundamental understanding of why the approximations succeed has not kept pace with the importance of the applications. An attempt to clarify the fundamental assumptions has been made by investigating their consequences in simple cases wherein details of the relationship between semiclassical concepts and wave-mechanical procedures can be exhibited. Whereas the usual theory emphasizes an integration over the volume of the nucleus, as though the deuteron should continue to disintegrate while crossing the region of the flat-bottom potential well, this study suggests that great importance should be attributed in the calculations to the disintegration of the deuteron on encountering the potential gradient at the edge of the nucleus. Some general features of stripping reactions can be understood in terms of semiclassical concepts here made plausible; it is hoped that further progress in this direction can be made in the future.

II - 5. Rotation of Gamma-Ray Symmetry Pattern Accompanying the Inelastic Scattering of Alphas

David R. Inglis

A good example of the way directly visualizable physical concepts can bring out the otherwise hidden meaning of extensive but somewhat obscure computations is found in an explanation of a striking phenomenon occurring in $(\alpha, \alpha'\gamma)$ reactions. As the angle of the inelastically scattered alpha, α', is varied from one of the characteristic maxima of the scattering pattern to the next, the symmetry pattern of the emitted gamma rays in some cases rotates rapidly in the reverse direction. The $0 \rightarrow 2$ excitation of a deformed nucleus forms a superposition of states with $m = \pm 2$, and these together form a pattern of charge distribution having the symmetry of a flower with four petals or a gear with four teeth. The relative phases of the two states (and hence the orientation of the pattern of γ rays emitted by the charge distribution) depend on the conditions of excitation, which are determined by interference of the incident and scattered waves.

When the incident beam α impinges on a nucleus horizontally toward the right and the scattered beam α' emerges upward toward the right, say, one may focus attention on the interference of the two waves as they bend around the bottom edge of the nucleus, for example. The superposition of these two waves, of slightly different wavelength, produces a "beat wave" of considerably longer wavelength. As the angle of the beam α' is increased (more steeply upward toward the right), the longer waves of α' at the bottom edge are pulled toward the right relative to the shorter waves of α. It is easily seen that, when the longer wave is pulled toward the right, the "beat wave" moves rapidly toward the left. The beat wave moving rapidly past the lower edge of the nucleus provides the excitation which determines the phases of the excited states and the orientation of the charge distribution and subsequent gamma rays. Its

rapid reverse motion thus causes the reverse rotation of the gamma ray pattern in a mechanism having a strong similarity to a rack-and-pinion gear arrangement.

II - 6. Statistical Properties of Nuclear States, Transitions, and Cross Sections

N. Rosenzweig

Generally speaking, the purpose of these studies is to help in the classification of nuclear properties according to the sensitivity with which these depend upon the details of the underlying structure. More specifically, the present work has largely consisted of isolating and treating those phenomena which depend only upon gross features of nuclear structure and upon general symmetry principles. The best known properties in that class are the distribution of energy levels, the transition probabilities, and the reaction cross sections.

Theoretical studies during the past year[1,2] have shown that virtually all of the above fluctuation phenomena (which occur in an energy range which is small compared with the energy of excitation) may be derived from a single statistical hypothesis such as the micro-canonical ensemble of matrices introduced by the writer in 1962. Thus, it was shown that both the observed energy-level statistics (as obtained in neutron resonance experiments) and the joint distribution of two or more reaction widths follow from the above matrix ensemble without further assumption.[1] In particular, the distribution of a sum of partial gamma-ray widths could be discussed on the basis of the invariant micro-canonical ensemble.[2]

---

[1] N. Rosenzweig, in Proceedings of the International Conference on Nuclear Physics with Reactor Neutrons, October 1963, Argonne National Laboratory Report ANL-6797, p. 302.

[2] N. Rosenzweig, Phys. Letters 6, 123 (1963).

It is clear that the Ericson fluctuations of reaction cross sections also follow without further statistical assumptions from the above-mentioned ensemble theory. Work which aims to show this in a particularly direct fashion is now under way.

II - 7. The Effect of Long-Range Perturbations in Scattering

J. E. Monahan and A. J. Elwyn

The treatment of a long-range weak interaction in the presence of a strong short-range force seems not to have received much consideration. Several problems arise. For example, the calculation of scattering from a short-range potential is conveniently carried out in terms of a partial-wave expansion. However, such an expansion does not converge rapidly enough to be practical for a long-range potential. Further, as a result of the long-range interaction, the radius at which the associated wave function can be considered to be that for noninteracting particles may be increased by orders of magnitude. Thus the difficulty of a purely numerical solution is increased considerably by the presence of potentials of widely different ranges.

We have been able to avoid these difficulties as follows. In the intermediate region where the short-range force vanishes but the long-range interaction is not yet negligible, the wave function for the system is calculated to first order in the strength of the weak interaction. This function is then used as an interpolation formula to continue the numerical solution from the region where the short-range potential is finite into the asymptotic region. Since the high-order partial-wave phase shifts approach the corresponding phase shifts of the plane-wave Born approximation for the long-range force, the contribution (to any observable) from these phase shifts can be summed analytically in this formulation. Thus the above-mentioned convergence difficulties are avoided.

This method has been used to calculate the polarization of neutrons scattered from an optical-model potential (including a spin-orbit interaction) plus a long-range potential of electromagnetic origin. This additional potential arises from the interaction between the electric field of the target nucleus and the magnetic moment of the neutron. The results of this calculation are compared with measured polarizations in Sec. I - 2.2(3).

II - 8. Analytic Criteria for Selecting an Optimum Set of Measurements (Project I-18)

J. E. Monahan and A. Langsdorf, Jr.

The purpose of this work is to formulate tractable criteria for the selection of a set of points at which a distribution $f(x, \underset{\sim}{a})$ should be measured to ensure that the resulting set of measured values will determine the parameters $\underset{\sim}{a}$ of the distribution with minimum uncertainty (for a given total expenditure of effort or cost). For example, the function $f(x, \underset{\sim}{a})$ might represent the angular distribution of particles scattered from some target as a function of x, the cosine of the angle of scatter. The "choice of measurements" implies selecting the points x at which the distribution should be measured and also the relative statistical accuracies of the individual measurements. This advance planning is in contrast to the standard statistical techniques, such as least squares and maximum likelihood, which can be applied to deduce a set of "best estimates" of the m independent parameters $\underset{\sim}{a}$ of a distribution measured at an arbitrary set of n distinct points ($n > m$) but which offer no explicit guidance in taking data efficiently.

Such criteria have been obtained for measurements of polynomial distributions, a frequently-encountered class. These criteria, which are easily coded for a digital computer, would, for example, enable the computer to make routine decisions on questions of the following kind.

Suppose that a distribution has been measured at n points (i.e., at n values of x). At what point should the (n + 1)st measurement be made in order to obtain the most accurate estimate of the parameters $\underset{\sim}{a}$ from the complete set of (n + 1) measurements? Traditionally this "choice of measurements" has been based largely on the intuition of the experimenter; but the increasing efficiency of computers makes the use of mathematical criteria practical or even necessary for the more complex or costly experiments. A paper is being prepared for publication.

The extension of these results to the case of a multivariable polynomial distribution $f(x, y, \cdots ; \underset{\sim}{a})$ would be of interest since various correlation and coincidence experiments could then be considered.

II - 9. Foundations of Quantum Mechanics

Melvin Hack

The branch of research in quantum theory that is notable for the range of viewpoints to which it has given rise is the quantum theory of measurement. Not unlike the situation in some other branches of physics, the problems connected with the foundational aspects were noted almost immediately after the theory's inception, and the discussions generated by them have continued up to the present. In the last year or so, the renewal of interest in this field has undergone a quantum jump. In the absence at the present time of a generally acknowledged description of the measuring process, the question naturally suggests itself: Does there exist an acceptable formulation of measurement within the framework of present quantum theory? Work on this problem is being continued.

II - 10. Observables in Relativistic Quantum Mechanics (Project V-44)

H. Ekstein and W. C. Davidon*

The conventional statement of statistical determinism is that "the expectation values of all (Heisenberg) observables are determined by the expectation values of the observables at one time." This requires that a full algebra of self-adjoint operators be in one-to-one correspondence with measurement procedures performed at one time; but no such procedure is known. The contrast between the positive assertion of the existence of certain laboratory procedures and the inability to describe them constitutes perhaps the weakest point of quantum mechanics.

In the present investigation, it was shown that the conventional statement of statistical causality is untenable in a relativistic theory. The alternative proposed is a weaker form of causality which (1) is restricted to states that are vacuum-like outside a finite space-volume and (2) uses measurements made within a truncated light cone rather than at one time for predictive purposes. Failure of the conventional causality statement implies that the set of quasi-local observables is not necessarily linear (i.e., if A and B are in a set, A + B is not necessarily in it). This remark may open the way to a systematic inquiry into the problems of associating laboratory procedures to self-adjoint operators.

---

*Haverford College, Haverford, Pennsylvania.

II - 11. Relativistic Theory of Multiparticle Scattering

F. Coester

The quantum mechanics of relativistic particles is a possible alternative to quantum field theory on one hand and analytic S-matrix theory on the other. The basic difficulties which stand in the way of such an approach have been overcome.

The scattering theory for one or several two-particle channels can be formulated in the rest frame of the center of mass along the same lines as the nonrelativistic theory. The existence and completeness of the scattering states and their asymptotic properties as well as the Lorentz invariance of the S operator follow from known mathematical theorems. Numerical methods appropriate to the nonrelativistic differential Schrödinger equation cannot be extended; but we can use algebraic methods which were first developed for the systematic approximation of nonrelativistic single-channel scattering amplitudes.[1]

To be consistent, multi-particle theory must satisfy the following requirements. The interaction of two particles should be the same when they are alone as when other particles are present at a large distance. A particle system may break up into two or more noninteracting clusters. The dynamical description of the entire system must also contain the correct Lorentz-invariant description of each of the clusters. These requirements have been satisfied for three-particle systems.

---

[1] F. Coester, Phys. Rev. 133, B1516 (1964).

II - 12. Structure of Elementary Particles (Project V-47)

K. Hiida

Pseudoscalar charge density of spin-$\frac{1}{2}$ particles. When interactions are renormalizable and are invariant under time reversal but not under space reflection, then under the requirement that the S matrix is free from divergences after the renormalization it was shown that any spin-$\frac{1}{2}$ particle with nonvanishing mass should have pseudoscalar charge density in addition to the usual scalar charge density.[1] To show

---

[1] K. Hiida, Phys. Rev. 134, B174 (1964).

clearly that the pseudoscalar charge density is a physical observable, the influence of the pseudoscalar charge density on the spin orientation of a charged spin-$\frac{1}{2}$ particle in time-independent electric and magnetic fields was considered.[2] In a longitudinal electric field, the interaction of the pseudoscalar charge density with the field causes the spin to rotate about the axis perpendicular to the direction of propagation and the spin orientation. In a transverse electric field, the interaction of the pseudoscalar charge density with the field causes the spin to rotate about the axis perpendicular to the spin and the direction of the field, whereas the interaction of the usual scalar charge density with the field causes the spin to rotate about the axis perpendicular to the direction of propagation and the direction of the field; at very low energies, the spin can be rotated through a larger angle in the former case than in the latter. There is no interaction between the induced pseudovector current and a magnetic field.

Theory of spin-$\frac{1}{2}$ particles with parity-nonconserving interactions.[3] It was shown that when interactions are not invariant under parity conjugation, both the self-mass term and the term $(-a\bar{\psi}\gamma_\mu\gamma_5 \cdot \partial\psi/\partial x_\mu)$ are induced by the self interaction of any spin-$\frac{1}{2}$ particle with nonvanishing mass (T invariance being assumed for simplicity). To avoid propagation in a vacuum at a speed greater than that of light and to avoid ghost states, it follows that $a^2 \leq 1/3$. Although a has no physical meaning for free particles, it is shown that it has a physical meaning when a charged particle is interacting with an external electromagnetic field.

---

[2] K. Hiida, Phys. Rev. (May 1964).

[3] K. Hiida, Phys. Rev. 132, 1239 (1963).

II - 13. Geometric Properties of Angular Distributions of Decay Products (Project V-5)

M. Peshkin

A maximum-complexity test has been found for the spin and parity of an unstable particle or state X, which is produced in a reaction A + B → C + X and decays according to X → D + E. This new test applies only when A, B, C, and D have spin zero and X is either a spinless particle or a gamma ray.

The angular distribution of the decay is written in the form

$$I_{\delta}(\theta) = \sum_{L=0}^{2j} a_L(\delta)\, P_L(\cos\theta),$$

where j is the spin of state X, angle δ is the production angle, and θ is the angle between the momentum direction of E and the normal to the production plane, in the rest frame of X. Then it is shown that $a_{2j}(\delta)$ cannot vanish, but lies between bounds which depend upon j. Moreover, the sign of a_{2j} determines the parity of state X.

This test has several unusual advantages: First, the bounds of $A_{2j}(\delta)$ are independent of δ. Therefore, it is permissible to average $I_{\delta}(\theta)$ over production angles δ to get an average a_{2j} before performing the test. This feature makes the method applicable to unusually small samples. Second, the largest L in $I(\theta)$ is unambiguously identified by the bounds of a_{2j}, if the statistical accuracy is good enough. The usual trouble, that a good fit can always be improved by adding higher L values, is averted. Third, the hypothesis that X has spin j and definite parity is tested by a single quantity whose statistical accuracy is easily estimated. Fourth, although the maximum-complexity test applies only to a restricted class of experiments, this class comprises just the cases for which the usual angular-correlation tests fail.

II - 14. A Model for the Low-Energy $\pi + N \rightarrow N^* + \pi$ Reaction

K. Itabashi

For the low-energy $\pi + N \rightarrow N^* + \pi$ reaction, it is shown that the exchange of a two-pion system (or the system of even G parity) with isotopic spin 2 and angular momentum 0 has a good chance to become dominant. If this is actually the case, then the reaction occurs predominantly from the $T = \frac{1}{2}$, $d_{3/2}$ state of the initial πN system. Therefore, in connection with the problem of the second πN resonance, this possibility is very interesting. It would play a very important role in producing the second resonance, even though it could not be the sole cause of the resonance. Some possible experimental tests of this possibility are suggested.

II - 15. Meson-Nucleon Interaction

K. Tanaka and K. Itabashi

In order to examine the validity of the symmetry of the unitary unimodular group in SU_3 in three dimensions, observable consequences of the decays of the vector meson (such as that into two pseudoscalar mesons and N photons or into a pseudoscalar meson and N photons) are obtained.

When 2 octets (8 representations of the group SU_3) transform into 2 octets, there are ordinarily eight channel amplitudes or reduced matrix elements. Invariance properties of the theory lead to various relations among the channel amplitudes. For various processes, the relation between channel amplitudes, the number of independent channel amplitudes, and spin selection rules are systematically obtained.

The relations among the amplitudes for nucleon-antinucleon annihilation into two mesons (pseudoscalar or vector) and also those into a baryon-antibaryon pair are obtained on the basis of SU_3 invariance.

It is of interest to attempt to verify the validity of the SU_3 symmetry in order to understand the nature of elementary particle physics.

II - 16. Unitary Symmetry and the $K \to 2\pi$ Decay

K. Itabashi

It is proved that, in the limit of strict SU_3 symmetry of strong interactions, all the $K \to 2\pi$ decays are forbidden provided only that the nonleptonic decay Lagrangian belongs to the CP-invariant representations (the irreducible representations whose $Q = 0$, $Y = 0$ members are CP invariant). For the case in which the decay Lagrangian belongs to an octet, the theorem has recently been proved by others; but the present theorem is much stronger.

The proof does not apply when the symmetry-breaking interactions are taken into account, and thus all the $K \to 2\pi$ decays should be attributed to the symmetry-breaking (and/or electromagnetic) corrections.

It is also argued that, in connection with the $(K_1^0 \to 2\pi)$-$(K^+ \to 2\pi)$ puzzle, the octet hypothesis of a nonleptonic decay Lagrangian is very attractive.

In the coming year, the other nonleptonic decays and the nature of the symmetry-breaking interactions will be investigated.

II - 17. Internal Symmetry and Lorentz Invariance

F. Coester, M. Hamermesh, and W. D. McGlinn

The known mesons, baryons, and their resonances have been successfully identified with irreducible representations of the group SU_3 even though the symmetry is badly broken—broken in the sense that the members of the same SU_3 multiplets have large mass differences. In fact, one of the great successes of SU_3 symmetry has been the mass formula of Gell-Mann

and Okubo, which relates the masses of the members of the same SU_3 multiplet.

Recent discussions have led to attempts to explain such mass formulas and broken symmetries by searching for an over-all symmetry group that contains SU_3 and the Lorentz group as sub-groups but not as a direct product. If it occurred as a direct product, then within the irreducible representation of the over-all symmetry group the multiplets of SU_3 could have the same mass. In particular, to obtain mass splittings the generators of SU_3 cannot in general commute with the translations.

We show that there are severe restrictions on such over-all symmetry groups. These restrictions are contained in the following two theorems, in each of which we assume that the generators of the over-all symmetry group G are those of the inhomogeneous Lorentz group L and an internal symmetry group I which is taken to be semi-simple. Theorem I: If the internal symmetry generators commute with the homogeneous Lorentz group, then $G = I \times L$ and thus no mass splittings result. Theorem II: If the complete set of commuting generators of I are Lorentz invariant, then $G = I \times L$ and therefore there can be no mass splittings.

In particular, if the internal symmetry is SU_3 and if T_z and Y are Lorentz invariant, then $G = SU_3 \times L$. In fact, for the case of SU_3, just the assumption that T_z is Lorentz invariant implies $G = I \times L$. Thus it is seen that if one wishes to obtain an over-all symmetry group that contains both I and L and if one wishes to maintain the condition of either Theorem I or II, then one must introduce generators other than those of I and L.

II - 18. Assignments of the $d_{3/2}$ Octet

Arthur W. Martin

The unitary-symmetry model of the strongly interacting particles has enjoyed quite remarkable success in establishing order among these particles. In particular the baryonic states, both bound states and resonances, have been successfully grouped into multiplets associated with irreducible representations of the group SU(3). This multiplet structure has provided a powerful theoretical tool for the prediction of new particles; yet at the same time it can be mischievously misleading. This will happen when the quantum numbers of a given particle allow its assignment to any of several irreducible representations. In such a case it is necessary to employ more subtle arguments in order to straighten out the classification scheme.

The case in point is the assignment of the 1520-MeV Y_0^* resonance, previously assumed to be a member of a $d_{3/2}$ octet. Arguments based on two independent considerations have been presented to the effect that this resonance is not a member of an octet but is instead a unitary singlet. The first consideration is that an analysis of the reduced resonance widths permits a comparison with the coupling-strength predictions of the unitary-symmetry model. The second is based upon an "effective threshold" model for the mass splittings between members of a baryonic multiplet (Fig. II-18-a). The important consequences of the

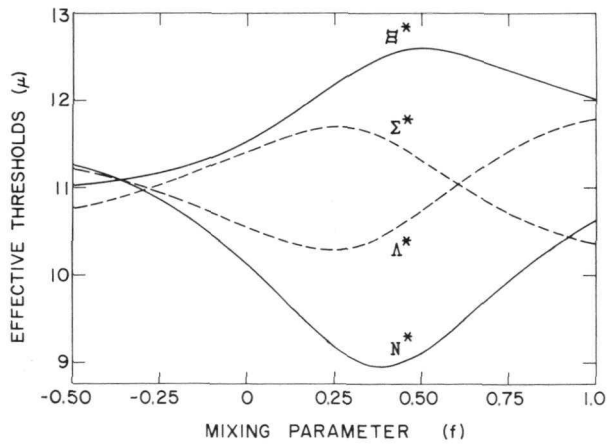

Fig. II-18-a. Mass splittings of a baryonic octet in the "effective threshold" model.

argument are the prediction of a new Y_0^* resonance, its location and width, and the location and width of a previously unobserved cascade-pion resonance that had been predicted (at the wrong location) by earlier theoretical arguments. Subsequently, preliminary experimental evidence supporting both of these predictions has been obtained.

II - 19. Approximate Bootstrap Technique

Arthur W. Martin

The notion that the existence of the strongly interacting particles is a dynamical consequence of their mutual interactions, that is, that they "bootstrap" each other into being, is the subject of intensive investigation by theoretical physicists. One technique of investigation is the N/D method, which leads to the formulation of the dynamical equations governing the basic interactions as integral equations of the Fredholm type. These integral equations, especially in the case of coupled channels, are of such complexity that rather drastic approximation schemes are frequently employed in order to obtain solutions. The most common approximation technique, the first-order "determinantal" method, has severe shortcomings; for one thing, its approximate solutions generally violate time-reversal invariance.

An alternative method, the "degenerate kernel" approximation, is suggested for the study of the "bootstrap" integral equations. The approximation reduces the solution of the integral equations to an algebraic problem. It further avoids the many drawbacks of the "determinantal" method. The technique has been applied to the vector-meson bootstrap problem, with the self-consistent solutions obtained by means of Argonne's IBM-704 computer. The results indicate features of the bootstrap notion that were obscured by the earlier approximation techniques. The "degenerate kernel" method is presently being applied to the problem of bootstrapping the

nondegenerate vector-meson octet in the unitary symmetry model of the strongly interacting particles.

II - 20. Meson-Baryon Resonances in the Octet Model

A. W. Martin and K. C. Wali

We have examined the consequences of the "bootstrap hypothesis" for meson-baryon states within the framework of the unitary symmetry, or octet model. Beginning with the requirement that all baryonic states introduced into the driving forces (the "potential") must emerge as dynamical consequences of those forces, we investigated the question of what other resonances would be predicted in a model in which the baryon octet and the decuplet of resonances were mutually self-supporting. It was found that this requirement led to the prediction of two additional baryon states, a $J^P = \frac{1}{2}^-$ unitary singlet and a $J^P = \frac{3}{2}^-$ unitary singlet.

These predicted states were identified with the 1405-MeV Y_0^* and the 1520-MeV Y_0^*, respectively, and were reinserted into the driving forces. The search for resonances was then repeated with the new driving forces. It was found that, within the limitations of our dynamical model, this set of four unitary-symmetry multiplets formed a closed and consistent system; they were mutually self-supporting. An immediate consequence of the model is the prediction that the Yukawa-coupling mixing parameter, the parameter which determines the baryon-pseudoscalar-meson couplings, should have the value $f = 0.39$. This prediction, as well as other predictions concerning the strength of interaction in various partial-wave channels, appears to be in agreement with the experimental data now available.

II - 21. Pion-Pion Scattering

Jack L. Uretsky, K. Smith (AMD), and A. M. Saperstein

This is a continuing attempt to incorporate relativistic perturbation theory into a sensible theory of the pion-pion interaction. The essence of the idea is to calculate a "generalized potential" from perturbation theory and then to use dispersion-theoretic techniques to obtain the scattering induced by the potential. Thus far the second- and third-order calculations have been completed[1] and it is believed that these have given a consistent model of s-wave scattering up to moderate energies and of p-wave scattering at low energies in terms of a single undetermined parameter λ (the "coupling constant"). The fourth-order calculation (now being prosecuted with W. McGlinn and A. Saperstein), if it predicts the known p-wave resonance at 750 MeV, will then determine λ.

---

[1] K. Smith and J. L. Uretsky, Phys. Rev. 131, 861 (1963); A. M. Saperstein and J. L. Uretsky, Phys. Rev. 133, B1340 (1964).

II - 22. Pion-Nucleon Scattering

Jack L. Uretsky and Arthur Martin

The implications of the so-called "one nucleon exchange force" for pion-nucleon scattering have been investigated. If this force actually describes the long-range part of the pion-nucleon interaction, then it should provide an adequate description of the observed high partial waves. It is also reputed to be responsible for the well-known $T = 3/2$, $J = 3/2$ pion-nucleon resonance. In fact, our calculations confirmed neither of the expectations. In the first place we learned that within the dispersion-theoretic computational framework it is not possible to give an unambiguous formulation of the problem. In terms of the most reasonable class of formulations, however, it turned out that the one-nucleon exchange force

was much too strong to give a reasonable description of "physics." A paper describing this work has been submitted to the Physical Review.

II - 23. Hypernuclei and ΛΛ Hypernuclei

A. R. Bodmer

Hypernuclei are being studied with the aim of elucidating their structure, of obtaining knowledge about the Λ-N interaction, and also of investigating the Λ particle in the role of a nuclear probe. A study of the hypertriton using meson theoretical potentials with a hard core is being considered with the aid of a new powerful and flexible variational method for three-body systems described in a paper with S. Ali, to appear in Nuclear Physics. Another problem under consideration is the modification of the Λ-N interaction in nuclear matter.

A study of ΛΛ-hypernuclei is in progress. Hard-core potentials, and in particular meson-theoretical potentials, are being considered for the Λ-Λ interaction. The three-body method referred to is also being used here. The effect of distortion of the core nucleus by the Λ particles is being studied and provisional estimates for ${}_{\Lambda\Lambda}Be^{10}$ show this to be quite appreciable.

III. EXTRANUCLEAR PROPERTIES OF MATTER

The largest program in Extranuclear Properties of Matter is the mass spectrometric studies. In addition, a modest effort in plasma physics concerns itself mainly with the properties of rf plasmas and the containment of plasmas in rf cavity fields.

III - 1. MASS SPECTROMETRIC INVESTIGATIONS

The mass-spectrometric investigations involve seven instruments, each designed for a specified task; and another (MA-24) is nearing completion. They include MA-15B, used primarily for the study of the molecular composition of high-temperature vapors and the kinetics of gas-phase reactions; two spectrometers designed for isotopic analysis applied to geochronometry (MA-16B employing surface ionization of solid samples, and MA-18 using electron-bombardment ionization for gaseous samples); MA-17, which incorporates an energy analyzer and is used for determining the kinetic energy of fragment ions; MA-23, having a high-speed pumping system necessary for the study of higher pressure phenomena, such as consecutive ion-molecule reactions and ionic fragments produced by nuclear decay; and a portable mass spectrometer (MA-27) which can be used in conjunction with particle accelerators for the study of ionization in gases and sputtering of solids by high-energy particles. In addition, an Atlas Werke mass spectrometer has been adapted so that interactions between ions or atoms and a metal surface can be studied by pulsed-beam techniques, and is also used for studying the diffusion of salts through metals.

In addition to the basic information that these studies provide about the fundamental atomic and molecular properties of matter (i.e., molecular structure, and the thermodynamics and kinetics of reactions), the results of these investigations can be directly applied to the solution of problems involving rocket propulsion, nuclear reactor technology, radiation chemistry, radiation damage to space vehicles, and re-entry behavior.

III - 1.1. High-Temperature Studies of Equilibria and Chemical Kinetics

(1) Gas-Phase Chemical Kinetics (Project II-28)

W. A. Chupka

In this program, a statistical theory has been used to calculate the kinetic energy released in the fragmentation of polyatomic molecular ions produced by electron impact. In most cases the results are in agreement with experimental values and provide support for the statistical model used to explain these decompositions. Resumption of experimental work on the unimolecular decomposition of excited molecular ions awaits the completion of the new mass spectrometer MA-24 together with the vacuum ultraviolet monochromator and associated photoionization apparatus.

(2) High-Temperature Studies (Project II-29)

J. Berkowitz, W. A. Chupka, and F. E. Stafford

We have used a mass-spectrometric technique to study the reaction of BaO (solid) with water vapor and have interpreted the observed $BaOH^+$ ion peak as originating from neutral BaOH and $Ba(OH)_2$ molecules. From a thermodynamic analysis of the data, the Ba—OH bond energy was shown to be much larger than had been believed. The larger ($\sim$ 100 kcal/mole vs $\sim$ 60 kcal/mole) bond energy implies that the concentration of BaOH in the spectral experiments of Sugden et al.[1] were around 10^5 times what had been thought. Hence, the "kinetic" chemiluminescence postulated by these workers need not be invoked;

---

[1] T. M. Sugden, in Annual Reviews of Physical Chemistry (Annual Reviews, Inc., Palo Alto, California, 1962), Vol. 13, p. 381.

"equilibrium" chemiluminescence[2] is the most probable interpretation.

The systems currently being studied include some hydroxides and intermetallic compounds—systems whose bond energies are poorly understood.

---

[2] F. E. Stafford and J. Berkowitz, J. Chem. Phys. (May 1964).

(3) Vaporization Phenomena Involving Sulfur[1]

J. Berkowitz and W. A. Chupka

In previous studies at this laboratory, sulfur vapor was investigated under equilibrium conditions and the bond energies of all species from S_2 to S_{10} were determined. Maximum stability was found for the S_8 molecule, in agreement with the prediction of Pauling.

During the course of the above study, various anomalies appeared in experiments on saturated sulfur vapor. They were shown to be due to lack of equilibrium, a circumstance rather rare in high-temperature research and due in this case to the relatively low temperature of the experiment and relatively high stability of the S—S bond (ca. 2.6 eV). It was found that the molecular composition of vapor evaporating from solid sulfur was strongly dependent on the form and past history of the sample and that, for example, at least 200 000 collisons of S_8 molecules with rhombic sulfur surfaces are necessary for the attainment of equilibrium. A very efficient catalyst (Al_2O_3) for equilibrium was found and its probable mechanism established. These findings reconcile a large amount of discordant data of earlier workers.

---

[1] J. Berkowitz and W. A. Chupka, J. Chem. Phys. 40, 287-295 (15 January 1964).

(4) Normal-Mode Vibrations of the S_6 Molecule

J. Berkowitz and W. A. Chupka

Although the preparation of pure but very unstable S_6 in crystals and solution has long been known, no successful infrared or Raman study of this molecule has been made. A comparison of the force constants of S_6 with those of the stable and oft-investigated S_8 would be a valuable addition to the comparison of bond energies of S_6 and S_8 obtained in earlier thermodynamic studies. A normal-coordinate analysis of S_6 was made and the force constants of S_8 were used to predict the normal-mode frequencies of S_6. Infrared investigations (with equipment of the Chemistry Division) led to the observation of two of the three infrared-active frequencies which are in reasonable agreement with calculation. Attempts to obtain a Raman spectrum failed because the commercial Raman apparatus available uses a mercury line which is strongly absorbed by S_6. Tentative plans have been made to use a laser light source for future Raman work on S_6.

(5) Vapor Ejected by Laser Light Focused on Various Solids[1]

J. Berkowitz and W. A. Chupka

One of the goals of this research has been to determine whether the molecular composition of ejected vapor corresponds to chemical equilibrium at temperatures difficult to attain in the steady state. The experimental technique involves pulsing a ruby laser, and focusing the emitted light on a target located inside a mass spectrometer. The neutral species ejected are then ionized by electron impact, mass analyzed, and detected by photographing an oscilloscope trace. With the two materials

---

[1] J. Berkowitz and W. A. Chupka, J. Chem. Phys. (May 1964).

studied thus far (graphite and boron), the evidence suggests that a molecular composition characteristic of the saturated vapor at ca. 4000°K would explain the results obtained. With graphite, molecules as large as C_{14} were detected; with boron targets, B_5 was observed. If further studies confirm the existence of chemical equilibrium in the jet, this represents a major extension of the range of pressure and temperature over which the high-temperature gas-phase behavior of matter can be studied.

(6) Optical Spectra of Laser-Ejected Jets

J. Berkowitz and W. A. Chupka

In an attempt to understand the phenomena occurring in the ejected jet following laser impact, the visible emission from this jet was studied photographically and spectrographically as a function of the ambient gas. A graphite jet ejected in an environment of argon at one atmosphere was found to produce ca. 100 times as intense an emission as that in helium. The spectrum consisted of the C_2 Swan bands and the 4050 Å pseudocontinuum of C_3, with another continuum centered around 5900 Å. Of the various hypotheses offered to explain this disparity in light emission, the most plausible at the moment involves the preferential cooling of vibrational excitation in carbon species by helium, relative to argon. The unquenched molecules can then convert vibrational excitation to electronic excitation in collision; this results in a higher apparent excitation in an argon environment.

An earlier spectrographic observation of the graphite jet in air revealed the presence of intense CN bands. Recent work at this laboratory has shown (surprisingly) that oxygen is a necessary ingredient for the production of these CN bands. The laser-impact technique shows promise as a tool for production of certain spectra and possibly for the study of some high-temperature chemical reactions.

III - 1.2. Atomic and Ionic Impact Phenomena on Metal Surfaces

M. Kaminsky

(1) Channeling of Energetic Recoil Atoms in fcc Monocrystals

The existence of preferred ejection directions in the back-sputtering of target particles from monocrystals under ion impact in the Rutherford collision region (reported tentatively earlier[1]) has been fully established. Such studies in the Rutherford collision region allow the first significant check on the different suggested types of atomic collision sequences (e.g., hard-sphere collision chain, lens focusing, channeling) since the mean free path λ for the production of the first primary knock-on becomes comparable to or even larger than the estimated ranges of the above-mentioned mechanisms of momentum transfer between energetic recoil atoms and quasi-stationary lattice atoms. Autoradiographs and optical transmission measurements of the deposit of particles back-sputtered from the (100) and (111) planes of copper and silver monocrystals under bombardment by 0.1—2-MeV deuterons at various angles of incidence reveal a pattern of spots along the [110], [100], and [112] directions (Fig. III-1-a), the densities of the deposits decreasing in that order (in contrast to low-energy sputtering). These results agree with the theoretically expected decrease in the effectiveness of channeling of energetic recoil atoms in fcc metals and indicate that the lens-focusing mechanism and the hard-sphere collision chains contribute relatively little to the observed pattern.[2]

---

[1] M. Kaminsky, Phys. Rev. 126, 1267 (1962).

[2] M. Kaminsky, Atomic and Ionic Impact Phenomena on Metal Surfaces, Monograph 25 in the series "Struktur und Eigenschaften der Materie," (Springer, Verlag, Heidelberg, Berlin), in press.

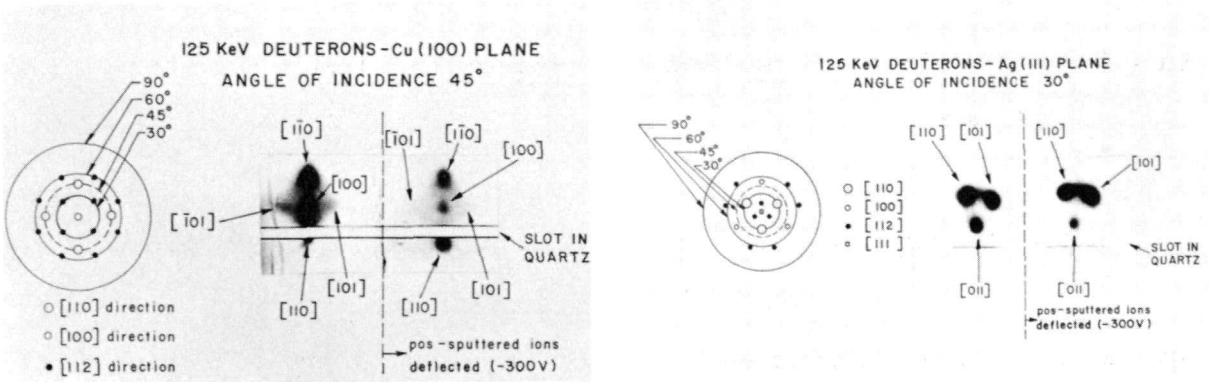

Fig. III-1-a. Patterns of preferential ejection for sputtered particles: left, for a (100) plane of Cu bombarded by 125-keV deuterons incident at 45° from the normal; right, for a (111) plane of Ag bombarded by 125-keV deuterons incident at 30°. In the photographs of the deposits, the patterns to the left of the dotted lines are due to both ions and neutrals; those to the right are due to neutral particles only. The numbers in brackets indicate the crystallographic directions along which the particles are ejected. The other spots indicated in the stereographic projections are faint but can be seen on the original negative.

These experiments will be extended to other fcc and bcc metals for various types of incident ions to establish the relative importance of the various types of atomic collision sequences. Also, the studies will be extended to transmission-sputtering experiments of evaporated monocrystalline foils.

(2) Studies of the Sputtering Ratio and the Ionic Etching of Monocrystals by Ion Impact

The dependence of the sputtering ratio S on the incident-ion energy (Fig. III-1-b), the angle of incidence, and the crystal structure of the target has been investigated in the Rutherford collision region with an experimental technique described earlier. These experiments provide the first adequate test of various theoretical models to explain back sputtering in this energy region.

Electron microscope studies of the target surfaces after

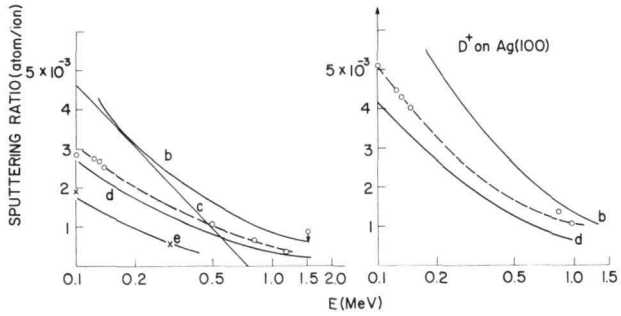

Fig. III-1-b. Comparison of the calculated sputtering ratios with those determined experimentally by bombarding the (100) planes of Cu and Ag monocrystals with deuterons at normal incidence and with energies in the Rutherford collision region. The experimental points are connected by dashed lines; the solid lines represent various theoretical predictions.

the high-energy ion bombardment revealed three types of surface etch pits and showed that the ionic attack is greater in close-packed crystal planes.

With the aid of the newly installed 2-MeV Van de Graaff, the study of the sputtering ratio will be extended over the energy region $150 < E < 500$ keV, where there is now a gap in the data.

(3) Species of Particles Leaving a Monocrystalline Target in a Charged or Uncharged State under High-Energy Ion Bombardment

A portable mass spectrometer (MA-27) has been used in conjunction with a 4.5-MeV Van de Graaff accelerator and a Cockroft-Walton generator to determine the species of particles leaving the (110) and (100) planes of monocrystals of copper and silver under the impact of protons, deuterons, and He^+ ions in the energy range from 0.1—0.25 MeV and from 0.7 to 2.0 MeV. The intensity of various neutral molecular species (such as Cu_2 and CuO) has been determined relative to the atomic species. In addition, singly-charged Cu ions have been observed, but no multiply-charged ions could be detected. The ratio of particles sputtered as positive ions to those as neutrals was determined

(1) mass spectrometrically, (2) by autoradiographic comparison, and (3) from additional measurements of the emitted secondary ions and their distributions in angle and energy. The results were interpreted in terms of charge-changing collisions between energetic recoil atoms and quasi-stationary lattice atoms.

(4) Secondary-Electron and Secondary-Ion Emission from Metal Monocrystal Planes under Ion Impact in the Rutherford Collision Region

Both the secondary-electron yield γ and the secondary-ion yield g for the (100) planes of copper and silver monocrystals bombarded by protons and deuterons have been measured as a function of the angle of incidence α and of the bombarding energy in the range 0.10—0.15 MeV and 0.5—2.0 MeV. In these energy regions the yield γ decreases with increasing energy of the incident ion. The data indicate a close relationship between $\gamma(v)$ and $\sigma_i(v)$, where v is the velocity of the incident ion and σ_i is the cross section for ionizing a lattice atom. The function $\gamma(\alpha)$ appears to have minima at the angles for which channeling of the incident beam is most effective and maxima at angles at which there is maximum density of lattice points projected onto the surface plane. Preliminary experiments indicate a similar angular dependence for the ion yield $g(\alpha)$. The studies of the functions $\gamma(E,\alpha)$ and $g(E,\alpha)$ will be continued with an improved collector system which will also allow a better determination of the angular distribution of secondary electrons and secondary ions.

(5) Studies with a Pulsed-Molecular-Beam Mass Spectrometer

In these experiments modulated atomic beams consisting predominantly of rubidium, or molecular beams of rubidium halides, impinge with thermal energies on heated atomically-clean surfaces of polycrystalline

and monocrystalline tungsten. The experimental arrangement[1] allows the direct determination of the desorption probabilities (inverse of the mean absorption lifetime) of the rubidium atoms and ions from the tungsten surface and the measurement of the ionization degree. The experiments are performed for various surface temperatures to allow the determination of the desorption energies for the atoms and ions, which in turn lead to a determination of the activation energy for the charge-transfer process between adatom and surface.[2] For each beam temperature used, the intensity of the incident beam is varied between approximately 10^{12} and 10^{16} particles/cm^2 to study how the surface coverage by the beam material itself affects the desorption probabilities. Both the composition of the incident beam and also the atomic and molecular species of particles desorbing from the target surface after the bombardment are determined mass spectrometically.

---

[1] M. Kaminsky, Phys. Verhandlung 1-2, 60 (1962).

[2] M. Kaminsky, Advanced Energy Conversion 3, 255 (1963).

III - 1.3. Installation and Modification of a 2-MeV Van de Graaff and an Associated Beam-Handling System

M. Kaminsky and J. R. Wallace

An electron accelerator shipped from Notre Dame University in the summer of 1963 has been converted into a positive-ion machine in order to aid in our studies of impact phenomena of energetic ions and neutral atoms (after charge exchange) on solids and of radiation damage effects in solids. The new machine fills the energy gap between the Cockcroft-Walton generators and the Van de Graaff accelerators already in operation at Argonne. J. R. Wallace, W. F. Evans, and G. Schultz have built an rf ion source for the machine. A positive-ion tube was installed, the focusing and voltage-control systems were modified, and shielded target and control

rooms were constructed. Preliminary tests in March 1964 indicated that a 70-μA mass-analyzed proton beam could be delivered over the energy range from 0.175 to 1.5 MeV; a better tune-up is expected to give considerably higher target currents. For experiments on back sputtering and transmission sputtering, the planned construction of a surface-ionization source to produce alkali and alkaline earth ions will allow the incident ions to be varied over a wide range of mass and atomic number sometimes exceeding those of the target atom.

A temporary beam-handling system (Fig. III-1-c) is being used in the present experiments on back sputtering of monocrystals

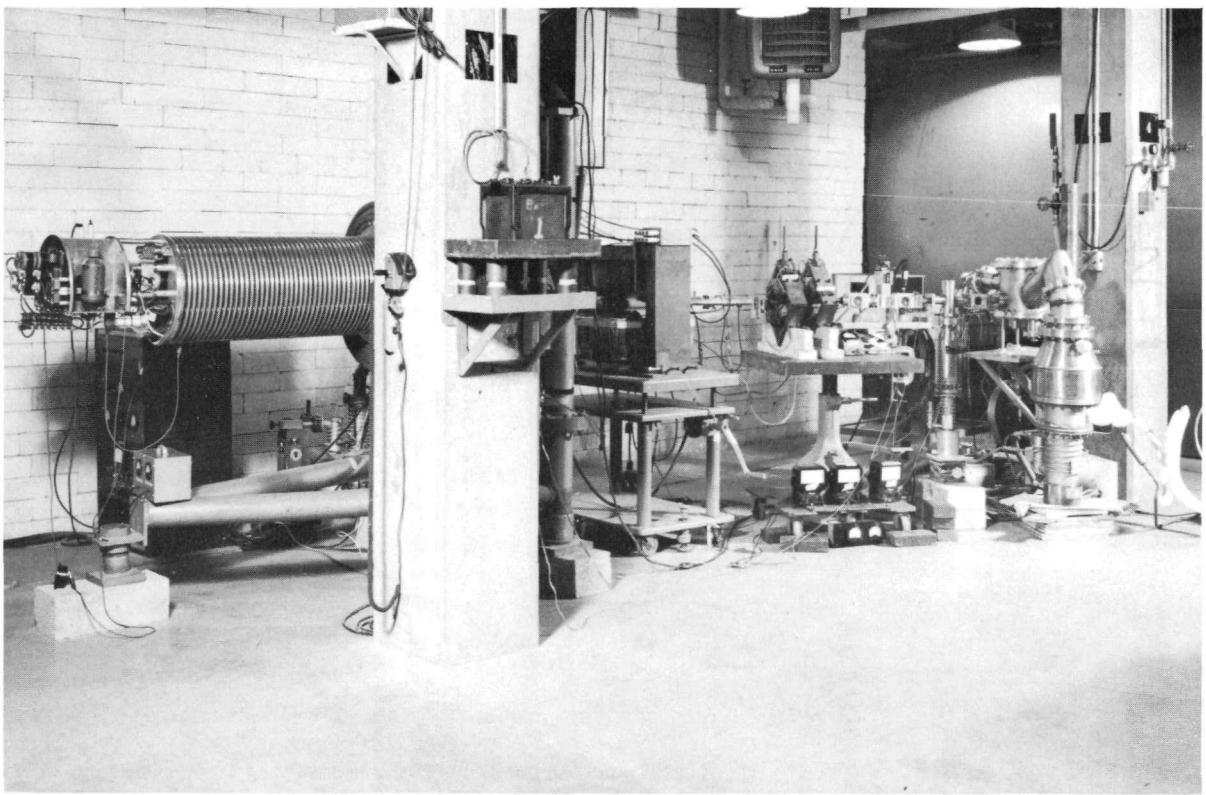

Fig. III-1-c. The 2-MeV Van de Graaff with the temporary beam-handling system.

by mass-analyzed deuterons. Beam currents up to 22 μA at energies as low as 150 keV have been focused on a target spot 1.5 mm in diameter. A beam-handling system purchased from the High Voltage Engineering Corp. is to be delivered in May. It consists of a double-focusing analyzing magnet, two magnetic alternating-gradient lenses, an electrostatic beam-steering system, and the associated slit systems, viewers, power supplies, and controls. It is designed to handle beams over the range from 150-keV protons to 1-MeV Cs^+ ions with a mass resolution $M/\Delta M = 200$ at 10% of the peak height and to focus the beam on a spot about 2 mm in diameter. Approximately 90% of the beam passing the entrance slit is to be focused on an area of about 3.1 mm^2 on the target. To increase the transmission of the ion beam, it is planned to install a quadrupole lens between the exit port of the Van de Graaff and the entrance slit of the analyzing magnet, and the acceleration tube may have to be modified or replaced for the heavy-ion acceleration.

III - 1.4. Fragmentation of Hydrocarbons (Project II-40)

H. E. Stanton and J. E. Monahan

Existing theories concerned with the fragmentation of organic molecules under electron impact postulate a distribution of the energy imparted by the electrons among the various modes of excitation of the molecule. The energy then becomes randomized in the molecule and the problem may be treated as a system in equilibrium.

It appears that some of the basic concepts may require some revision as a result of studies of molecular fragmentation with higher electron energies. The fragmentation pattern for several hydrocarbon molecules was measured for energies of bombarding electrons from about 150 eV to over 2000 eV and the various fragment yields were examined as a function of this energy. It was found that two classes of

fragments were defined by this energy dependence of their yields. One class, which was more numerous and contained fragments with ordinarily larger yields, decreased less rapidly with electron energy than the other which comprised the ions with smaller yields. The former class corresponded to fragments formed in transitions characterized by dipole coupling between the initial and final states whereas the corresponding matrix element for the others was zero. If this interpretation is correct, the initial molecule-ion may be formed in either one of two possible classes of noninteracting excited states. Complete interchange of energy between these two sets of states would, therefore, be inhibited.

III - 2. HIGH-FREQUENCY PLASMAS

The central purpose of this research is to advance the understanding of the basic properties of low-pressure gaseous discharges and plasmas produced by high-frequency fields. The dynamic properties of all plasmas—irrespective of the means of excitation—are manifested by several resonant and cutoff frequencies in the megacycle and gigacycle range. Although the unusual cooperative phenomena in high-frequency plasmas will have technological applications involving excitation, heating, and containment, the primitive state of present knowledge of these phenomena demands that current emphasis be placed mainly on the basic dynamical processes per se.

The two lines along which the plasma research at Argonne is proceeding are (1) the experimental and theoretical study of plasmas produced in the approximately uniform electric field between plane parallel electrodes, and (2) the experimental and theoretical study of plasmas produced in the nonuniform standing-wave electromagnetic fields in resonant cavities. The dynamic properties of underlying interest in the present work are the Langmuir-Tonks frequency for cooperative longitudinal electron plasma oscillations, and the associated cutoff electron density above which field penetration into the plasma is highly attenuated. All of the experimental work is performed in a newly installed rf-shielded room 16 ft × 24 ft × 8 ft high.

III - 2.1. Plasmas in Uniform Electric Fields

A. J. Hatch, R. J. Freiberg, and S. V. Paranjape

This is a comprehensive comparative study of the eight known types of discharges and plasmas observed to occur within a 6-decade pressure range that includes the collision-frequency transition (i.e., the pressure at which the collision frequency equals the radian frequency of the applied field). The plasmas are produced in air between plane parallel metal electrodes 25 cm in diameter and 15 cm apart at a frequency of 15 Mc/sec. A recent result shown in Fig. III-2-a is the first measurement of the complex admittance of the various types of discharge, all at approximately constant input rf power. Of major interest here are the

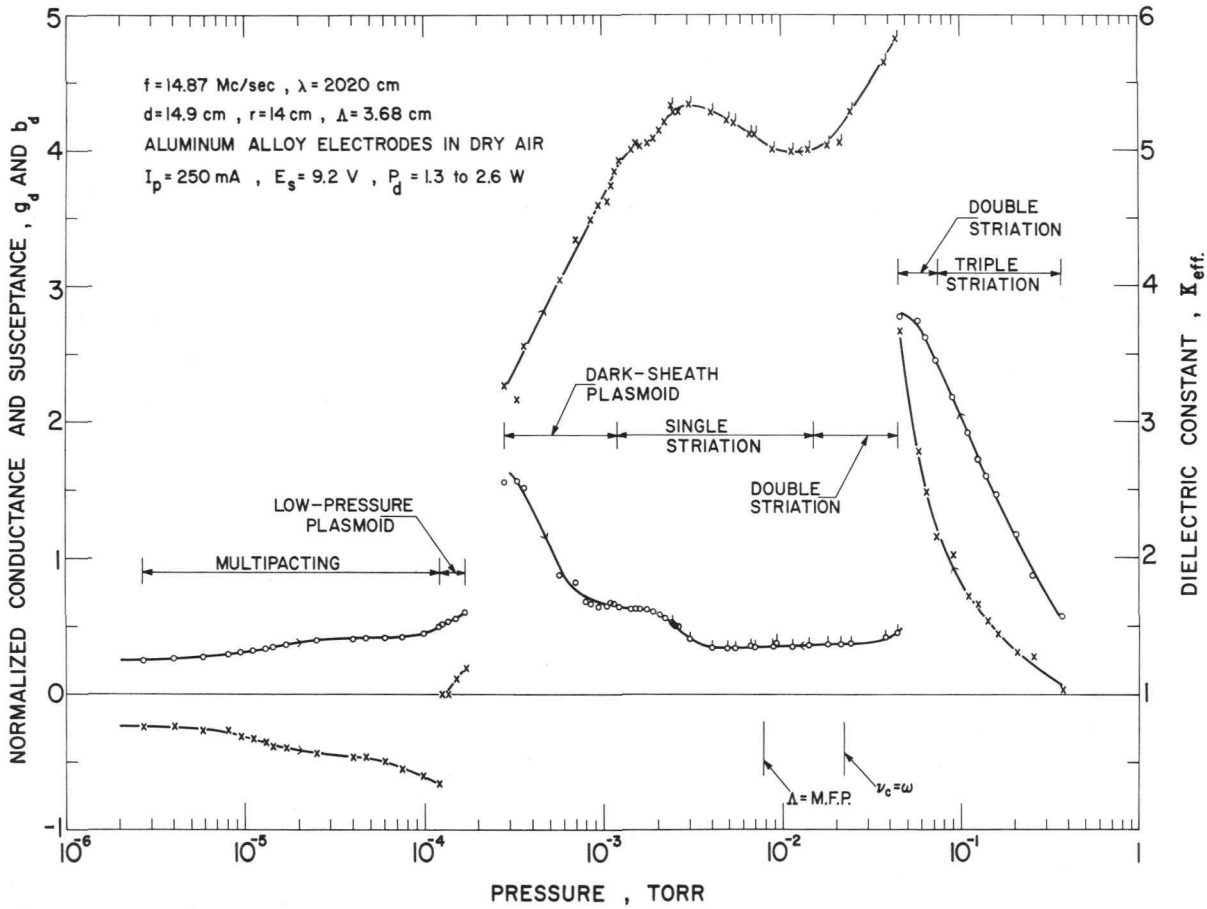

Fig. III-2-a. Admittance components of high-frequency discharges and plasmas, normalized to susceptance of electrodes without plasma. Conductance indicated by open circles; susceptance indicated by crosses.

large positive values of susceptance and the associated large values of effective dielectric constant κ at pressures above 2×10^{-4} Torr. The significance of this result is that it helps to clarify a 40-year controversy that is now seen to hinge mainly on the hitherto unappreciated distinction between the intrinsic $\kappa < 1$ of a free electron plasma and the effective $\kappa > 1$ of a quasi-bound electron plasma. The mechanism involved appears to be the forced cooperative axial oscillations of electrons bound to the central plasma by space charge in the surrounding sheath regions.

Other phases of the research in preliminary stages include (a) photographic studies of the visible structure of the discharges as

related to internal properties,[1] and (b) dc and rf probe studies of electric fields,[1] electron temperatures, and electron and ion densities. In addition, a theoretical study begun during the past year has as its goal the machine computation of admittance for free electrons and for quasi-bound electrons, both as a function of a wide range of the significant parameters of electron density and collision frequency. A new ultra-high-vacuum system now nearing completion will permit measurements to be made in pure gases rather than in air.

III - 2.2. Plasmas in Nonuniform (Cavity) Electromagnetic Fields

A. J. Hatch

A new facility for the study of discharges and plasmas in the nonuniform standing-wave fields of resonant cavities is expected to come into operation by mid-1964. This facility includes a tunable 2-kW CW 4-cavity klystron power amplifier which will excite plasmas in copper-lined cylindrical cavities in the UHF frequency range from 610 to 985 Mc/sec. The first observations will be the systematic exploration and mapping of the domains of visibly distinguishable plasma phenomena as a function of input rf power and gas pressure, and the subsequent measurements of plasma admittance and other properties. Special attention will be given to coherent radiation pressure caused by gradients in the standing-wave electromagnetic fields and to indications of plasma containment near the central nodal points in quadrupole modes.[2]

The potential-well theory of radiation pressure containment of dense plasmas has recently been applied to the related problem of electromagnetic levitation of nonmagnetic metallic bodies.

---

[1] A. J. Hatch, Proceedings of the Fifth International Conference on Ionization Phenomena in Gases (North Holland Publishing Co., Amsterdam, 1962), Vol. I, p. 748.

[2] A. J. Hatch, U.S. Patent No. 3,120,477, February, 1964.

IV. PUBLICATIONS FROM 1 APRIL 1963 THROUGH 31 MARCH 1964

The papers listed here are those whose publication was noted by the reporting unit of the Laboratory in the 1-year period stated above. The dates on the journals therefore are often earlier. The list of papers and books includes letters and notes; the list of abstracts includes all papers presented at meetings—even in cases in which the complete text was published in a volume of proceedings.

IV - 1. PUBLISHED PAPERS AND BOOKS

1. DISTRIBUTION OF PARTIAL RADIATION WIDTHS
   L. M. Bollinger, R. E. Coté, R. T. Carpenter, and J. P. Marion
   Phys. Rev. 132, 1640-1662 (15 November 1963).

2. SLOW-NEUTRON CAPTURE GAMMA RAYS IN Hg^{200}
   R. E. Segel, R. K. Smither, and R. T. Carpenter
   Phys. Rev. 133, B583-B590 (10 February 1964).

3. DOUBLE ISOMERISM IN As^{73}
   H. H. Bolotin
   Phys. Rev. 131, 774-777 (15 July 1963).

4. PROPERTIES OF CAPTURE GAMMA-RAY SPECTRA OF s-WAVE AND p-WAVE RESONANCES IN Zr, Nb, AND Mo
   H. E. Jackson
   Phys. Rev. 131, 2153-2162 (1 September 1963).

5. TOTAL RADIATION WIDTHS FOR s-WAVE AND p-WAVE NEUTRON CAPTURE IN Nb^{93}
   H. E. Jackson
   Phys. Rev. Letters 11, 378-380 (15 October 1963).
   ERRATUM: Phys. Rev. Letters 11, 488 (15 November 1963).

6. ON THE LIFETIME OF THE ODD-PARITY LEVEL IN ^{144}Nd
   P. Rice-Evans
   Proc. Phys. Soc. (London) 82, 914-917 (1 December 1963).

7. NONLOCAL OPTICAL-MODEL ANALYSIS OF NEUTRON SCATTERING FROM NUCLEI NEAR A = 100 AT ENERGIES BELOW 1 MEV
   A. J. Elwyn, R. O. Lane, A. Langsdorf, Jr., and J. E. Monahan
   Phys. Rev. 133, B80-B93 (13 January 1964).

8. POLARIZATION AND DIFFERENTIAL CROSS SECTION OF NEUTRONS SCATTERED FROM Be^{9}: PARITIES OF THE 7.37- AND 7.54-MEV STATES IN Be^{10}
   R. O. Lane, A. J. Elwyn, and A. Langsdorf, Jr.
   Phys. Rev. 133, B409-B419 (27 January 1964).

9. NUCLEAR LEVELS OF F^{20}
   C. T. Hibdon
   Phys. Rev. 133, B353-B369 (27 January 1964).

10. (n,2n) REACTION CROSS SECTIONS FROM 12 TO 19.6 MEV
    L. A. Rayburn
    Phys. Rev. 130, 731-734 (15 April 1963).

11. 3.86-MEV LEVEL IN F^{17}
    R. E. Segel, P. P. Singh, R. G. Allas, and S. S. Hanna
    Phys. Rev. Letters 10, 345-347 (15 April 1963).

12. TECHNIQUES FOR THE STUDY OF RADIATIVE ALPHA-CAPTURE REACTIONS
    J. A. Weinman
    Nucl. Instr. Methods 24, 390-394 (October 1963).

13. THE EFFECT OF TARGET THICKNESS AND BEAM STRAGGLING ON THE MAGNITUDE OF RESONANCES IN ELASTIC SCATTERING EXPERIMENTS
    J. A. Weinman
    Nucl. Instr. Methods 21, 181-182 (1963).

14. STATES IN Si^{28} WITH $12.7 < E_x < 13.7$ MEV BY (α,γ) AND (α,α) REACTIONS ON Mg^{24}
    J. A. Weinman, L. Meyer-Schützmeister, and L. L. Lee, Jr.
    Phys. Rev. 133, B590-B597 (10 February 1964).

15. THE OBSERVATION OF Be^{8} IN THE GROUND STATE
    J. A. Weinman and R. K. Smither
    Nucl. Phys. 45, 260-272 (1963).

16. A TEST OF THE STATISTICAL NATURE OF FLUCTUATIONS IN NUCLEAR CROSS SECTIONS
    L. L. Lee, Jr., and J. P. Schiffer
    Phys. Letters 4, 104-105 (15 March 1963).

17. MEASUREMENT OF SPINS OF SOME STATES IN Ca^{41}
    L. L. Lee, Jr., J. P. Schiffer, and D. S. Gemmell
    Phys. Rev. Letters 10, 496-498 (1 June 1963).

18. EXPERIMENTAL EVIDENCE FOR THE J DEPENDENCE OF THE ANGULAR DISTRIBUTION FROM (d,p) REACTIONS
    L. L. Lee, Jr., and J. P. Schiffer
    Phys. Rev. Letters 12, 108-110 (27 January 1964).

19. SEARCH FOR A PARTICLE-STABLE TETRA NEUTRON
    J. P. Schiffer and R. Vandenbosch
    Phys. Letters 5, 292-293 (15 July 1963).

20. PROTON WIDTHS IN A DIFFUSE WELL
    J. P. Schiffer
    Nucl. Phys. 46, 246-250 (July 1963).

21. THE PREPARATION OF THIN SELF-SUPPORTING BORON FILMS
    J. R. Erskine and D. S. Gemmell
    Nucl. Instr. Methods 24, 397-398 (October 1963).

22. THE $Ta^{181}(d,p)Ta^{182}$ REACTION AND A BAND-MIXING ANALYSIS OF THE OBSERVED ENERGY LEVELS
    J. R. Erskine and W. W. Buechner
    Phys. Rev. 133, B370-B377 (27 January 1964).

23. COLLECTIVE EXCITATIONS IN $Ni^{58,60,62}$ AND $Zn^{64,66,68}$
    H. W. Broek
    Phys. Rev. 130, 1914-1925 (1 June 1963).

24. (d,p) REACTION ON THE TITANIUM ISOTOPES
    J. L. Yntema
    Phys. Rev. 131, 811-817 (15 July 1963).

25. STEREOSCOPIC TELEVISION SYSTEM
    W. J. O'Neill
    Nucl. Instr. Methods 24, 45-48 (July 1963).

26. NUCLEAR SPIN AND MAGNETIC HYPERFINE INTERACTION OF 12-DAY Ge^{71}
    W. J. Childs and L. S. Goodman
    Phys. Rev. 131, 245-250 (1 July 1963).

27. MAGNETIC HYPERFINE INTERACTION OF Cr^{53}
W. J. Childs, L. S. Goodman, and D. von Ehrenstein
Phys. Rev. 132, 2128-2135 (1 December 1963).

28. DETERMINATION OF ISOTOPIC DIFFERENCES IN MESIC X RAYS IN CALCIUM
H. L. Anderson,* C. S. Johnson,* E. P. Hincks,† S. Raboy, and C. C. Trail
Phys. Letters 6, 261-264 (15 September 1963).

29. THE MÖSSBAUER EFFECT FOR Fe^{57} IN BERYLLIUM, COPPER, TUNGSTEN, AND PLATINUM
J. P. Schiffer, P. N. Parks, and J. Heberle
Phys. Rev. 133, A1553-A1557 (16 March 1964).

30. MÖSSBAUER EFFECT IN CHEMICAL COMPOUNDS OF Xe^{129}
C. L. Chernick, C. E. Johnson, J. G. Malm, G. J. Perlow, and M. R. Perlow
Phys. Letters 5, 103-104 (15 June 1963).

31. STRONG M1 TRANSITIONS IN LIGHT NUCLEI
D. Kurath
Phys. Rev. 130, 1525-1529 (15 May 1963).

32. PHASE RELATION IN NUCLEAR SCATTERING
D. R. Inglis
Nucl. Phys. 44, 460-471 (July 1963).

33. THE DEFORMATION ENERGY OF A CHARGED DROP: PART V: RESULTS OF ELECTRONIC COMPUTER STUDIES
S. Cohen and W. Swiatecki (Lawrence Radiation Laboratory)
Ann. Phys. 22, 406-437 (June 1963).

34. CALCULATION OF DEUTERON STRIPPING AMPLITUDES USING S-MATRIX REDUCTION TECHNIQUES
A. M. Saperstein
Phys. Rev. 130, 2054-2060 (1 June 1963).

---

*University of Chicago, Chicago, Illinois.

†National Research Council of Canada, Ottawa, Ontario, Canada.

35. STATISTICAL MECHANICS OF EQUALLY LIKELY QUANTUM SYSTEMS
    N. Rosenzweig
    Section II in Statistical Physics by G. E. Uhlenbeck, N. Rosenzweig, A. F. Siegert, E. Jaynes, and S. Fujita (W. A. Benjamin, Inc., New York, June 1963), pp. 91-158.

36. ANOMALOUS STATISTICS OF PARTIAL RADIATION WIDTHS
    N. Rosenzweig
    Phys. Letters 6, 123-125 (15 August 1963).

37. NOTE ON A CRUDE NUCLEON-NUCLEON POTENTIAL
    F. Coester and E. Yen (University of Iowa)
    Nuovo Cimento 30, 674 (1963).

38. AN S-STATE INTERACTION WITH PAIRING-TYPE PROPERTIES IN THE NUCLEAR SHELL MODEL
    S. P. Pandya
    Phys. Letters 7, 342-343 (15 December 1963).

39. REVIEW OF "LIAPUNOV'S METHODS IN AUTOMATIC CONTROL THEORY" PARTS 1 AND 2 BY P. C. PARKS
    J. E. Monahan
    Computing Reviews 4, 161 (July-August 1963).

40. THE PRINCIPLE OF EQUIVALENCE
    F. Rohrlich
    Ann. Phys. 22, 169-191 (May 1963)

41. PREACCELERATION IN ELECTRON THEORY
    M. N. Hack
    Nuovo Cimento 29, 298-301 (1963).

42. FLUXOID QUANTIZATION, PAIR SYMMETRY, AND THE GAP ENERGY IN THE CURRENT-CARRYING BARDEEN-COOPER-SCHRIEFFER STATE
    M. Peshkin
    Phys. Rev. 132, 14-20 (1 October 1963).

43. SPIN AND PARITY ANALYSIS AT ALL PRODUCTION ANGLES
    M. Peshkin
    Phys. Rev. 133, B428-B430 (27 January 1964).

44. COUPLED-CHANNEL APPROACH TO $J = \frac{3}{2}^+$ RESONANCES IN THE UNITARY SYMMETRY MODEL
A. W. Martin and K. C. Wali
Phys. Rev. 130, 2455-2467 (15 June 1963).

45. A DYNAMICAL MODEL FOR ω-φ MIXING
A. Katz and H. J. Lipkin
Phys. Letters 7, 44-47 (15 October 1963).

46. UNITARY SYMMETRY IN PHOTOPRODUCTION AND OTHER ELECTROMAGNETIC INTERACTIONS
C. A. Levinson,* H. J. Lipkin, and S. Meshkov†
Phys. Letters 7, 81-84 (15 October 1963).

47. ON THE PRODUCTION OF THE Z^- (Ω^-) BARYON
H. J. Lipkin, C. A. Levinson,* and S. Meshkov†
Phys. Letters 7, 159-161 (1 November 1963).

48. BOSON COUPLINGS AND HIGHER SYMMETRIES
H. J. Lipkin
Phys. Letters 7, 221-222 (15 November 1963).

49. THREE-NEUTRINO HYPOTHESIS
K. Hiida
Nuovo Cimento 27, 1439-1449 (1963).

50. Σ BREAKUP AND THE $\Sigma\Lambda$ RELATIVE PARITY
K. Hiida, J. L. Uretsky, and R. J. Oakes
Nuovo Cimento 27, 1262-1265 (1 March 1963).

51. THEORY OF SPIN-$\frac{1}{2}$ PARTICLES WITH PARITY-NONCONSERVING INTERACTIONS
K. Hiida
Phys. Rev. 132, 1239-1248 (1 November 1963).

52. FAIRLY LOW-ENERGY PION-PION SCATTERING II
A. M. Saperstein and J. L. Uretsky
Phys. Rev. 133, B1340-B1343 (9 March 1964).

---

*Weizmann Institute of Science, Rehovoth, Israel.

†National Bureau of Standards, Washington, D.C.

53. LOW-ENERGY PION-PION SCATTERING
K. Smith and J. L. Uretsky
Phys. Rev. 131, 861-867 (15 July 1963).

54. NONLEPTONIC DECAYS OF HYPERONS
S. N. Gupta
Phys. Rev. 130, 1180-1181 (1 May 1963).

55. A NOTE ON THE MEASURABLE ELECTRIC CHARGE OF SPIN-$\frac{1}{2}$ BOSONS
R. Spitzer
Nuovo Cimento 28, 364-367 (16 April 1963).

56. THE PARITY OF THE NEUTRAL K MESON
R. Spitzer
Nucl. Phys. 47, 367-384 (September 1963).

57. EQUILIBRIUM COMPOSITION OF SULFUR VAPOR
J. Berkowitz and J. R. Marquart
J. Chem. Phys. 39, 275-283 (15 July 1963).

58. DISSOCIATION ENERGIES OF SOME METAL SULFIDES
J. R. Marquart and J. Berkowitz
J. Chem. Phys. 39, 283-285 (15 July 1963).

59. VAPORIZATION PROCESSES INVOLVING SULFUR
J. Berkowitz and W. A. Chupka
J. Chem. Phys. 40, 287-295 (15 January 1964).

60. IONIZATION BY IONS IN THE MEV RANGE
S. Wexler and D. C. Hess
J. Chem. Phys. 38, 2308-2309 (1 May 1963).

61. INTERFERENCE OF LINEARLY POLARIZED LIGHT WITH PERPENDICULAR POLARIZATIONS
A. Langsdorf, Jr.
Am. J. Phys. 31, 624 (August 1963).

62. REFLECTION OF A PLANE SOUND WAVE FROM A SINUSOIDAL SURFACE
J. L. Uretsky
J. Acoust. Soc. Am. 35, 1293-1294 (1963).

IV - 2. PUBLISHED ABSTRACTS

Applications of Computers to Nuclear and Radiochemistry, Proceedings of a Symposium, Gatlinburg, Tennessee, 17-19 October 1962, edited by G. D. O'Kelley (National Academy of Sciences—National Research Council, Washington, D.C.), NAS-NS 3107.

1. A COMPUTER PROGRAM FOR ANALYSIS OF COMPLEX CONTINUOUS BETA-RAY SPECTRA
   S. B. Burson, R. G. Helmer, and T. Gedayloo
   pp. 51-60.

2. ANALYSIS OF GAMMA-RAY SPECTRA
   J. E. Monahan, S. Raboy, and C. C. Trail
   pp. 213-216.

---

3. THE ARGONNE 3-PARAMETER ANALYZER
   L. M. Bollinger
   Proceedings of the Conference on Utilization of Multiparameter Analyzers in Nuclear Physics, Grossinger's, New York, 1962 (U. S. Atomic Energy Commission Report NYO 10595), p. 59.

4. ANGULAR DISTRIBUTIONS OF NEUTRONS
   A. Langsdorf, Jr.
   in Progress in Fast Neutron Physics, the Proceedings of the International Conference on Fast Neutron Physics, Rice University, Houston, Texas, 26-28 February 1963, edited by G. C. Phillips, J. B. Marion, and J. R. Risser (University of Chicago Press, Chicago, 1963), pp. 257-267.

Conference on Compound Nuclear States, Gatlinburg, Tennessee, 10-12 October 1963.

5. POLARIZATION OF NEUTRONS SCATTERED FROM Be^9; PARITIES OF 7.37- AND 7.54-MEV STATES IN Be^{10}
   R. O. Lane, A. J. Elwyn, and A. Langsdorf, Jr.
   Bull. Am. Phys. Soc. 9, 166 (27-29 February 1964).

6. SOME MEASUREMENTS OF FLUCTUATIONS IN NUCLEAR CROSS SECTIONS
   L. L. Lee, Jr., and J. P. Schiffer
   Bull. Am. Phys. Soc. 9, 169 (27-29 February 1964).

American Physical Society meeting, Chicago, 18-19 October 1963.

7. POPULATION OF THE FIRST T = 1 STATE IN B^{10} BY THE REACTION $C^{12}(d,\alpha)B^{10}$
   R. G. Allas, J. R. Erskine, L. Meyer-Schützmeister, and D. von Ehrenstein
   Bull. Am. Phys. Soc. 8, 538 (18-19 October 1963).

8. CAPTURE REACTIONS $Al^{27}(p,\gamma)Si^{28,28*}$ IN THE GIANT-DIPOLE REGION OF Si^{28}
   R. G. Allas, S. S. Hanna, L. Meyer-Schützmeister, R. E. Segel, and P. P. Singh
   Bull. Am. Phys. Soc. 8, 538 (18-19 October 1963).

9. ISOTOPE SHIFT IN THE K_α TRANSITION OF μ-MESIC ATOMS OF Ca^{40} AND Ca^{44}
   H. L. Anderson, C. S. Johnson, E. P. Hincks, S. Raboy, and C. C. Trail
   Bull. Am. Phys. Soc. 8, 522 (18-19 October 1963).

10. LEVELS IN Ga^{66} FROM THE DECAY OF Ge^{66}
    H. H. Bolotin
    Bull. Am. Phys. Soc. 8, 524 (18-19 October 1963).

11. ACCURACY OF THE QUASIPARTICLE RANDOM-PHASE APPROXIMATION (QPRPA) IN NUCLEAR-STRUCTURE CALCULATIONS
    S. Cohen, R. D. Lawson, M. H. Macfarlane, and M. Soga
    Bull. Am. Phys. Soc. 8, 523 (18-19 October 1963).

12. POLARIZATION OF NEUTRONS SCATTERED FROM F, Na, Al, AND P
    A. J. Elwyn, R. O. Lane, and A. Langsdorf, Jr.
    Bull. Am. Phys. Soc. 8, 513 (18-19 October 1963).

13. p-γ ANGULAR CORRELATIONS IN THE REACTION $Fe^{54}(d,p\gamma)Fe^{55*}$
    D. S. Gemmell, L. L. Lee, Jr., A. Marinov, and J. P. Schiffer
    Bull. Am. Phys. Soc. 8, 523-524 (18-19 October 1963).

14. FLUCTUATIONS IN PARTIAL RADIATION WIDTHS OF U^{239}
    H. E. Jackson
    Bull. Am. Phys. Soc. 8, 513-514 (18-19 October 1963).

American Physical Society meeting, Chicago, 18-19 October 1963 (cont'd.).

15. DYNAMICAL ASPECTS OF MESON-BARYON SCATTERING IN THE OCTET MODEL
    A. W. Martin and K. C. Wali
    Bull. Am. Phys. Soc. 8, 515 (18-19 October 1963).

16. OPTICAL-MODEL ANALYSIS OF NEUTRON SCATTERING FROM NUCLEI NEAR A = 100 AT LOW ENERGIES
    J. E. Monahan, A. J. Elwyn, R. O. Lane, and A. Langsdorf, Jr.
    Bull. Am. Phys. Soc. 8, 513 (18-19 October 1963).

17. SPIN-PARITY ANALYSIS AT ARBITRARY PRODUCTION ANGLE
    M. Peshkin
    Bull. Am. Phys. Soc. 8, 514 (18-19 October 1963).

18. SEARCH FOR BOUND STATES IN He^4
    J. L. Yntema, S. S. Hanna, and R. E. Segel
    Bull. Am. Phys. Soc. 8, 537 (18-19 October 1963).

American Physical Society meeting, New York, 22-25 January 1964.

19. STATES IN Ar^{36} WITH EXCITATION ENERGIES BELOW 7 MEV
    R. G. Allas, L. Meyer-Schützmeister, and D. von Ehrenstein
    Bull. Am. Phys. Soc. 9, 79 (22-25 January 1964).

20. NUCLEAR RESONANCE FLUORESCENCE IN Cu^{65}
    G. B. Beard
    Bull. Am. Phys. Soc. 9, 9 (22-25 January 1964).

21. MÖSSBAUER ABSORPTION IN Mg_2Sn^{119}
    F. R. Berg and J. Heberle
    Bull. Am. Phys. Soc. 9, 111 (22-25 January 1964).

22. LEVELS IN Sn^{116} POPULATED BY THE DECAY OF 54-MIN In^{116}
    H. H. Bolotin
    Bull. Am. Phys. Soc. 9, 17 (22-25 January 1964).

23. MAGNETIC HYPERFINE STRUCTURE OF Sn^{117} AND Sn^{119}
    W. J. Childs and L. S. Goodman
    Bull. Am. Phys. Soc. 9, 11-12 (22-25 January 1964).

American Physical Society meeting, New York, 22-25 January 1964 (cont'd.).

24. $Ca^{48}(He^3,d)Sc^{49}$ REACTION
J. R. Erskine, J. P. Schiffer, and A. Marinov
Bull. Am. Phys. Soc. 9, 80 (22-25 January 1964).

25. THE $Fe^{54}(d,n)Co^{55}$ REACTION
D. S. Gemmell, L. L. Lee, Jr., J. P. Schiffer, and A. B. Smith
Bull. Am. Phys. Soc. 9, 92 (22-25 January 1964).

26. MAGNETIC FIELD AT THE NUCLEUS IN A FREE IRON ATOM
L. S. Goodman and W. J. Childs
Bull. Am. Phys. Soc. 9, 12 (22-25 January 1964).

27. ISOMER SHIFTS AND NUCLEAR ZEEMAN EFFECT IN Nb_3Sn^{119}
J. Heberle
Bull. Am. Phys. Soc. 9, 10 (22-25 January 1964).

28. SPIN ASSIGNMENTS OF NEUTRON RESONANCES IN Pd^{105}
H. E. Jackson and R. E. Coté
Bull. Am. Phys. Soc. 9, 21 (22-25 January 1964).

29. HYPERFINE FIELDS AND ISOMER SHIFTS IN BINARY AND TERNARY Fe ALLOYS WITH THE α-MANGANESE STRUCTURE
C. W. Kimball, M. V. Nevitt, and R. S. Preston
Bull. Am. Phys. Soc. 9, 112 (22-25 January 1964).

30. STUDY OF THE REACTION $Fe^{54}(d,p)Fe^{55}$
L. L. Lee, Jr., and J. P. Schiffer
Bull. Am. Phys. Soc. 9, 92 (22-25 January 1964).

31. ISOMERIC STATE OF SCANDIUM-43
F. J. Lynch, K.-E. Nystén, and R. E. Holland
Bull. Am. Phys. Soc. 9, 79-80 (22-25 January 1964).

32. MEASUREMENT OF THE RATIO OF QUADRUPOLE MOMENTS OF Xe^{129*} AND Xe^{131}
G. J. Perlow
Bull. Am. Phys. Soc. 9, 11 (22-25 January 1964).

33. ISOMER SHIFTS IN VANADIUM-RICH bcc V-Fe ALLOYS
R. S. Preston, C. W. Kimball, D. J. Lam, and D. O. Van Ostenburg
Bull. Am. Phys. Soc. 9, 112 (22-25 January 1964).

American Physical Society meeting, New York, 22-25 January 1964 (cont'd.).

34. MISSING TRANSITIONS IN B^{10}
P. P. Singh, R. E. Segel, R. G. Allas, S. S. Hanna, and M. A. Grace
Bull. Am. Phys. Soc. 9, 56 (22-25 January 1964).

35. NEUTRON-CAPTURE GAMMA RAYS FROM Ca^{42}
C. C. Trail and S. Raboy
Bull. Am. Phys. Soc. 9, 21 (22-25 January 1964).

36. DEGENERATE LIMITS OF BROKEN MULTIPLETS AND THE OKUBO MASS FORMULA
K. C. Wali and R. L. Warnock (Illinois Institute of Technology)
Bull. Am. Phys. Soc. 9, 115 (22-25 January 1964).

International Symposium on Direct Interactions and Nuclear Reaction Mechanisms, Padua, Italy, 3-8 September 1962.

37. (d,t) REACTIONS ON NUCLEI NEAR N = 28
T. H. Braid and B. Zeidman
p. 556.

38. COLLECTIVE LEVELS IN 11 ISOTOPES OF Ti, Ni, AND Zn
H. W. Broek and J. L. Yntema
pp. 769-771.

39. DIRECT INTERACTIONS AND NUCLEAR STRUCTURE
M. H. Macfarlane
pp. 3-17.

40. (n,2n) REACTION CROSS SECTIONS IN F^{19}, Cu^{63}, Cu^{65}, AND Zn^{64}
L. A. Rayburn
pp. 322-324.

41. CALCULATION OF REDUCED WIDTHS FROM RESONANT SCATTERING OF PROTONS BY A DIFFUSE POTENTIAL
J. P. Schiffer
pp. 139-142.

42. THE (d,p) REACTION AT 21.4 MEV DEUTERON ENERGY
J. L. Yntema
pp. 553-555.

International Symposium on Direct Interactions and Nuclear Reaction Mechanisms, Padua, Italy, 3-8 September 1962 (cont'd.).

43. THE (d,t) REACTION ON THE TITANIUM ISOTOPES
J. L. Yntema
p. 566.

44. THE (α,d) REACTION ON TITANIUM
J. L. Yntema and W. J. O'Neill
pp. 1084-1086.

45. (d,He^3) REACTIONS ON F^{19} AND Al^{27}
B. Zeidman and T. H. Braid
p. 566.

46. SENIORITY MIXING IN $1f_{7/2}$ NUCLEI
B. Zeidman and R. D. Lawson
pp. 845-847.

---

47. THE MÖSSBAUER EFFECT IN CHEMICAL COMPOUNDS OF Xe^{129}
G. J. Perlow, C. E. Johnson, and M. R. Perlow
in Noble Gas Compounds, the Proceedings of the Conference on Inert-Gas Compounds, Argonne National Laboratory, 22-23 April 1963, edited by H. H. Hyman (University of Chicago Press, Chicago, 1963), pp. 279-283.

Third International Conference on the Mössbauer Effect, Cornell University, 4-7 September 1963.

48. ISOMER SHIFTS IN Fe^{57} FROM Co^{57} DIFFUSED IN V-Al ALLOYS
S. S. Hanna and D. J. Bailey
Rev. Mod. Phys. 36, 395 (January 1964).

49. MANGANESE-TIN ALLOYS IN LARGE EXTERNAL MAGNETIC FIELDS
S. S. Hanna, J. Heberle, J. Diaz, and R. W. Reno
Rev. Mod. Phys. 36, 407 (January 1964).

50. MÖSSBAUER CROSS SECTION IN METALLIC IRON
S. S. Hanna, R. S. Preston, and W. S. Denno
Rev. Mod. Phys. 36, 469-470 (January 1964).

Third International Conference on the Mössbauer Effect, Cornell University, 4-7 September 1963 (cont'd.).

51. SUPERCONDUCTING MAGNETS FOR MÖSSBAUER EXPERIMENTS
J. Heberle
Rev. Mod. Phys. 36, 408-409 (January 1964).

52. MÖSSBAUER EFFECT IN Fe^{57} AND Sn^{119} METALS IN LARGE EXTERNAL MAGNETIC FIELDS
J. Heberle, M. Schulhof, and S. S. Hanna
Rev. Mod. Phys. 36, 407 (January 1964).

53. INTERNAL MAGNETIC FIELD IN GADOLINIUM
L. Meyer-Schützmeister, S. S. Hanna, J. Heberle, J. Diaz, and R. W. Reno
Rev. Mod. Phys. 36, 392 (January 1964).

54. THE MÖSSBAUER EFFECT IN XENON COMPOUNDS
G. J. Perlow and M. R. Perlow
Rev. Mod. Phys. 36, 353-357 (January 1964).

55. MÖSSBAUER ANALYSIS OF IRON IN METEORITES
E. L. Sprenkel-Segel, S. S. Hanna, and D. J. Bailey
Rev. Mod. Phys. 36, 360 (January 1964).

---

56. A PROPOSED SYSTEM TO OBTAIN HIGHER SPACE RESOLUTION IN NUCLEAR EMULSIONS
J. H. Roberts, P. C. Chow, and G. R. Ringo
Korpuskularphotographie IV, Vorträge und Diskussionen auf dem IV. Internationalen Kolloquium über Korpuscular-photographie, Munich, 1962, edited by H. Frieser and G. Heimann (Institut für Wissenschaftliche Photographie der Technischen Hochschule München, Munich, 1963), pp. 587-601.

Midwest Conference on Theoretical Physics, University of Notre Dame, May 31—June 1, 1963.

57. "ELEMENTARY" PARTICLE THEORY OF NUCLEAR REACTIONS
F. Coester
pp. 108-112.

Midwest Conference on Theoretical Physics, University of Notre Dame, May 31—June 1, 1963 (cont'd.).

58. THEORY OF SPIN-$\frac{1}{2}$ PARTICLES WITH PARITY-NONCONSERVING INTERACTIONS
K. Hiida
pp. 96-100.

59. THE BOOTSTRAP METHOD IN THE PHYSICS OF STRONG INTERACTIONS
B. M. Udgaonkar
pp. 65-79.

Proceedings of the Third Conference on Reactions Between Complex Nuclei (Asilomar, Pacific Grove, California, 14-18 April 1963), edited by A. Ghiorso, R. M. Diamond, and H. E. Conzett (University of California Press, Berkeley and Los Angeles, 1963).

60. EQUILIBRIUM SHAPES OF A ROTATING CHARGED DROP AND CONSEQUENCES FOR HEAVY-ION-INDUCED NUCLEAR REACTIONS
S. Cohen, F. Plasil,* and W. J. Swiatecki*
pp. 325-331.

61. THE $B^{10}(d, Li^6)Li^6$ REACTION AT DEUTERON ENERGIES FROM 8 TO 13.5 MEV
D. S. Gemmell, J. R. Erskine, and J. P. Schiffer
pp. 186-190.

62. SIMPLE INTERFERENCE CONCEPTS IN SCATTERING AND STRIPPING
D. R. Inglis
pp. 81-84.

---

63. QUANTUM THEORY OF MEASUREMENT
M. N. Hack
Bull. Am. Phys. Soc. 9, 148 (27-29 February 1964).

64. FAIRLY LOW-ENERGY PION-PION SCATTERING II
A. M. Saperstein and J. L. Uretsky
Bull. Am. Phys. Soc. 8, 617 (December 1963).

---

*Lawrence Radiation Laboratory, University of California, Berkeley.

65. MASS SPECTROMETRIC STUDIES OF HIGH-TEMPERATURE SYSTEMS

W. A. Chupka, J. Berkowitz, D. J. Meschi, and H. A. Tasman

Advances in Mass Spectrometry, Vol. 2, the Proceedings of a Conference Held in Oxford, September 1961, edited by R. M. Elliott (Pergamon Press, Oxford, 1963), pp. 99-109.

66. THERMODYNAMICS AND KINETICS OF VAPORIZATION PROCESSES STUDIED BY MASS SPECTROMETRY

W. A. Chupka and J. Berkowitz

Appl. Spectroscopy 17, 130 (September 1963).

67. ATOMIC COLLISION SEQUENCES REVEALED IN THE SPUTTERING OF METAL MONOCRYSTALS BY ION BOMBARDMENT IN THE RUTHERFORD COLLISION REGION

M. Kaminsky

Bull. Am. Phys. Soc. 8, 428 (24 June 1963).

68. A PULSED-MOLECULAR-BEAM MASS SPECTROMETER FOR STUDIES OF ATOMIC AND IONIC IMPACT PHENOMENA ON METAL SURFACES

M. Kaminsky

Advanced Energy Conversion (Pergamon Press, Oxford, 1963), Vol. 3, pp. 255-263 (January-March 1963).

See also the fourteen additional abstracts of papers presented at Argonne—sponsored conferences and included in the volumes of Proceedings issued as ANL topical reports. These are listed in the next section under the appropriate conference headings.

IV - 3. ANL TOPICAL REPORTS

1. Proceedings of the International Conference on Nuclear Physics with Reactor Neutrons, Argonne National Laboratory, 15-17 October 1963, edited by F. E. Throw, Argonne National Laboratory Topical Report ANL-6797 (490 pages). The following are the Argonne papers included in this conference.

   a. DISTRIBUTION OF PARTIAL RADIATION WIDTHS
      L. M. Bollinger, R. E. Coté, R. T. Carpenter, and J. P. Marion
      Proceedings, ANL-6797, pp. 322-323.
      Bull. Am. Phys. Soc. 9, 177 (27-29 February 1964).

   b. MEASUREMENT OF THE POLARIZATION OF THERMAL-NEUTRON BEAMS BY MAGNETIZED MIRRORS
      M. T. Burgy, G. R. Ringo, S. Ketudat, P. Rice-Evans, and S. Barkan
      Proceedings, ANL-6797, pp. 35-44.
      Bull. Am. Phys. Soc. 9, 174 (27-29 February 1964).

   c. GAMMA-RAY ANGULAR CORRELATIONS IN Ca^{45}, Fe^{55}, Ni^{59}, Ni^{61}, AND Ni^{63}
      R. E. Coté, H. E. Jackson, Jr., L. L. Lee, Jr., and J. P. Schiffer
      Proceedings, ANL-6797, p. 270.
      Bull. Am. Phys. Soc. 9, 176-177 (27-29 February 1964).

   d. TOTAL RADIATION WIDTHS FOR s-WAVE AND p-WAVE NEUTRON CAPTURE IN Nb^{93}
      H. E. Jackson
      Proceedings, ANL-6797, pp. 294-300.
      Bull. Am. Phys. Soc. 9, 177 (27-29 February 1964).

   e. FLUCTUATIONS IN PARTIAL RADIATION WIDTHS OF U^{239}
      H. E. Jackson
      Proceedings, ANL-6797, pp. 333-341.
      Bull. Am. Phys. Soc. 9, 178 (27-29 February 1964).

   f. THE NEUTRON-ELECTRON INTERACTION
      V. E. Krohn
      Proceedings, ANL-6797, pp. 15-20.

Nuclear Physics with Reactor Neutrons (cont'd.).

g. STUDY OF THE NEUTRON-CAPTURE GAMMA RAYS IN Ca^{48}
S. Raboy and C. C. Trail
Proceedings, ANL-6797, pp. 243-246.
Bull. Am. Phys. Soc. 9, 176 (27-29 February 1964).

h. STATISTICAL PROPERTIES OF NUCLEAR STATES AND TRANSITIONS
N. Rosenzweig
Proceedings, ANL-6797, pp. 302-321.

i. SEARCH FOR PARTICLE-STABLE TETRANEUTRONS AND DINEUTRONS IN FISSION
J. P. Schiffer and R. Vandenbosch
Proceedings, ANL-6797, pp. 27-29.
Bull. Am. Phys. Soc. 9, 173 (27-29 February 1964).

j. ROTATIONAL AND VIBRATIONAL EFFECTS IN NEUTRON-CAPTURE GAMMA-RAY SPECTRA
R. K. Smither
Proceedings, ANL-6797, pp. 89-110.

k. NEUTRON CAPTURE BY DEUTERIUM
C. C. Trail and S. Raboy
Proceedings, ANL-6797, pp. 247-258.
Bull. Am. Phys. Soc. 9, 176 (27-29 February 1964).

---

2. NUCLEAR SPECTROSCOPY WITH DIRECT REACTIONS. I. CONTRIBUTED PAPERS (the first volume of proceedings of the Symposium on Nuclear Spectroscopy with Direct Reactions which was sponsored by Argonne National Laboratory and was held at the Center for Continuing Education, University of Chicago, 9—11 March 1964), edited by F. E. Throw, Argonne National Laboratory Report ANL-6848, March 1964 (248 pages). The following are the Argonne papers included in this conference.

a. A HIGH-RESOLUTION STUDY OF (d,p) REACTIONS ON TARGETS OF W^{182}, W^{184}, AND W^{186}
J. R. Erskine
I. Contributed Papers, ANL-6848, pp. 86-97.

NUCLEAR SPECTROSCOPY WITH DIRECT REACTIONS (cont'd.).

b. A STUDY OF (d,n) REACTIONS ON Fe^{54} AND Ni^{58}
D. S. Gemmell, L. L. Lee, Jr., J. P. Schiffer, and A. B. Smith
I. Contributed Papers, ANL-6848, pp. 98-103.

c. NUCLEON CAPTURE REACTIONS NEAR A = 40
J. L. Yntema and G. R. Satchler
I. Contributed Papers, ANL-6848, p. 177.

---

3. FORTRAN PROGRAMS FOR COMPUTING ANGULAR DISTRIBUTIONS AND Q VALUES OF NUCLEAR REACTIONS
H. W. Broek
Argonne National Laboratory Topical Report ANL-6718 (May 1963).

4. EQUILIBRIUM SHAPES OF A ROTATING CHARGED DROP AND CONSEQUENCES FOR HEAVY-ION-INDUCED NUCLEAR REACTIONS
S. Cohen, F. Plasil, and W. J. Swiatecki
University of California Lawrence Radiation Laboratory report UCRL-10775 (29 April 1963).

5. A SIMPLE GRAPHICAL METHOD IN THE ANALYSIS OF SU_3
S. Gasiorowicz
Argonne National Laboratory Topical Report ANL-6729.

6. THE PARITY OF THE NEUTRAL K MESON
R. Spitzer
University of California Radiation Laboratory Report UCRL-7332-T (30 April 1963).

V. STAFF MEMBERS OF THE PHYSICS DIVISION

The Physics Division staff as of 1 April 1964 is listed below. Although the members are classified by programs, it must be understood that many of them work in two or more of the areas. In such cases, the classification indicates only the current primary interest.

In the period from 1 April 1963 through 31 March 1964, there were 35 temporary staff members (26 staff members from universities and other laboratories and 9 post-doctoral fellows), 3 graduate students (including 2 doing thesis research), and 35 undergraduates (10 in the Argonne Semester program of the Associated Colleges of the Midwest, 9 in cooperative programs, 15 on summer appointments, and 1 other).

RESEARCH AT THE REACTOR CP-5

Permanent Staff

Lowell M. Bollinger,* Ph. D., Cornell University, 1951

Merle T. Burgy, B. S., University of Chicago, 1939

Robert E. Coté, Ph. D., Columbia University, 1953

Harold E. Jackson, Jr., Ph. D., Cornell University, 1959

Victor E. Krohn, Ph. D., Case Institute of Technology, 1952

Allen P. Magruder, B. S., University of Chicago, 1959

J. P. Marion, M. S., DePaul University, 1959

Sol Raboy, Ph. D., Carnegie Institute of Technology, 1950

G. R. Ringo, Ph. D., University of Chicago, 1940

Robert K. Smither, Ph. D., Yale University, 1958

George E. Thomas, Jr., B. A., Illinois Wesleyan University, 1943

Carroll C. Trail, Ph. D., Texas A & M College, 1956

Resident Research Associates

Harnam S. Hans, Ph. D., Aligarh Muslim University, 1953

Arthur I. Namenson, Ph. D., Columbia University, 1963

---

*Director of Physics Division

FAST-NEUTRON REACTIONS

Permanent Staff

Alexander Elwyn, Ph. D., Washington University, 1956

Carl T. Hibdon, Ph. D., Ohio State University, 1944

Raymond O. Lane, Ph. D., Iowa State University, 1953

Alexander Langsdorf, Jr., Ph. D., Massachusetts Institute of Technology, 1937

F. P. Mooring, Ph. D., University of Wisconsin, 1951

CHARGED-PARTICLE REACTIONS

Permanent Staff

Thomas H. Braid, Ph. D., Edinburgh University, 1950

John R. Erskine, Ph. D., University of Notre Dame, 1960

Donald S. Gemmell, Ph. D., Australian National University, 1960

David C. Hess, Ph. D., University of Chicago, 1949

Robert E. Holland, Ph. D., University of Iowa, 1950

Linwood L. Lee, Jr., Ph. D., Yale University, 1955

Frank J. Lynch, B. S., University of Chicago, 1944

Luise Meyer-Schützmeister, Ph. D., Technical University of Berlin, 1943

John P. Schiffer,* Ph. D., Yale University, 1954

Ralph E. Segel, Ph. D., Johns Hopkins University, 1955

J. L. Yntema, Ph. D., Free University of Amsterdam, 1952

Benjamin Zeidman, Ph. D., Washington University, 1957

Resident Research Associates

Richard G. Allas, Ph. D., Washington University, 1961

Dietrich Dehnhard, Ph. D., University of Marburg/Lahn, 1964

---

*Associate Director of Physics Division

Amnon Marinov, Ph. D., Hebrew University, 1962

Karl-Edvard Nystén, Ph. D., University of Helsinki, 1960

Rolf H. Siemssen, Ph. D., University of Hamburg, 1963

P. Paul Singh, Ph. D., University of British Columbia, 1959

Zeev Vager, Ph. D., Weizmann Institute of Science, 1952

Dieter von Ehrenstein, Dr, rer. nat. degree, University of Heidelberg, 1960

GAMMA- AND BETA-RAY SPECTROSCOPY

Permanent Staff

Herbert H. Bolotin, Ph. D., Indiana University, 1955

S. B. Burson, Ph. D., University of Illinois, 1946

Resident Research Associates

Teymoor Gedayloo, M. S., University of Washington, 1960

William C. Johnston, B. S., Alma College, 1961

E. Brooks Shera, Ph. D., Western Reserve University, 1962

ATOMIC-BEAM STUDIES

Permanent Staff

William J. Childs, Ph. D., University of Michigan, 1956

John Dalman

Leonard S. Goodman, Ph. D., University of Chicago, 1952

MÖSSBAUER STUDIES

Permanent Staff

Juergen Heberle, Ph. D., Columbia University, 1955

Gilbert J. Perlow, Ph. D., University of Chicago, 1940

Richard S. Preston, Ph. D., Yale University, 1954

Stanley Ruby, B. A., Columbia University, 1947

VARIABLE-ENERGY CYCLOTRON

Permanent Staff

John J. Livingood, Ph. D., Princeton University, 1929

THEORETICAL PHYSICS

Permanent Staff

Stanley Cohen, Ph. D., Cornell University, 1955

Fritz Coester, Ph. D., University of Zurich, 1944

Hans Ekstein, Ph. D., University of Berlin, 1934

Melvin Hack, Ph. D., Princeton University, 1956

David R. Inglis, Ph. D., University of Michigan, 1931

Dieter Kurath, Ph. D., University of Chicago, 1951

Donald Lang, Ph. D., Australian National University, 1961

Robert D. Lawson, Ph. D., Stanford University, 1953

Malcolm H. Macfarlane, Ph. D., University of Rochester, 1959

James E. Monahan, Ph. D., St. Louis University, 1953

Murray Peshkin,* Ph. D., Cornell University, 1951

Norbert Rosenzweig, Ph. D., Cornell University, 1951

---

*Associate Director of Physics Division

Resident Research Associates

Arnold Bodmer, Ph. D., Manchester University, 1955

Sudhir Pandya, Ph. D., University of Rochester, 1957

John K. Perring, Ph. D., Cambridge University, 1952

MASS SPECTROMETRY

Permanent Staff

Joseph Berkowitz, Ph. D., Harvard University, 1955

William A. Chupka, Ph. D., Harvard University, 1955

Manfred Kaminsky, Ph. D., University of Marburg, Germany, 1952

Henry E. Stanton, Ph. D., University of Chicago, 1944

RADIOFREQUENCY PLASMAS

Permanent Staff

Albert J. Hatch, M. S., University of Illinois, 1947

ADMINISTRATIVE

Permanent Staff

Charles Eggler, B. S., Virginia Polytechnic Institute, 1944

Francis E. Throw, Ph. D., University of Michigan, 1940